JPRS-UMS-92-004
19 MARCH 1992

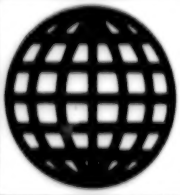

FOREIGN
BROADCAST
INFORMATION
SERVICE

# JPRS Report

# Science & Technology

## Central Eurasia: Materials Science

# Science & Technology
## Central Eurasia: Materials Science

JPRS-UMS-92-004 19 March 1992

CONTENTS

### ANALYSIS, TESTING



### COATINGS



### COMPOSITE MATERIALS

## CORROSION



## FERROUS METALS



## NONFERROUS METALS, ALLOYS, BRAZES, SOLDERS

## NONMETALLIC MATERIALS

## TREATMENTS



## WELDING, BRAZING, SOLDERING

## EXTRACTIVE METALLURGY, MINING



## MISCELLANEOUS

## Magnetic Properties of Multilayer Co/Cu Films

*927D0110B Yekaterinburg FIZIKA METALLOV I METALLOVEDENIYE in Russian No 12, Dec 91 pp 43-49*

[Article by V.M. Fedosyuk, O.I. Kasyutich, N.N. Kozich, Institute of Solid State and Semiconductor Physics at the Belarus Academy of Sciences]

UDC (669.3+669.25):539.216.2:537.622

[Abstract] The outlook for using multilayer hard magnetic cobalt and iron films with alternating platinum and palladium layers and with a high perpendicular magnetic anisotropy constant (KPMA) as data media in vertical recording memory devices (VZS) is discussed and the magnetic properties of multilayer structures with ultrathin alternating copper and cobalt layers (on the order of one nanometer) are investigated. Torque, rotational hysteresis loss, and rotational hysteresis integral curves are plotted and analyzed and the conclusion is drawn that the magnetization polarity of such films can be easily reversed by moving their domain walls. It is shown that in some Co/Cu films, 80 kA/m and 0.45 characteristics may be attained, which substantially exceed the corresponding characteristics of today's best single-layer Co-Cr films with vertical memory recording. The multilayer Co/Cu films can be produced by pulsed electrolytic precipitation from a single electrolyte. PARC-155 and PARC-4500 vibrational magnetometers are used in the study. Figures 6; References: 5 Western.

## Diffusional Thermoelectromotive Force and Electric Conductivity of $GdZn_xCu_{1-x}$ Compounds

*927D0110C Yekaterinburg FIZIKA METALLOV I METALLOVEDENIYE in Russian No 12, Dec 91 pp 50-55*

[Article by N.I. Kourov, Yu.G. Karpov, Institute of Physics of Metals at the Urals Branch of the USSR Academy of Sciences]

UDC 669.3'5'73:537.31/32

[Abstract] The effect of the narrow *d*-band, probably formed by the 5*d*-states of $Gd^{3+}$ ions, on the behavior of electron characteristics of the $GdZn_xCu_{1-x}$ compounds prompted an investigation of their diffusional thermoelectromotive force and resistivity at $TT_c$ and $T_N$ because these properties of the quasibinary solid solutions in which a phase transition from a CdCu antiferromagnetic to a GdZn ferromagnetic is realized are the most indicative of Mott's scattering mechanism with a throw-over of the majority light charge carriers to another band with a low mobility. To this end, the thermoelectromotive force of 17 samples is examined in a 80-350K band and the electric resistivity of 14 samples in a 300-650K band. The heat capacity, transport properties, and temperature-insensitive component of paramagnetic susceptibility are examined as a function of temperature, concentration, and structural transition in samples with $x$ close to zero. An analysis shows that the behavior of these characteristics is determined primarily by the parameters of the narrow *d*-band located in the neighborhood of Fermi's level $E_f$ and that a change in the position and shape of the *d*-band as a function of temperature, especially at $TT_N$ and $T_c$, and concentration and during phase transitions indeed determines the electron characteristics of the system both in the vicinity of the concentrational phase transition from ferromagnetic to antiferromagnetic and in the paramagnetic state. Figures 4; references 13: 10 Russian, 3 Western.

## Annealing Under Tensile Stress of $Fe_{73.5}Cu_1Nb_3Si_{13.5}B_9$ Nanocrystalline Alloy

*927D0110D Yekaterinburg FIZIKA METALLOV I METALLOVEDENIYE in Russian No 12, Dec 91 pp 56-61*

[Article by A.A. Glazer, N.M. Kleynerman, V.A. Lukshina, A.P. Potapov, V.V. Serikov, Institute of Physics of Metals at the Urals Branch of the USSR Academy of Sciences]

UDC 669.15'3'293'781'782:537.624.2

[Abstract] Thermomechanical treatment—annealing under tensile stress—of amorphous alloys which leads to the development of magnetic anisotropy with the axis of easy magnetization (OLN) perpendicular to the tension axis is discussed and an attempt to examine the effect of annealing under tensile stress on new nanocrystalline Fe-based alloys produced by crystallizing the initial amorphous alloy is reported. Twenty μm-thick alloy strips are made by the rapid quenching method on a spinning copper drum. Hysteresis loops of the nanocrystalline alloy annealed at 530°C for 1 h under tensile stress and the nuclear γ-resonance (YaGR) spectra are plotted and the subspectrum parameters are summarized. An analysis shows that annealing under tensile stress is efficient in that it induces uniaxial anisotropy in the rapidly quenched alloy but only after it has passed to the nanocrystalline state and if its magnetostriction is low. This induced "easy plane" anisotropy is perpendicular to the thermomechanical treatment axis while the value of the $K_u$ is several times higher than that of a typical Co-based amorphous alloy. Furthermore, the temperature stability of the induced anisotropy in the nanocrystalline alloy is substantially higher than that of the amorphous alloy. The above findings are explained in the framework of the "cluster in a shell" model. Figures 4; tables 1; references 5: 2 Russian, 3 Western.

## Dynamic Response and Micromagnetic Structure Parameters of Fe-Cr-Co-Based Hard Magnetic Alloys

*927D0110E Yekaterinburg FIZIKA METALLOV I METALLOVEDENIYE in Russian No 12, Dec 91 pp 62-64*

[Article by M.A. Libman, F.I. Stetsenko, V.S. Boruta, N.N. Potapov, Central Scientific Research Institute of Ferrous Metallurgy imeni I.P. Bardin, Moscow]

UDC 669.15'25'26:537.613

[Abstract] A range of Fe-Cr-Co system compositions, within which the high-temperature α-solid solution decays into two isomorphous phases—the $\alpha_1$ and $\alpha_2$—enriched with ferromagnetic elements (Fe and Co) and chromium, respectively, resulting in the development of a structural state with a high coercive force, is discussed and interest in examining the parameters of the micromagnetic structure, i.e., $\alpha_1$ phase particle distribution in size and anisotropy field, forming as a result of the above decay is reported. This investigation is carried out using the method of dynamic response which is based on the relaxation origin of the coercive force in heterogeneous magnetic systems, i.e., its dependence on the application duration of the external magnetic field and temperature during the measurements. The influence of the effective magnetic anisotropy energy and mean volume of particles with a reversed magnetization polarity on the magnetization force is plotted for an iron alloy containing 26% Cr and 15% Co doped with 1-2% Mo and Ti. Figures 1; tables 1; references 5: 2 Russian, 3 Western.

## Characteristics of Natural Ferromagnetic Resonance in Amorphous Microconductor

*927D0110F Yekaterinburg FIZIKA METALLOV I METALLOVEDENIYE in Russian No 12, Dec 91 pp 172-174*

[Article by S.A. Baranov, S.K. Zotov, V.S. Larin, A.V. Torkunov, Kishinev Scientific Research Institute of Electric Instrument-Making at the Mikroprovod Scientific Production Association]

UDC 539.213:(537.635:537.611.44)

[Abstract] The natural ferromagnetic resonance (YeFMR) discovered in a 2-12 GHz frequency band in cast amorphous microconductors encased in soda-lime glass sheathing which is peculiar to these metallic materials with a positive magnetostriction is discussed; the greater the magnetostriction, the higher the natural ferromagnetic resonance frequency. Formulas of the dependence of the natural ferromagnetic resonance frequency on the microconductor parameters are derived. The consistency of theoretical data and the experimental results is noted. The dependence of the natural ferromagnetic resonance frequency on temperature is investigated in order to check the theoretical findings; an analysis demonstrates that the frequency is proportionate to temperature while the extrapolated value of the soda-lime glass congelation point (400-500°C) is consistent with experimental data. Figures 3; references 5.

## Galvanomagnetic Properties of Mo Single Crystals Under Static Skin Effect in Strong Magnetic Fields

*927D0110G Yekaterinburg FIZIKA METALLOV I METALLOVEDENIYE in Russian No 12, Dec 91 pp 65-74*

[Article by A.N. Cherepanov, V.V. Marchenkov, V.Ye. Startsev, Institute of Physics of Metals at the Urals Branch of the USSR Academy of Sciences]

UDC 669.28:537.312.8

[Abstract] Efforts to establish whether static skin effect exists in high-purity single crystal molybdenum with $\rho_{293.2K}/\rho_{4.2K} > 30{,}000$ in magnetic fields of up to 15 T and—if it does—to investigate its contribution to the development of magnetoresistance and ascertain whether an increase in the Hall coefficient detected in tungsten is also characteristic of other compensated metals with closed Fermi surfaces, such as molybdenum, are reported. To this end, the anisotropy and magnetic field behavior of transverse magnetoresistance and Hall resistivity of single crystal molybdenum with the above resistivity ratio is examined in 0.8-15 T magnetic fields and at 4.2K. Static skin effect accompanied by a high direct current distrubution nonuniformity is observed; the ratio of the surface current density to the steady volume current density in magnetic fields above 10 T reaches 500-900. The results shown that in Mo crystals, (100) faces scatter conductivity electrons in a more specular way than similar tungsten single crystal faces and that the Hall coefficient under static skin effect conditions increases linearly with the magnetic field strength, pointing to the fact that this Hall effect behavior is common to compensated metals with a closed Fermi surface. It is speculated that this phenomenon may be detected in other metallic crystals with a static skin effect. The authors are grateful to N.Ye. Alekseyevskiy for support and interest in the study and V.A. Sazonova for the crystallographic orientation of the samples. Figures 6; tables 1; references 13: 11 Russian, 2 Western.

## Investigation of Grain Boundary, Dislocation, and Precipitate Distribution in Stainless Steel 04Kh17N14M3G2

*927D0110H Yekaterinburg FIZIKA METALLOV I METALLOVEDENIYE in Russian No 12, Dec 91 pp 80-86*

[Article by V.Yu. Gertsman, O.V. Mishin, O.K. Korotkova, S.V. Averin, V.A. Safonov, Institute of Metal Superplasticity Problems at the USSR Academy of Sciences]

UDC 669.15'24'26'28'74-194:548:620.186.8

[Abstract] The recently proposed concept of "grain boundary" designing, i.e., controlling the properties of the materials by manipulating the grain boundary distribution in them, is discussed and an attempt to comprehensively examine various distributions which characterize the structure of stainless steel 04Kh17N14M3G2 in a statically recrystallized state is reported. Two tube-shaped samples of austenitic steel 04Kh17N14M3G2, one produced by rolling single crystals (M) and one by rolling polycrystals (P) are investigated for this purpose. To this end, the grain boundary distribution in the reciprocal density of coincident angles Σ, misalignment angles and axes, dislocation densities, and inclusions both inside the grains and on their boundaries are

analyzed and the relationships among these parameters are examined. Metallographic studies are carried out under a Neofot-32 optical microscope and a JSM-840A scanning electron microscope while electron microscope studies are carried out in a JEM-2000EX transmission electron microscope. The structure of both samples in the rolled state is highly fragmented and is characterized by a high dislocation density while an equiaxial uniform grain structure with a large number of twins forms in both samples during annealing. An analysis shows the structure of M and P samples differs mostly in the grain size while the grain boundary distribution in both samples is similar to that of other statically recrystallized materials with a tendency toward twinning during annealing. $Me_{23}C_6$ carbide precipitates during annealing along the grain boundaries except for the Σ3 twins. Figures 5; tables 1; references 16: 6 Russian, 10 Western.

### Argon Analysis in Natural Gas

*927D0109F Moscow RAZVEDKA I OKHRANA NEDR in Russian No 10, Oct 91 pp 34-35*

[Article by N.K. Devitskaya, Luganskgeologiya Production Geology Association]

UDC 543.544:546.293

[Abstract] The difficulties of argon analysis in natural gas related to the chromatograph column design or preliminary oxygen absorption in the VTI-2 in a pyrogallol solution are discussed and a new method of using CaX molecular sieves is proposed. The procedure of argon analysis in a chromatograph column with the help of the CaX molecular sieve is outlined and calibration curves are plotted for two injection methods—by a syringe and by a dispenser—using 99.9% pure argon. The chromatography conditions are as follows: a 70 mA detector current, a 30 ml/min carrier gas rate, a 40°C column temperature, and a 100°C detector temperature. A 1 $cm^3$ sample is analyzed and oxygen is used as the carrier gas; the need to find a less corrosive carrier gas is identified. Figures 1; tables 1.

### Effect of Silicide Particle Precipitation on Two-Phase Titanium Alloy Properties

*927D0099G Yekaterinburg FIZIKA METALLOV I METALLOVEDENIYE in Russian No 11, Nov 91 pp 129-135*

[Article by A.A. Popov, O.A. Yelkina, A.V. Trubochkin, Urals Polytechnic Institute imeni S.M. Kirov and Institute of Physics of Metals at the Urals Branch of the USSR Academy of Sciences]

UDC 669.295:539.4.015

[Abstract] Although it is known that the addition of silicon to titanium alloys improves their high-temperature strength, the mechanism of this effect remains unclear; consequently, the effect of complex titanium and zirconium silicides on the toughness of the VT9 two-phase titanium alloy is examined. To this end, 20 mm dia. rods are heated to 1,100°C, exposed for 2 h, and transferred to a 700°C furnace and exposed there for 2 h, then cooled in the air. The resulting laminated structure with colonial α-phase flakes actually simulates the initial stages of the thermal cycle in semifinished products for the VT8 and VT9 alloys. The effect of the cooling rate on the toughness of the VT8 and VT9 alloys and the effect of the testing temperature on the toughness of the VT8 and VT9 alloys is examined and plotted and the alloys' fracture surface and microstructure are analyzed. The mechanical properties of the VT8 and VT9 alloys are summarized after various treatment procedures. It is established that $(Ti, Zr)_5Si_3$ silicides precipitate in the VT9 alloy and are transformed due to isothermal exposure to $(Ti, Zr)_6Si_3$ silicides, i.e. are enriched with zirconium atoms. This precipitation is responsible for a decrease in the alloy toughness. It is recommended that silicides be dissolved in order to increase the alloy's high-temperature strength by heating it to 950°C and subsequently cooling it a 1-16K/s rate; this helps to neutralize the silicide particle formation on the one hand but does not result in the martensite phase formation during the cooling on the other. Figures 4; tables 2; references 15: 1 Russian, 14 Western.

### Effect of C, Cu, and Nb on Crystal Structure of Martensite in Co-Fe and Co-Ni Alloys

*927D0099F Yekaterinburg FIZIKA METALLOV I METALLOVEDENIYE in Russian No 11, Nov 91 pp 117-121*

[Article by B.I. Nikolin, T.L. Sizova, Institute of Physics of Metals at the Ukrainian Academy of Sciences]

UDC 669.225:666.046.516:620.186.1

[Abstract] The effect of martensite comprehensively alloyed with both interstitial and substitutional elements in binary cobalt systems in which multilayer structures do not form either as a result of hardening or due to multiple reversible FCC-HCP phase transformations or aging is examined in single crystals produced by water quenching of large-grained ingots smelted in a microwave furnace in an argon medium. Niobium, copper, and carbon which have a limited solubility in cobalt and binary alloys differing by the type of solid solutions—substitutional (Co-Ni and Co-Fe) and interstitial (Co-C)—are used as the alloying elements. An analysis demonstrates that in binary cobalt systems alloyed by Nb, a 138R or 46T multilayer martensite structure forms during hardening while reversible β-NR or RT transitions in the Co+Ni+Nb alloy facilitate the modulated structure development in the β-phase. In Co-Nb and Co-Cu alloys, nickel decreases the critical Nb and Cu concentration of the RT or NT martensite structure formation in binary systems; moreover, a $7T_1$ structure forms in single crystals of the Co+Fe+Cu alloy after

hardening and as a result of reversible β-α phase transitions. It is noted that additional studies are needed to determine why NR or NT martensite structures do not form in Co-Ni-Cu alloys. Figures 2; references 9.

### Phase Transformations in Fe-Ni-Co-Ti Strip Produced by Melt Spinning Method

*927D0099E Yekaterinburg FIZIKA METALLOV I METALLOVEDENIYE in Russian No 11, Nov 91 pp 108-111*

[Article by I.G. Zakrevskiy, L.Ye. Kozlova, I.V. Feofilov, V.A. Chernenko, O.M. Shevchenko, V.M. Kachalov, Institute of Physics of Metals at the Ukrainian Academy of Sciences]

UDC 669.15'24'25'295:669-156:620.186.1

[Abstract] Phase transformations occurring in rapidly quenched alloys are discussed and an attempt to ascertain the possibility, in principle, of producing a shape memory material from a Fe-Ni-Co-Ti alloy by quenching from a molten state as well as investigate the characteristics of phase transitions in the rapidly quenched strip under the effect of temperature is reported. An alloy containing 27% Ni, 18% Co, and 5% Ti by weight melted in an induction furnace in an inert atmosphere and rolled into bar and strip is used; for comparison, rapidly quenched 20 μm strips are produced by pouring the melt onto a copper disc spinning at a 1,500 RPM rate. Diffraction patterns of the initial strip and strips aged at 923K for 10 min, the tensile strain of a strip loaded with a constant force as a function of temperature, and the calorimetric dependence of the initial strip and a strip aged at 923K for 10 min are examined and plotted. An analysis of the results demonstrates that the strip prepared by spinning is capable of undergoing a reversible martensite transformation and thus recovering strain and generating mechanical stress. Experimental data also indicate that strip shape memory materials can be produced from Fe-Ni-Co-Ti alloys; a need for subsequent research in order to improve the structure, composition, and property homogeneity of the material is identified. The authors are grateful to V.V. Kokorin for discussing the finding and I.N. Vitenko for help with the experiment. Figures 4; tables 1; references 6: 5 Russian, 1 Western.

### Effect of Structural Characteristics of $R_{33}Fe_{67}$ Rapidly Quenched Alloys on Hysteretic Properties

*927D0110A Yekaterinburg FIZIKA METALLOV I METALLOVEDENIYE in Russian No 12, Dec 91 pp 37-42*

[Article by Ye.V. Ivanova, I.I. Yakimov, M.I. Bartashevich, Irkutsk Teachers Institute]

UDC 669.85/86.018:537.622

[Abstract] The use of rapid melt quenching for producing alloys of iron with rare earth elements or rare earth metals (R) whose coercive force can be increased significantly compared to cast and sintered magnets is discussed and the need to examine and analyze data on the structure of rapidly quenched Fe-R alloys (BZS) is identified. Thus, the magnetic properties and structural state of rapidly quenched $R_{33}Fe_{67}$ alloys (R=Sm, Tb, Ho, Er, and Dy) produced by quenching the melt on a spinning disc in an atmosphere of argon are investigated and it is shown that the noticeable difference between the coercive force of alloys with light and heavy rare-earth element atoms can be attributed to the solidification characteristics of peritectic alloys. The highest coercive force is attained in $Sm_{33}Fe_{67}$ alloy (close to 4 MA/m). The high coercivity state as well as an unusual magnetic behavior of these alloys is attributed to the paramagnetic samarium shell which separates highly anisotropic $SmFe_2$ crystals from each other. The morphological characteristics of the nonequilibrium structure and the presence of soft and hard magnetic phases separated by the paramagnetic Sm shell are noted. Figures 6; references 4: 3 Russian, 1 Western.

## Emission-Spectral and Roentgenographic Investigation of Germanium Coatings Deposited Onto Copper and Niobium by Electroprecipitation From an Ethylene Glycol Solution

*927D0046E Kishinev ELEKTRONNAYA OBRABOTKA MATERIALOV in Russian No 3, May-Jun 91 (manuscript received 31 Jul 90) pp 29-31*

[Article by V.D. Kalugin, A.M. Gavrish, T.A. Naumenko, and L.V. Lapchinskaya, Chemistry Scientific Research Institute, Kharkov University, Kharkov]

[Abstract] The authors of the study used the methods of emission-spectral and roentgenographic analysis to examine the structure of germanium coatings electrolytically precipitated onto copper and niobium substrates from an ethylene glycol solution. The germanium layers studied were precipitated from an electrolyte consisting of 98.4% ethylene glycol and 1.6% $H_2O$ plus 3% (volume) $GeCl_4$. The electrolysis was implemented at a current of 50 A/dm$^2$ and electrolyte temperature of 55 +/- 1°C in an open electrolytic cell with plate-type germanium electrodes. The electrolysis time was dictated by the required coating thickness and generally ranged from 600 to 2,400 seconds. Before being subjected to the germanium plating, the copper substrates were etched in $HNO_3$ (1:1), rinsed in distilled water and acetone, and dried in air at 30 +/- 3°C. Before the niobium substrates were plated with germanium, they were treated as described elsewhere to remove their oxide layer and then rinsed in water and acetone and air-dried. The studies of the germanium scraped off the Cu and Nb electrodes were completely unexpected. The presence of the characteristic Ge spectral lines in the spectrograms of the powders scraped from both the Cu and Nb electrodes indicated that metallic germanium was precipitated during the electrolysis process. In the case of the copper electrode, the spectral lines obtained for the powder were the same as in the case of the standards. These findings led the researchers to hypothesize that either compounds (impurities) with different degrees of metal oxidation are included in the galvanic germanium precipitates on the Cu and Nb electrodes or else the structure of the electrolytic condensates changes. Comprehensive studies of the electrolytic germanium condensates confirmed that at high current densities (50 A/dm$^2$), the specific electrochemical nature of the substrate material (either Cu or Nb) does not appear. Precipitates having an x-ray amorphous nature and a weakly expressed crystalline structure are formed on the Cu and Nb substrates. Figures 2, table 1; references 6 (Russian).

## The Gas Permeability of VT1-0 Titanium With Microarc Anodic Oxidation Coatings

*927D0046F Kishinev ELEKTRONNAYA OBRABOTKA MATERIALOV in Russian No 3, May-Jun 91 (manuscript received 9 Aug 90) pp 35-39*

[Article by P.S. Gordiyenk, S.B. Bulanova, O.A. Krisanfova, and N.G. Vostrikova, Chemistry Institute, Far Eastern Department, USSR Academy of Sciences, Vladivostok]

[Abstract] The authors of the study examined the gas permeability of VT1-0 titanium with oxide coatings applied by the method of microarc anodic oxidation. For the studies, specimens of VT1-0 titanium measuring 5 x 10 x 1 mm were polished, degreased, and dried with filter paper. A titanium plate whose area was several times that of the specimen to be oxidized was used as the cathode. The electrolyte temperature was kept between 22 and 25°C. The coatings were applied in a mode of sparking at the anode at potentials of 200 to 400 V. The oxidation time ranged from 5 to 10 minutes. The gas permeability of the coatings produced was estimated on the basis of experimental data on the increase in the specimens' mass upon annealing in air. This estimate was based on data recorded by on Q-1500D derivative thermogravimetric analyzer. The specimens were annealed in open platinum crucibles in a dynamic mode with heating at a rate of 5 °/min to 1,000°C. To clarify the effect of annealing time on the coatings' properties, the specimens were annealed in an isothermal mode at temperatures above the temperature of the onset of oxidation (>650°C). The effect of isothermal annealing at temperatures of 800, 825, and 850°C was studied. Sixteen different electrolyte compositions were studied. Computer processing of the data collected during the experiments enabled the authors to derive the following equation linking the increase in specimen mass and temperature: $\Delta m\ [d(\Delta m)d(\Delta t)] = B exp\ [-(E/RT)]$. The coatings produced in the 16 different electrolytes studied shifted the temperature of the onset of oxidation from 650°C for specimens of pure titanium to 750-830°C for specimens of VT1-0 titanium coated by the microarc anodic oxidation technique. The average rate of oxidation of the shielded material at the working temperatures studied was also found to be an important parameter of the protective coatings. The coating produced in one of the 16 electrolytes studied was a high-temperature titanium dioxide phase of rutile modification. The authors hypothesized that it is likely more perfect than a titanium dioxide phase formed during thermal oxidation. Two of the other electrolytes tested were also deemed very promising. The authors concluded that the coatings formed in electrolytes at sparking potentials are distinguished by the diversity of their chemical compounds

and phases when compared with those of coatings produced by anodization or thermal oxidation and that the coatings studied herein appear to offer new possibilities with respect to modifying titanium surfaces in various ways (including improving their heat resistance). Figures 3, tables 5; references 9: 7 Russian, 2 Western.

## The Effect of Argon Pressure on the Structure of Multicomponent Vacuum Electroarc Coatings

*927D0046B Kishinev ELEKTRONNAYA OBRABOTKA MATERIALOV in Russian No 3, May-Jun 91 (manuscript received 10 Sep 90) pp 19-22*

[Article by B.A. Eyzner, G.V. Markov, and V.I. Ivashneva, Physics Technology Institute, Minsk]

[Abstract] The authors of the study examined one possible way of improving the structure of multicomponent vacuum electroarc coatings. Specifically, they conducted a series of experiments to determine the effect that adding an inert gas, in this case argon, to the vacuum chamber would have on the structure of the said coatings. The pressure of the argon was selected so that the length of the ions' free run was less than the distance from the erosion surface of the cathode (the ion source) to the substrate. The researchers hypothesized that under such conditions, the ions ionized the argon atoms upon colliding with them. This ionization in turn resulted in an increase in the ion concentration and, consequently, in a decrease in the thickness of the Debye layer. This decrease in Debye layer thickness in turn reduced separation and helped produce a coating with a more uniform composition. This hypothesis was verified experimentally by using a 01NI vacuum electroarc unit to apply a type NiCrAlY refractory coating with an arc current of 80 A and with a normal ion drop. Studies performed by using a 252 profilometer-profilograph, JEM-100CX scanning electron microscope, and Kamebaks x-ray fluorescent analyzer confirmed that coatings applied in an argon medium had more uniform structures. The coatings produced in the argon medium also had a lesser surface roughness and higher heat resistance than analogous coatings produced without the use of argon. An argon pressure of $2.7 \times 10^{-2}$ Pa appeared to be best. Figures 4; references 6 (Russian).

## Stochastic Magnetic Structure Characteristics of Laser Sputtered Amorphous Tb-Fe Films

*927D0099A Yekaterinburg FIZIKA METALLOV I METALLOVEDENIYE in Russian No 11, Nov 91 pp 62-71*

[Article by L.A. Yudina, S.G. Kraynova, L.N. Sovetnikova, V.V. Yudin, Far Eastern State University]

UDC (669.15'863-539.2162):537.662

[Abstract] The use of rare-earth and transition metal-based (RZ-PM) materials in optical memory devices—double-sublattice ferrimagetic films which are amorphous within a broad concentration range—is discussed and attempts to investigate amorphous Tb-Fe films with a 500 angstrom thickness sputtered on KBr cleavages by the methods of bright field, transmission, and Lorentz electron microscopy (JEM-100B and EVM-100AK units) and electron microdiffraction and laser diffraction pattern analyses are reported. The films are produced by the frequency laser sputtering method in the nanosecond pulse mode at a varying laser radiation defocusing. The fine structure of magnetic distribution which may become a medium suitable for orthogonal data recording is suggested and the advantages of magnetic quasilattice structures are summarized. An analysis of magnetic inhomogeneities and the character of interaction among them makes it possible to speculate that the size of the elements used for thermomagnetic data recording in this medium is on the order of single micrometers. The above magnetic bubble (TsMD) materials are distinguished by the need for two magnetic anisotropy components for making a magnetic recording. The authors are grateful to Yu.A. Bykovskiy for formulating the problem and expressing interest in our work, L.I. Litinskaya and A.G. Dudoladov for making facilities available, and T.M. Kozlova and A.G. Shishkov for discussions and advice. Figures 4; references 15: 14 Russian, 1 Western.

## Natural and Induced Aging of Bronze Used as $Nb_3Sn$-Based Composite Matrices

*927D0099D Yekaterinburg FIZIKA METALLOV I METALLOVEDENIYE in Russian No 11, Nov 91 pp 90-98*

[Article by T.P. Krinitsina, Ye.P. Popova, S.V. Sudareva, Ye.P. Romanov, A.D. Nikulin, A.K. Shikov, A.Ye. Vorobyeva, Institute of Physics of metals at the Urals Branch of the USSR Academy of Sciences and VNIINM imeni Academician Bochvar, Moscow]

UDC 669.3'6:621.785.78

[Abstract] Precipitation of the hard brittle $Cu_3Sn$ ε-phase during the cold straining of copper-based composites prompted an investigation of natural and induced aging of bronze with 8.5 and 13% Sn by mass following cooling at various rates from the diffusion annealing temperature as well as after hot and cold working. Samples of FCC bronze are studied under a JEM-150 transmission electron microscope and their microhardness behavior is plotted. An analysis of test data reveals that the microhardness of naturally aged bronze with 13% Sn increases by 40% and that a decrease in the natural cooling rate decreases the natural aging effect somewhat, indicating that thermal elastic stress relaxation is the principal mechanism responsible for the ε-phase precipitation in cooled bronze. Moreover, naturally aged bronze undergoes an incomplete recovery at 200°C during annealing accompanied by a 20% decrease in microhardness and a partial ε-phase dissolution. As a result, it is recommended that annealing at 200°C for 15 hours be used to soften the initial bronze matrix state since such "softened" bronze is not as susceptible to ordering after hold plastic working of the Nb/Cu-Sn composite. Figures 11; references 10.

## Modification of the Surface Layer of Fiber-Based Composites in a Glow Discharge

*927D0046C Kishinev ELEKTRONNAYA OBRABOTKA MATERIALOV in Russian No 3, May-Jun 91 (manuscript received 5 Oct 90) pp 22-25*

[Article by Ch.M. Dzhuvarly, Yu.V. Gorin, and F.Kh. Kulakhmetov, Physics Institute, AzSSR Academy of Sciences, Baku]

[Abstract] Others have established that treatment in a glow discharge makes it possible to purify and activate the surface of dielectric, semiconductor, and metal materials and products. In a continuation of this line of research, the authors of the study examined the possibility of modifying the surface layer of carbon fiber-based composites in a glow discharge. For their experiments, they used 15 x 15 x 1-$mm^3$ specimens of carbon-filled plastics in the form of oriented carbon fibers and polymerized epoxy compound along with specimens of the same material whose surface had been formed by multilayer impregnated glass fiber. The specimens were treated in a glow discharge in nitrogen, argon, sulfur hexafluoride, and residual air. The working gap was formed by parallel disk electrodes with an area of 12 $cm^2$ located 20 cm apart. The treatment in all of the gases was conducted at a pressure of 2 x $10^{-2}$ mm Hg (2.7 Pa). The glow discharge at currents of 0.5 to 4 mA was stable in all of the gases used. Specimens were arranged at the anode, at the cathode, close to the cathode parallel to the axis of the gap, and at the edge of the positive column of the glow discharge. The initial pressure before the glow discharge was admitted was 5 x $10^{-5}$ mm Hg. The treatment time was varied from 15 seconds to 3 minutes at fixed discharge currents of 0.5 and 1.0 mA and voltages in the gap of 1.2 and 2.1 kV. All coatings deposited by the thermovacuum method after treatment in a glow discharge had better adhesion than did analogous non-glow discharge-treated specimens. The maximum increase in specimen surface adhesion was achieved in the case of specimens treated in a glow discharge in residual air when the specimens were placed at or near the cathode. Figures 2; references 7 (Russian).

## Modification of Composites' Surfaces in a Flash Discharge

*927D0046G Kishinev ELEKTRONNAYA OBRABOTKA MATERIALOV in Russian No 3, May-Jun 91 (manuscript received 12 Nov 90) pp 48-52*

[Article by Yu.V. Gorin, F.Kh. Kulakhmetov, E.D. Kurbanov, R.N. Mekhtizade, and A.K. Gerasimov, Physics Institute, AzSSR Academy of Sciences, Baku]

[Abstract] The authors of the study examined the possibility of using a flash discharge to modify the surface of two types of composites: carbon-filled plastics with an epoxy binder and carbon-filled plastics with glass fiber underlayers. The flash discharge treatment experiments were conducted on a laboratory unit consisting of a high voltage source, limiting and instrument resistors, a discharge gap, and an oscillograph. A core made of a refractory material (molybdenum) 1.5 mm in diameter was used to form the flash. The treatment, which was carried out at ambient temperature, included a stable flash discharge during the positive half-period of the alternating voltage and a corona discharge during the negative half-period. The voltage of the stable flash ranged from 22 to 28 kV. Specimens were treated at alternating voltages of 15.5 and 19 kV with average flash currents of 32 and 136 A and average corona currents in the negative half-periods of 20 and 30 μA, respectively. At voltages of 15.5 kV the currents of the corona and flash differ by a factor of about 1.5. When subjected to such surface treatment, the carbon-filled plastics with the epoxy binder experienced a monotonic increase in adhesion, with most of this increase occurring in the first 100 seconds of treatment. Treatment of the carbon-filled plastics with the underlayer also produced a monotonic increase in adhesion (as indicated by an increase in $\cos\theta$), with most of the increase occurring in the first 50 seconds of treatment. At a voltage of 19 kV, the flash current exceeded the corona current by a factor of 4. At

that voltage, both types of carbon-filled plastics experienced a monotonic increase in adhesion. The adhesion achieved at a voltage of 19 kV was greater than that at 15.5 kV. Treating the specimens at voltages greater than 21 kV provided even greater increases in $\cos\theta$; however, the simultaneous presence of sparks and the flash discharge and their localization on certain spots of the specimens' surfaces resulted in uneven treatment. The experiments confirmed that a bipolar mode of combining a flash discharge with a negative corona may be optimal in actual electric discharge modification of the surface of a composite material. The strongest treatment effects were achieved in a static mode. A comparison of the adhesion of 1-μm-thick aluminum coatings applied to carbon-filled plastics subjected to flash discharge treatment and the adhesion of the same coatings to untreated control specimens revealed that flash discharge treatment results in a 50 to 70% improvement in adhesion. Figures 3, table 1; references 8 (Russian).

## Electron Microscope Structural Study of Nb/Cu-Sn Composites With Ti-Doped Niobium Filaments

*927D0110I Yekaterinburg FIZIKA METALLOV I METALLOVEDENIYE in Russian No 12, Dec 91 pp 100-110*

[Article by L.A. Rodionova, Ye.N. Popova, S.V. Sudareva, Ye.P. Romanov, N.V. Nikolayeva, A.Ye. Vorobyeva, Ye.A. Dergunova, O.V. Malafeyeva, A.D. Nikulin, K.A. Mareyev, N.Ye. Khlebova, A.K. Shikov, Institute of Physics of Metals at the Urals Department of the USSR Academy of Sciences and VNIINM imeni Academician A.A. Bochvar]

UDC (669.3'6+669.293):620.187.3

[Abstract] The effect of alloying on the critical properties of $Nb_3Sn$ superconductors is discussed and the effect of alloying with titanium on the structure of the superconducting layer, niobium filaments, and bronze matrix of $Nb_3Sn$-based multifilament composites fabricated by the "bronze" technology with various methods of Nb filament alloying is investigated; the study is carried out by the transmission electron microscopy and scanning electron microscopy method under JEM-200CX and JSM-U3 microscopes and Camebax Microbeam Link-860 microanalyzer. The sample composition and treatment methods are summarized and the microhardness of various components of a nonalloyed composite and a composite with metallurgical alloying (but without diffusion annealing) is measured. The titanium distribution in artificially alloyed composites is determined. The results indicate that in both conventional metallurgical alloying and artificial alloying of niobium filaments with titanium, titanium intensively diffuses through niobium and the $Nb_3Sn$ layer into the bronze matrix and forms intermetallic compound with copper and tin. In addition, $Ti_6Sn_5$ intermetallic compound particles are observed in $Nb_3Sn$ layers. Titanium's positive impact amounts to increasing the superconducting layer thickness as well as decreasing or completely eliminating the grain anisotropy in the layer. The mean grain size in the $Nb_3Sn$ layer is 62 nm. Figures 11; tables 3; references 9: 1 Russian, 8 Western.

## High-Temperature Oxidation of Ti-Nb Alloys

*927D0094F Moscow ZASHCHITA METALLOV in Russian Vol 27 No 6, Nov-Dec 91 pp 945-951*

[Article by V.I. Dyachkov, Leningrad State University]

UDC 620.193.5:669.295.5

[Abstract] High temperature oxidations of titanium's alloys with niobium is investigated. To this end, ingots of alloys containing 0.7, 1.8, 4.5, and 8.1% Nb by mass are remelted, fettled, forged, rolled, etched, and annealed while samples cut from the resulting strips are scraped, degreased by ethanol, and annealed in an evacuated twin-walled quartz vial; then alloy oxidation is studied by the precision gravimetric method and the oxidation products are analyzed micrographically and by the methods of metallographic, electron diffraction, and radiographic analyses and their microhardness is measured. The results show that alloying with niobium increases the heat resistance within a 700-1,200°C range, especially at low Nb concentrations, and that the alloy oxidation kinetics within this temperature range are governed by the parabolic, cubic, and Evans law, respectively, depending on the Nb content and the test duration and temperature. An addition of Nb to titanium decreases the scaling rate and increases the oxygen proportion in the diffusion layer and the depth of its penetration. The slope of the temperature dependence of parabolic oxidation rate increases sharply above 1,000°C. Figures 5; tables 2; references 14: 9 Russian, 5 Western.

## Cerium's Effect on Corrosion-Electrochemical Properties and Structure of Cast Ferrite Chromium Steel

*927D0094B Moscow ZASHCHITA METALLOV in Russian Vol 27 No 6, Nov-Dec 91 pp 904-910*

[Article by G.P. Chernova, L.A. Chigirinskaya, Ngo Kuok Long, R.Kh. Zalavutdinov, K.G. Bykov, N.D. Tomashov, Physical Chemistry Institute at the USSR Academy of Sciences]

UDC 620.193.01

[Abstract] The resistance of cast ferrite chromium steel 06Kh18T, inoculated by Ce in the amount of 0.1 and 0.5% of burden mass, to general, intercrystalline, and pitting corrosion in $H_2SO_4$ and HCl solutions, respectively is studied. The dependence of the mean corrosion rate and corrosion potential on the cerium concentration are plotted and the pickling behavior of cast steel with and without cerium is examined under a microscope. The results demonstrate that the resistance of cast chromium ferrite steel to general, intercrystalline, and pitting corrosion increases in proportion to the cerium concentration while the pitting corrosion potential depends on the smelting conditions and the ingot location from which the sample is cut out. Cerium also has a favorable effect on the microstructure of steel by reducing the ferrite grain size and lowering the chromium carbide and titanium sulfide concentration along the grain boundaries. The drawback of steel inoculation by cerium is the increase in the amount of nonmetallic inclusions and their behavior. Depending on the smelting conditions, cerium is unevenly distributed in the ingot and affects the steel's electrochemical properties. It is shown that the longer the metal remains in the molten state after inoculation, the lower the residual cerium concentration in the ingot. Figures 4; tables 1; references 15: 14 Russian, 1 Western.

## Effect of Cr and Admixtures on Electrochemical and Corrosion Properties of Fe-Cr-Al System Alloys

*927D0094C Moscow ZASHCHITA METALLOV in Russian Vol 27 No 6, Nov-Dec 91 pp 911-916*

[Article by N.V. Vyazovikina, N.A. Zhalenko, Yu.A. Kurpanov, A.V. Samelyuk, V.N. Adeyev, V.A. Zhabokritskiy, Institute of Materials Science Problems at the Ukrainian Academy of Sciences]

UDC 620.193.01

[Abstract] The effect of the chromium and admixture concentration on the electrochemical and corrosion properties of commercial ferrite alloys of the Fe-Cr-Al system is investigated. To this end, commercial alloys Kh27Yu5 and Kh15Yu5 and model alloy Kh45Yu5 are smelted in an induction furnace. The chemical composition of the alloys is summarized and their microstructure is studied under an electron microscope; Auger spectra of the fracture surfaces, i.e., grain boundaries, and anode potentiostatic and potentiodynamic curves are plotted. The electrochemical properties are examined in a 0.5 M solution of $H_2SO_4$; an analysis demonstrates that the alloys display a tendency toward localized corrosion. The conclusion is also drawn that chromium's effect on the electrochemical properties is dominant and that as the chromium concentration increases, the alloys' tendency to passivation in 0.5 M $H_2SO_4$ and 3% NaCl solutions rises. Various admixtures and excess phases decrease the corrosion resistance of commercial alloys in the passive state compared to the model alloy of the corresponding compositions. Figures 4; tables 2; references 12: 10 Russian, 2 Western.

## Surface Treatment and Electrochemical Characteristics of Rapidly Quenched Zr Alloy

*927D0094D Moscow ZASHCHITA METALLOV in Russian Vol 27 No 6, Nov-Dec 91 pp 917-921*

[Article by V.B. Yakovlev, V.I. Chicherina, Yu.K. Kovneristyy, Ye.A. Trofimova, K.V. Volkov, E.K. Osipov]

UDC 620.193:539.213.2

[Abstract] The effect of the chemical composition and structural state on the electrochemical properties of rapidly quenched alloys (BZS) and the difference between the properties of the surface and internal layers and the free and contact sides of the rapidly quenched alloy strip are discussed; the effect of the surface treatment on the electrochemical properties of rapidly quenched zirconium alloys is investigated. To this end, a 2-7 mm thick strip of the Zr48Ti46Si6 alloys with a 30-70 μm thickness is made by rapidly spinning the melt in an inert atmosphere in a copper drum. The alloy's electrochemical characteristics are analyzed by plotting potentiodynamic polarization and potentiodynamic pulse (PDI) curves in solutions of 5 M $H_2SO_4$ and 0.5 M $H_3PO_4$ after different types of surface treatment at room temperature and comparing them. Three types of treatment are used—simple degreasing, electrolytic polishing, and ultrasonic (UZ) purification in alcohol. The element distribution in the alloy depth is determined by Auger analysis before and after electropolishing. The results show that the electrochemical characteristics do not differ statistically, so the above electrochemical surface treatment techniques are not sensitive to the alloy structure within the amorphous-microcrystalline range of states. Figures 2; tables 1; references 15: 12 Russian, 3 Western.

## Effect of Phase Composition on Corrosion Properties of Mg-Y System Alloys in Neutral Solutions

*927D0094E Moscow ZASHCHITA METALLOV in Russian Vol 27 No 6, Nov-Dec 91 pp 922-926*

[Article by V.V. Krasnoyarskiy, L.M. Petrova, T.V. Dobatkina, I.G. Korolkova, Physical Chemistry Institute at the USSR Academy of Sciences]

UDC 620.193.01

[Abstract] The effect of the phase ratio on the corrosion rate of Mg-Y alloys is discussed and an attempt is made to determine the dependence of the magnesium alloy dissolution rate on the phase composition. To this end, the effect of the phase composition of binary Mg+8.2% Y alloys on the corrosive dissolution is investigated. The microstructure of the alloy in the cast and annealed state is examined under an NU-2E microscope and the surface structure is ana'yzed in the elastically reflected electron beam using a "Camebax micro beam" analyzer; the sections are polished with the help of an "Elipovist" unit. The results show that changes in the binary alloy phase composition have little effect on the corrosion rate in neutral solutions while the dissolution occurs gradually and without pitting. During the galvanostatic anode polarization, the alloy phase composition noticeably affects the dissolution rate only after pitting develops; an increase in the two-phase (DF) alloy self-dissolution rate during pitting is due to the significant cathode effect of the intermetallic phase ($Mg_{24}Y_5$). Figures 5; tables 1; references 5.

## Inhibiting Zn Corrosion in Primary Cells Without Using Hg Compounds

*927D0094G Moscow ZASHCHITA METALLOV in Russian Vol 27 No 6, Nov-Dec 91 pp 952-956*

[Article by I.S. Pogrebova, G.I. Dremova, L.Ye. Sribnyy, A.A. Babich, V.T. Fomin, L.I. Antropov, Kiev Polytechnic Institute]

UDC 621.352.1

[Abstract] The advantages of Mn-Zn chemical electric energy sources (MTsKhIT) with salt electrolytes vs. the negative impact of mercury chloride contained in them are discussed; consequently, attempts are made to avoid using mercury compounds in primary cells or substitute them with other substances. Mercury-free Mn-Zn primary cells were developed on the basis of regular type 373 Orion M salt and the corrosion indices of zinc electrodes and their electrode potential, the cell discharge time, initial voltage, and short circuit current were measured and used as diagnostic variables. The cells were made at the Sirius Scientific Production Complex in Klaipeda. The zinc anode corrosion in chloride salt electrolytes is examined and the dependence of the zinc anode self-discharge rate as a result of its corrosion on the storage duration and the dependence of the initial voltage on the storage duration are plotted. The development of various corrosion inhibitors with substitute mercury chloride is reported and the results of corrosion tests in the presence of various inhibitors are summarized. Discharge curves of the Orion M batteries after a 12-month storage period are plotted and the effect of combined corrosion inhibition agents (ID) on the zinc anode self-dissolution rate is examined. The characteristics of the new mercury-free storage cell containing new corrosion inhibitors are analyzed and found to be in conformity with TU 16-729 and TU 125-78; the anticipated environmental impact of mercury substitution is close to 500,000 rubles. Figures 3; tables 2; references 8: 6 Russian, 2 Western.

## Degradation of Decorative and Protective Properties of Polymer Coats on Roll-Formed Steel Sections in Maritime Atmosphere

*927D0094H Moscow ZASHCHITA METALLOV in Russian Vol 27 No 6, Nov-Dec 91 pp 993-1004*

[Article by Yu.M. Panchenko, P.V. Strekalova, L.V. Markina, Physical Chemistry Institute at the USSR Academy of Sciences]

UDC 620.193.01

[Abstract] The results of two 5-year full-scale tests of four types of polyvinyl chloride film coats on roll-formed steel section in open air and in a semi-enclosed atmosphere inside rooms with louver walls are presented. The tests of 100-120 μm-thick films were conducted in the moderately cold, temperate humid, and warm humid climate on the coast of the Barents, Black and Japan Seas whereby the state of the coats was evaluated after various exposure lengths by the deterioration of their decorative (luster and color) and protective properties. The decorative properties deteriorate at the fastest pace in the subtropical and temperate humid climate with an elevated sea salt concentration in the air and strong solar radiation. In the semi-enclosed atmosphere, the protective properties after a 5-year exposure can be regarded as good or satisfactory for the NGS and DPO-15 PVC film and poor for the PLKhV-122 film. The full-scale tests conducted on the open coast and in semi-enclosed atmosphere reflect the true PVC film behavior on steel as a function of the weather factor variability and the level of air contamination with the sea salt. It is speculated that without frequent condensation of moisture on the metallic surfaces, the minimum service life of the above films indoors is at least 8-10 years. Figures 3; tables 3; references 2

## Development of Corrosion-Resistant Surface Layers on Ti by Successive Si and Pd Ion Implantation Into It

*927D0094I Moscow ZASHCHITA METALLOV in Russian Vol 27 No 6, Nov-Dec 91 pp 1014-1017*

[Article by N.D. Tomashov, O.A. Zhiltsova, R.Kh. Zalavutdinov, A.Ye. Gorodetskiy, M.I. Guseva, B.G. Vladimirov, Physical Chemistry Institute at the USSR Academy of Sciences]

UDC 620.193.01

[Abstract] The superior corrosion-resistance qualities of metal-like titanium silicides are discussed and an attempt to develop corrosion-resistant surface silicide layers on a titanium base by direct implantation of silicon ions into titanium are reported; the possibility of increasing the protective life of the resulting layers by additionally doping them with palladium ions is studied. Potentiometric anode and cathode polarization curves are plotted and the behavior of Ti irradiated by $Pd^{2+}$ and $Si^{+}$ ions in a 20% $H_2SO_4$ is investigated. It is shown that the joint effect of the palladium and silicon ions is not additive; palladium on the Ti surface substantially lowers the cathode hydrogen liberation reaction overvoltage and ensures stable titanium base passivation in the pores and other silicide layer discontinuities. Thus, the protective action of titanium silicides is complemented by electrochemical protection by palladium; as a result, the service life of titanium surfaces thus treated increases by more than twofold compared to titanium doped with palladium ions alone. In less corrosive media, the double protection effect may be even greater and may extend the service life by an order of magnitude, i.e., to 3-4,000 hours. Figures 2; tables 1; references 9: 8 Russian, 1 Western.

## Corrosion Behavior of Porous Iron Silicate Material

*927D0094J Moscow ZASHCHITA METALLOV in Russian Vol 27 No 6, Nov-Dec 91 pp 1022-1024*

[Article by V.D. Glukhovskiy, R.F. Runova, E.V. Kryatchenko, A.B. Yamenko, Kiev Civil Engineering Institute]

UDC 666.973.6

[Abstract] The effect of lamination, shrinkage, and increased porosity which accompany the compaction and roasting of powder metallurgy products on their quality and operating properties is discussed and the corrosion behavior of porous iron silicate materials used in seals of pumps for slightly alkaline mortar is investigated electrochemically by plotting the anode and cathode polarization curves in a NaOH solutions with pH=7-13 with the help of a P-5827 potentiostat. The study shows that the corrosion potential of the composite material in a diluted electrolyte with pH = 9.5 is less negative than that of iron, thus arresting its anodic dissolution, and leads to the conclusion that a composite combination of iron powders and unused silicates in combination with thermal compaction, making it possible to use the resulting material efficiently in a weak alkaline medium. Figures 1; references 6

## Effect of Fire-Proofing Polyethylene Components on Corrosion in Steel

*927D0094K Moscow ZASHCHITA METALLOV in Russian Vol 27 No 6, Nov-Dec 91 pp 1045-1050*

[Article by A.M. Dorfman, V.I. Mikhaylov, N.V. Semakina, V.I. Kodolov, V.I. Povstugar, Izhevsk Mechanical Institute]

UDC 620.193:678.742

[Abstract] The relative advantages of fire retardants which decrease the combustibility of polyolefins vs. the corrosive effect of fireproof coats on the metallic base are

discussed and secondary polyethylene containing carbonyl and hydroxyl groups with a total saponification number of 26.6 mg/equiv KOH/g modified by a fire-retardant system is investigated; the fire-retardant system is produced from an alkyl resorcin epoxy resin (ARES). Steel 20's cathode and anode polarization curves in various fire-retardant solutions are plotted and the characteristics of these solutions are summarized. The mass loss and corrosion rate of steel 20 in these solutions are examined and the conclusion is drawn that oxidized polyethylene containing 1-17% of fire-retardant composition by mass can be used in contact with steel structures; it is recommended however that the concentration of this fire-retardant composition be kept under 14% in order to prevent the possibility of corrosion. Figures 2; tables 1; references 8.

## On Equalizing Copper Electrodeposition in Narrow Hole in Electrolyte Flow

*927D0094L Moscow ZASHCHITA METALLOV in Russian Vol 27 No 6, Nov-Dec 91 pp 1032-1034*

[Article by M.I. Savelyev, S.S. Kruglikov, M.M. Yarlykov, Ye.V. Braun, A.N. Menglishev, Moscow Chemical Engineering Institute imeni D.I. Mendeleyev]

UDC 621.357.7

[Abstract] The nonuniformity of electrolytic precipitation of metal in narrow through holes due to a number of factors is discussed and an attempt is made to demonstrate that sufficient copper distribution uniformity in deep through holes with a small diameter in conventional processes may be attained only at a very low current density. In the study, the electrolyte flow rate is manipulated and the copper distribution is measured by transverse section metallographic specimens. The effect of the relative copper-plating thickness in the middle of the hole on the electrolyte flow rate is measured and plotted at various current densities. An analysis of the data leads to the conclusion that by using electrolytes with a high scattering ability, e.g., modified by "Moscow Chemical Engineering Institute (MKhTI)" agents, for copper-plating deep through holes with a small diameter, one can produce galvanic deposits which are highly uniform in thickness at relatively high electrolytic precipitation rates with a forced electrolyte flow. Figures 1; tables 3; references 3: 2 Russian, 1 Western.

## Electrochemical Heterogeneity and Corrosion Resistance of Ti-Zr Welded Joint

*927D0094A Moscow ZASHCHITA METALLOV in Russian Vol 27 No 6, Nov-Dec 91 pp 898-903*

[Article by S.G. Polyakov, A.B. Goncharov, L.M. Onoprenko, O.D. Smiyan, Electric Welding Institute imeni Ye.O. Paton at the Ukrainian Academy of Sciences]

UDC 620.193.4

[Abstract] Since the corrosion resistance and mechanical properties of welded Ti-Zr joints largely depend on the properties of the heat-affected area (ZTV), the fusion zone, and the weld itself, the electrochemical behavior and corrosion resistance of dissimilar argon arc welded joints of the N-2.5 Zr alloy (with 2.5% Nb) with the VT1 technical titanium are investigated; in so doing, the weld's electrochemical heterogeneity is examined by measuring the potential distribution on the surface and galvanic currents and plotting the polarization of various weld zones in $H_2SO_4$, HCl, and $CH_3COOH$ solutions of various strengths at different temperatures. An analysis demonstrates that electrochemical heterogeneity of the weld accelerates the cathode process on the weld and the anode process along the fusion line on the titanium side which are characterized by the highest hydrogen absorption by the metal and corrosion failure, respectively. In the experiment, tubes are welded to the tube plates in a heat exchanger and are tested by the above method. A heat exchanger inspection after 15,000 hours of operation revealed no traces of corrosion or other fractures, thus confirming the possibility and efficiency of making commercial Ti-Zr chemical devices. Figures 3; tables 3; references 4: 3 Russian, 1 Western.

## The Effect of Surfactants on the Electroerosion Process

*927D0046A Kishinev ELEKTRONNAYA OBRABOTKA MATERIALOV in Russian No 3, May-Jun 91 (manuscript received 22 Oct 90) pp 16-18*

[Article by E.T. Abdukarimov, V.G. Krakov, and R.M. Rustamov, Electronics Institute imeni U.A. Arifov, UzSSR Academy of Sciences, Tashkent]

[Abstract] The authors of the study examined the effect of surfactants on the electroerosion process. Specifically, they studied the electroerosion machining of three current-conducting materials, i.e., M1 copper, L-63 brass, and 12Cr18Ni10Ti stainless steel, in an active medium containing a surfactant additive. The studies were performed on an experimental electroerosion unit equipped with an RC-generator with a no-load voltage of 120 V, a discharge capacitor capacitance of 130 μF, a pulse discharge energy of approximately 0.5 J, a pulse frequency of 500 to 2000 Hz, and an automatic system to track the gap between the electrodes and the combination electrode-tool. Tap water with a 40% solution of $[C_{12}H_{23}NC_5H_5]^+HSO_4^-$ was used as the active medium. The tap water and surfactant were mixed in a tank under high pressure at room temperature for 10 minutes. The resultant dielectric medium was used for electroerosion broaching of holes drawn under a pressure of 3 to 5 kgf/cm$^2$. A type A1-252 profilograph-profilometer was used to study the effect of the said surfactant on the properties of the machined metal. Those specimens that were machined in ordinary water were found to have a characteristic, very developed surface consisting of solidified burrs of the melted metal. As the concentration of

surfactant in the water was increased, the height of the irregularities dropped sharply, the pore diameter decreased, and the overall microrelief of the specimen surface became smoother. A surfactant concentration of about 0.06% by volume was found to result in the minimum degree of surface roughness. Broaching time was also found to increase as surfactant concentration was increased. A surfactant concentration of 0.04% was found to result in the highest process productivity regardless of material machined. The rate of increase in process speed when surfactant-treated water was used turned out to be approximately 37% regardless of the individual material in question. As the process concentration increased, the relative consumption of the electrode-tool ($\gamma$) began to decrease slowly and reached a minimum at a surfactant concentration of 0.04% (after which point it began to slowly increase again). Figures 6; references 4 (Russian).

## Iron Melt Properties and Structure

*927D0097A Moscow STAL in Russian No 10, Oct 91 pp 13-17*

[Article by G.N. Yelanskiy, V.A. Kudrin, Moscow Metallurgical Continuing Education Institute]

UDC 621.186.12

[Abstract] The physical properties and structure of pure iron melts in which the total concentration of 39 known impurities reaches 0.04794% are investigated and the resulting data are statistically processed. The density, kinematic viscosity, viscous flow activation energy, surface tension, and magnetic susceptibility of Fe-C melts as a function of the temperature and carbon concentration is plotted and the structure of the short-range order of Fe-C melts is examined; in addition, polythermal density curves of steel 40Kh and 25KhGT, the dependence of density of steel 40Kh and 25KhGT on the blast duration, and the dependence of kinematic viscosity of steel 40Kh and 25KhGT on the blast duration are plotted. An analysis of a range of physical properties of iron, Fe-C alloy, and steel melts reveals an anomaly on the density polytherm of molten iron which is attributed to a transition of the short-range low-temperature BCC-like melt structure to a statistical structure of superheated melts. The physical properties change nonmonotonically with the carbon content due to a gradual transition of the short-range melt order from BCC-like to FCC-like. A study of the short-range order structures shows that argon-blasting of the steel in the ladle increases the microhomogeneity of the melt and improves the steel quality; the optimum blasting duration is 6 min. Figures 7; references 8.

## Local Dust Removal in Charging Troughs of Sinter Cake and Blast Furnace Sections

*927D0097I Moscow STAL in Russian No 10, Oct 91 pp 80-81*

[Article by Ye.S. Makarenko, E.Ya. Livshits, O.G. Litvinova, Energostal Scientific Production Association]

UDC 669.1.015.7.074

[Abstract] The negative impact of the dust fractions released during the transfer of ore, concentrates, limestone, sinter cake, and pellets, especially the fractions with a particle size from under 5 to 60 μm prompted an attempt to develop local dedusting techniques. A method of reducing the dust exhaust in the lump material transport sections, including the sinter cake charging troughs in the blast furnace section, developed at the Energostal Scientific Production Association is described. The method makes it possible to reduce the dust exhaust along the entire sinter charging path or its long sections. A block diagram of the sinter cake transport system is cited and its operation is examined. The method involves pneumatic separation by means of plenum and exhaust ventilation systems and is capable of removing virtually 100% of all dust particles with a size of ≤300 μm. The method is efficient regardless of the sinter transport system length and its complexity or the possibility and installation conditions of aspiration suction systems. Figures 1; references 2.

## Comprehensive Methods of $NO_x$ Neutralization in Reheating Furnaces

*927D0097H Moscow STAL in Russian No 10, Oct 91 pp 78-80*

[Article by A.V. Aksenov, I.I. Ionochkin, A.G. Zenkovskiy, Moscow Metallurgical Continuing Education Institute]

UDC 621.783.2:662.95

[Abstract] The urgency of reducing toxic nitrous oxide discharges into the atmosphere in order to improve the air quality prompted efforts to develop comprehensive methods of $NO_x$ neutralization in reheating furnaces; simple and comprehensive nitrous oxide neutralization methods developed and tested at the Moscow Metallurgical Continuing Education Institute for natural gas-burning reheating furnaces are summarized. The methods are based on the theoretically proven possibility of decreasing the duration of the combustion product stay in the high-temperature flame zone, equalizing the flame's temperature pattern while maintaining its thermal energy, and enhancing the convective heat transfer from the flame to the screen surfaces. The results of preliminary studies conducted in fire test benches of the "Serp i Molot" Plant confirm the efficiency of the methods. The effect of the screen material and design on the oxidation process is examined and the effect of the screen perforation on the nitrous oxide yield and the nitrous oxide neutralization efficiency are plotted. Test data and the experimental results reveal the simplicity and reliability of the above comprehensive methods, moreover, the use of pulsating burners in a furnace with a perforated screen considerably increases the neutralizing action and improves the furnaces' ecological indicators. Figures 2, references 6.

## New Bearing Steel Compositions With Specified Hardenability

*927D0097G Moscow STAL in Russian No 10, Oct 91 pp 62-65*

[Article by B.K. Ushakov, V.N. Yefremov, V.V. Kolodyazhnyy, V.I. Skryagin, L.G. Dub, Moscow Metallurgical Continuing Education Institute and State Bearing Plants Nos. 8 and 9]

UDC 669.14.018.24

[Abstract] New compositions of steel ShKh4 developed for the raceways of railroad journal box bearings under

the leadership of K.Z. Shepelyakovskiy and their hardenability limitations are discussed and the need to improve steel ShKh4 and select new compositions in order to decrease its hardenability is identified; this need prompted an analysis of the effect of the chemical composition of steel ShKh4 on its hardenability. The study was carried out in a lab using more than 200 commercial smeltings from the Chelyabinks Integrated Iron and Steel Works and Dneprospetsstal Plant. Most of the analyses involved raceways made at GPZ-8 and GPZ-9 whereby the samples were heat treated by the methods which approximate the bearing plant technology to the utmost. The effect of the nickel and chromium composition on the hardenability of steel ShKh4 is examined and the effect of nitrogen and aluminum concentration on this parameter of steel ShKh4 is plotted. An alignment chart is drawn for determining the hardened layer thickness in raceways with a varying wall thickness as a function of steel ShKh4 hardenability. The studies indicate that within a 0.7 to 1.0% range, the carbon concentration has little effect on hardenability, provided that all other components remain unchanged, while an increase in the chromium concentration from 0.2 to 1% increases the hardenability of steel ShKh4. Nickel has the greatest effect on hardenability, prompting a recommendation that its concentration be maintained below 0.10%. Optimum composition ranges and applications of steel ShKh4 with various component ratios are proposed. Several pilot smeltings of steel with the proposed compositions demonstrate that its critical hardenability rate is 230-400 K/s. Figures 2; references 3: 2 Russian, 1 Western.

## Proportionate Strip Coating With One-Sided Current Supply

*927D0097F Moscow STAL in Russian No 10, Oct 91 pp 46-48*

[Article by S.V. Vilkul, L.Ye. Kuznetsova, V.M. Shmakova, Ye.A. Cherneva, L.P. Sarychev, Magnitogorsk Integrated Iron and Steel Works]

UDC 621.771.23:621.357.75

[Abstract] Proportionate strip coating in making the electrodeposited tin-plate by applying current of varying magnitude to both sides and to one side of a moving strip is discussed and the results of a statistical analysis of the resulting tin-plate are presented. Cathode polarization curves are plotted in a phenol sulfonic tin-plating electrolyte at various surface active substance (PAV) concentrations and the mass of the coat and its standard deviation are summarized. Comparative tests of tin-plate with a proportionate coat produced by the two-sided and the new one-sided current supply method made it possible to determine the coat mass, corrosion in $SO_2$, and porosity. The results indicate that the method of proportionate tin coat application during the making of electrolytic tin-plate by supplying current only to one side of the steel strip at a time is quite promising; the principal conditions for implementing the method are as follows: using an electrolyte with 20-25 g/l of surface active agents with a high dispersing ability and ensuring the optimum anode series/steel strip width ratio of 1.2. The proportionate coat produced by the mew method displays satisfactory corrosion-resistance properties and a considerably smaller mass. Figures 1; tables 2; references 3.

## Steel Smelting Characteristics of 200-Ton Electric Furnace With Water-Cooled Roof

*927D0097E Moscow STAL in Russian No 10, Oct 91 pp 27-28*

[Article by A.S. Morozov, O.M. Sosonkin, M.V. Yevdokimov, V.P. Kirpichenkov, Moscow Metallurgical Continuing Education Institute and Krasnyy Oktyabr Metal Works]

UDC 669.046.54

[Abstract] The characteristics of the water-cooled roof (VOS) of the DSP200 steel-making arc furnace operating at the Krasnyy Oktyabr Metal Works are examined by experts from the Moscow Metallurgical Continuing Education Institute on the basis of more than 1,000 smelting of various brands of steel, including ShKh15, and the results are statistically processed. An analysis of the sulfur and phosphorus removal rates during the smelting of steel ShKh15 in arc furnaces with water-cooled and brick roofs reveals that there is virtually no difference in the smelting process. To examine the skin formation process on the slag surface, the process is simulated in a lab using a Tammann furnace and the change in the specific heat flux with the height over the slag melt surface is examined and plotted. The results demonstrate once again that the technological conditions of the sulfur and phosphorus removal during the steel-making process in an arc furnace with a water-cooled roof differ little from those of an arc furnace with a brick roof despite the considerable process differences; on the other hand, the economic impact from using the water-cooled roof in a 200-ton furnace reaches 150,000 rubles. Figures 2; references 2.

## Microcomputer-Based Prediction of Technical and Economic Indicators of Steel-Making Arc Furnaces

*927D0097D Moscow STAL in Russian No 10, Oct 91 pp 26-27*

[Article by L.Ye. Nikolskiy, Moscow Metallurgical Continuing Education Institute]

UDC 669.187.25

[Abstract] The use of microcomputers in order to expand the arc furnace design and equipment capabilities and estimate the performance indicators of steel-making arc

furnaces is discussed and a BASIC microcomputer program developed at the Moscow Metallurgical Continuing Education Institute which makes it possible to calculate the transformer power for steel-making arc furnaces of varying capacity, the specific electric power consumption, the total smelting duration, and the daily and annual furnace output is described. A flow chart of the analysis algorithm is cited and the effect of the oxyfuel burner (TKG) operation on the technical and economic indicators of a 100 ton steel-making arc furnace with water-cooled wall and roof elements fueled by natural gas is investigated. The program is realized on IBM, DVK-3, and "Mazoviya" microcomputers. Figures 1; tables 2.

## New Method of Extending Arc Furnace Lining Life During Bearing Steel Smelting

*927D0097C Moscow STAL in Russian No 10, Oct 91 pp 24-26*

[Article by A.I. Kosyrev, L.L. Grigoryan-Chtents, O.M. Sosonkin, K.P. Verbitskiy, S.S. Kazakov, Moscow Metallurgical Continuing Education Institute and Dneprospetsstal Metal Works]

UDC 669.187.25

[Abstract] Improvements in the arc furnace smelting process which lead to an increase in the inside wall lining surface temperature necessitated a study of methods of extending the service life of the arc furnace lining under high-temperature conditions. A new electrical condition developed at the Moscow Metallurgical Institute and the Dneprospetsstal Metal Works in order to extend the normal life of arc furnace lining during the smelting of steel ShKh15 or ShKh15SG is described; the method is based on a sinusoidal change in the arc length at any given transformer voltage step. The arc length is manipulated automatically using the arc length control unit (BIDD) which is connected to the control panel or power regulator. The arc length characteristics, the dependence of the lining temperature rise rate on its initial temperature during the arc furnace operation under the original and pulsing arc conditions, and the dependence of the specific electric power demand on the secondary transformer voltage during the furnace operation under the conventional and new pulsing arc conditions are plotted. An analysis of the results shows that the electric furnace operation in the automatic pulsing arc mode helps to extend the service life of the lining from 109 to 146 smeltings and decrease the electric power consumption under a constant temperature condition. Figures 3.

## Increasing Steel Desulfuration Efficiency by Ladle Treatment With Powder

*927D0097B Moscow STAL in Russian No 10, Oct 91 pp 18-21*

[Article by N.A. Smirnov, I.A. Magidson, Moscow Metallurgical Continuing Education Institute]

UDC 669.187.2.046.546.2

[Abstract] A method of increasing the efficiency of steel desulfuration in the ladle by adding a slag-forming calcium mixture or alloy powder to the jet during tapping or adding it with a gas blast is discussed and an equation is derived for calculating the desulfuration rate. The desulfuration degree of this method reaches 89% while the residual sulfur concentration in the metal decreases to 0.002%. Twenty pilot smeltings are performed to examine the phenomenon and their principal characteristics are summarized. The mass transport of sulfur from the metal to the slag and the characteristics of sulfur absorbed by the slag and removed by interaction with calcium vapors are summarized and the sulfur concentration behavior in the melt is plotted. The effect of the blast mixture mass on the specific sulfur mass transport factor is determined and plotted. An analysis of the experimental findings reveals that sulfur and oxygen interact with calcium vapor bubbles during the blasting of powders through the melt while at the same time sulfur is absorbed by the slag phase forming in the bulk of the metal and on its surface, thus raising the desulfuration rate and fullness. The relative mass of sulfur absorbed by the slag phase is proportionate to the mean coefficient of sulfur distribution between the metal and slag during the blasting. It is shown than an addition of aluminum to the silicocalcium powder increases the calcium utilization factor and helps to produce metal with a lower sulfur content. Figures 3; tables 3; references 6: 3 Russian, 3 Western.

## Surface Laser Alloying of Steels and Cast Irons by the Boron Carbide Injection Method

*927D0046D Kishinev ELEKTRONNAYA OBRABOTKA MATERIALOV in Russian No 3, May-Jun 91 (manuscript received 5 Oct 90) pp 25-28*

[Article by A.M. Bernshteyn, Ye.M. Yandimirkin, O.A. Yermakova, and B.B. Somov, Moscow Institute of Steel and Alloys, Moscow]

[Abstract] In an effort to find ways of producing thicker and harder boron layers on steels and cast irons, the authors of the study examined the method of laser-alloying steels and cast irons by boron carbide injection. In their experiments the researchers used specimens of three steels (45, U8, and 4Cr4MoWVSi) and VCh-70 gray cast iron. Specimens measuring 10 x 15 x 50 mm were alloyed by using an LT1-2 continuous-wave laser with a power-flow density of 600 +/- 30 MJ/m$^2$. As an alloying element they used $B_4C$ powder with a dispersivity of 80 to 200 μm. The powder was fed in at a rate varying from 15 to 60 mg/s. The resultant layers were subjected to metallographic and x-ray analyses, and their microhardness was determined. The studies performed revealed that depending on the given alloying conditions, the alloyed layers 1.2 to 1.5 mm deep on specimens of 45 and U8 steel and VCh-70 cast iron may contain iron boride, borocementite [$Fe_3CB$)], a solid solution of B and C in ferrite, and undissolved $B_4C$

particles. Layers produced on 45 steel and U8 cast iron by using an alloying powder feed rate of 60 mg/s were found to have the greatest microhardness (18 to 20 GPa). These layers were shown to have a peritectic structure and to contain an excess $Fe_2B$ phase with inclusions of undissolved $B_4C$ particles. These layers also contained pores and cracks that were mainly due to the high heat stresses arising during rapid cooling owing to the difference in the thermal expansion coefficients of the $B_4C$ particles and the carboboride layer. Reducing the powder feed rate to 30 mg/s resulted in the formation of peritectic layers without the $B_4C$ inclusions. A powder feed rate of 20 mg/s resulted in layers without an excess $Fe_2B$ phase. In the case of the 4Cr4MoWVSi steel, laser alloying resulted in a microhardness of 12 to 18 GPa. The resultant carboboride layers did have a tendency to crack, however. In the case of VCh-70 cast iron, a powder feed rate of 15 mg/s was required for complete dissolution of the $B_4C$ particles. Laser treatment was found to result in the formation of ledeburite structures with a hardness of 12-14 GPa. Tests established that at the said powder feed rate, laser treatment with boron carbide results in the pulverization of the ledeburite. When laser hardening was used, the average thickness of the cementite wafer formed was about 8 μm as opposed to 4 μm after alloying. The tests performed thus confirmed that in the range of process parameters studied, layer alloying results in carboboride layers that are significantly deeper than and at least as hard as diffusion layers. Figures 2; references 4 (Russian).

## The Metal Science Aspects of Creating Combined Products From Refractory Nickel Alloys

*927D0072G Kiev METALLOVEDENIYE I TERMICHESKAYA OBRABOTKA METALLOV in Russian No 12, Dec 91 pp 18-20*

[Article by Ye.N. Rudnitskiy, O.Kh. Fatkullin, V.I. Yeremenko, and L.A. Pravikova]

UDC 62-144:669.245:669.17

[Abstract] One advantage of powder metallurgy is that it can be used to produce combination products consisting of different alloys. The ability to produce combination blanks in turn makes it possible to produce materials that can better meet various temperature-and-force and operating conditions as well as to produce blanks with inserts possessing improved technological properties (including improved machinability and weldability). Because most refractory alloys contain one and the same alloy-forming elements, there is no danger of interface embrittlement due to intermetallides that are not part of the materials being joined as sometimes happens when various metals and ceramics are subjected to solid-phase diffusion joining. Refractory nickel alloys are, however, subject to a variety of factors that may reduce the strength of the grain boundaries between nickel alloys formed during the process of hot isostatic pressing. One such factor is the separation of carbides (mainly TiC) at the interface of the two alloys. Another such factor is separation of the large particles of the γ'-phase. A third factor reducing interface strength is the presence of defects related to bugs in the process used to manufacture the nickel alloys. The first two factors are connected with the nature of the alloys being joined, and their effect cannot be eliminated by modifying the process used to produce and heat-treat blanks. Achieving an interface strength greater than that of one of the two alloys being joined requires selecting matching pairs of alloys or correcting their chemical composition. It has, for example, been demonstrated that the alloy EP698M (which contains ≤0.02% carbon) is advisable for use as an insert in disk blanks made of the heavily doped alloys EP741NP and EP962P. No problems related to achieving a quality interface have been found to occur during combined hot isostatic pressing of two heavily doped granulated alloys (EP962P-EP975P, EP741NP-EP975P). It is also important that the two alloys to be joined be compatible from the standpoint of acceptable heat treatment regimen. The selection of heat treatment conditions for use with combination blanks made of two granulated alloys or a granulated alloy and a casting alloy must be based on the results of a study of the laws governing the mechanical properties of these alloys as a function of the temperatures of their hardening and their first and second stages of aging and as a function of the cooling speed used during the hardening process. The following heat treatment conditions have been shown to result in products with a good set of mechanical properties when used with the heavily doped alloys EP962P, EP741NP, and EP975P: hardening temperature, 1,150 to 1,200°C; temperature during first aging, 850 to 950°C; temperature during second aging, 750 to 850°C; and rate of cooling during hardening, 6 to 6 x $10^3$°C/min. In addition to having good mechanical properties and being highly compatible with the alloys EP962P and EP741NP, the weldable alloy EI698MP (the granule version of EI698M) has also been shown to have a stable grain structure after protracted superheating above temperatures of 120-150°C. Figures 2; references 2: 1 Russian, 1 Western.

## Characteristic Features of Structure Formation During the Manufacture of Disk Blanks From Refractory Nickel Alloys

*927D0072A Kiev METALLOVEDENIYE I TERMICHESKAYA OBRABOTKA METALLOV in Russian No 12, Dec 91 pp 25-29*

[Article by O.N. Vlasova, N.N. Korneyeva, V.I. Yeremenko, O.Kh. Fatkullin, N.M. Semenova, S.N. Petrova, and D.D. Vaulin]

UDC 669.245:621.77:620.186

[Abstract] The authors of the study worked to develop a technology to manufacture disk blanks from the alloys EP962 and EP741NP with high performance characteristics. Specifically, they set out to design a process that would permit the following: 1) production of a structurally uniform disk blank; 2) use the hereditary effect of deformation hardening during final heat treatment; and 3) develop ways of achieving cooling speeds during hardening that would ensure formation of γ'-phase separations with the required dispersivity, as well as the absence of deformations and cracks. The process developed to produce disk blanks from EP741NP consisted of a homogenizing regimen, thermomechanical shaping regimen, and final heat treatment regimen. The homogenizing regimen, actually a homogenizing isostatic treatment regimen, designed has the following process parameters: pressure, 150 to 160 MPa with holding at a temperature of 1,150°C for 4 hours following by holding at 1,210°C for 4 hours, holding at 1,150°C for 4 hours, and holding at 1,100°C for 4 hours. This is followed by a thermomechanical shaping regimen calling for the following: deformation by upsetting at 1,160°C with a degree of deformation of 50% plus upsetting at 1,160°C with a 40% deformation plus recrystallization annealing at 1,180°C for 3 hours plus upsetting at 1,130°C with a deformation of 30% (at the rim of the blank) or 50% (at its center). Final heat treatment in the said regimen includes the following: holding at 1,090°C for 4 hours plus holding at 870°C for 16 hours plus holding at 760°C for 16 hours. A second two-step regimen was also developed for disks made from EP741NP. It calls for homogenizing treatment (consisting of holding at 1,150°C for 4 hours, at 1210°C for 4 hours, at 1,150°C for 4 hours, and at 1,100°C for 4 hours) plus final heat treatment (consisting of holding at 1,130°C for 4 hours plus holding at 1,000°C for 4 hours plus holding at 870°C for 16 hours

plus holding at 760°C for 16 hours). A three-stage process consisting of homogenization, thermomechanical shaping, and final heat treatment was developed for use in manufacturing disk blanks from the alloy EP962. Its homogenization stage calls for homogenizing isostatic treatment at a pressure of 140 to 160 MPa that included holding at the following temperatures (°C) for 4-hour periods: 1,130, 1,200, 1,130, and 1,100. The thermomechanical treatment stage of the process calls for deformation by upsetting at 1,100°C with a deformation of 40% followed by recrystallization annealing at 1,170°C for 4 hours followed by upsetting at 1,100°C with a deformation of 40% followed by annealing at 1,170°C for 4 hours following by upsetting at 1,080°C with a deformation of 30%. The heat treatment stage of the process calls for holding at 1,050°C for 4 hours followed by holding at 780°C for 16 hours, holding at 1,090°C for 4 hours, and holding at 780°C for 16 hours. Figures 5, tables 4; references 2 (Russian).

### The Structure and Mechanical Properties of Refractory Granulated Nickel Alloys

*927D0072D Kiev METALLOVEDENIYE I TERMICHESKAYA OBRABOTKA METALLOV in Russian No 12, Dec 91 pp 8-11*

[Article by V.I. Yeremenko, N.F. Anoshkin, and O.Kh. Fatkullin]

UDC 669.245:621.762:620.17:620.186

[Abstract] The granulated refractory nickel alloys EP741P, EP741NP, EP962P, and EP975P have recently been developed and have begun to be produced. They are intended for use at temperatures up to about 750°C. In their cast state, the said alloys have been demonstrated to include a γ'-phase and type $M_6C$ and MC carbides, as well as eutectic components (as many as three types) based on γ'-phase particles with different chemical compositions and segments of a carbide (carboboride) eutectic. The authors of the study worked to develop a combined hot isostatic pressing and heat treatment process that would allow for the aforesaid distinctions of the new nickel alloys. They conclude that preventing the development of intergrain fractures in the said alloys and the subsequent deterioration of their mechanical and performance characteristics requires the following steps: 1) strict control of granule production and processing to prevent their significant (>0.007% O) oxidation; 2) control of the carbon content in the alloy within the range from 0.02 to 0.08%; and 3) execution of the hot isostatic pressing process while simultaneously heating and exerting pressure on the granules so as to achieve a monolithic material at temperatures lower than the temperature of intensive formation of MC carbides on the free surfaces of the granules, i.e., between 1,000 and 1,050°C. Furthermore, they recommend that a hot medium be used for hardening so as to reduce residual stresses. When high mechanical and performance characteristics are required (as in the case of EP962P), hardening from the single-phase γ-region should be used. The authors also caution that the characteristic temperatures at which secondary carbides may be released during the aging process must be taken into consideration when designing aging regimens. Calculations based on fracture mechanics methods and experimental data led the authors to conclude that defects larger than 400 μm are unacceptable in the alloys EP741P and EP741NP with $\sigma_{0.2}$ = 900-1,000 N/mm$^2$ and that defects larger than 170 μm must not be permitted in alloys such as EP962P with $\sigma_{0.2}$ = 1,100 N/mm$^2$. Figures 7, tables 2; references 3: 2 Russian, 1 Western.

### The Design Strength of Plates of Aluminum Alloys for New-Generation Aircraft

*927D0072I Kiev METALLOVEDENIYE I TERMICHESKAYA OBRABOTKA METALLOV in Russian No 12, Dec 91 pp 23-25*

[Article by G.S. Neshpor, A.A. Armyagov, and V.V. Teleshov]

UDC 669.715:624.046.5

[Abstract] In the coming decades deformable high-strength aluminum alloys will be the main aircraft construction material. The creation of wide-bodied jets with an extended useful life will necessitate the manufacture of intermediate products from aluminum alloys that besides being characterized by high degrees of strength and plasticity, are also characterized by an adequate durability, low rate of fatigue crack formation, and high fracture toughness. This article presents the results of many years of study of the strength and durability of series-produced plates of the following "new-generation" aluminum alloys: 1163T, 1163T7, V96pchT2, V95ochT2, and 1973T2. A table is presented that details the values obtained when each of the aforesaid alloys was subjected to tests to determine its strength, static and cyclic crack resistance, and resistance to low-cycle fatigue. Series-produced plates of 1163T were found to have higher fracture toughness but a lower fatigue crack formation rate than plates of the alloy D16chT. Compared with plates of the alloy 1163T7, plates of the alloy 1163T had lower strength properties and a lower fracture toughness, but also a markedly slower rate of fatigue crack growth. Their strength properties were shown to be better than those stipulated in their respective specifications. Half of the V95pchT2 and V95ochT2 plates tested had fatigue crack growth rates that were even better than the desired level. Plates of the alloy 1163T7 were found to have a fibrous structure with an initial recrystallization stage and between 0.6 and 1.9% intermetallides by volume. Plates of the alloys V95pch, V95och, and 1973 had a partially recrystallized structure, with the V95pch and V950ch containing between 5 and 20% and the 1973 containing about 30%. The total volume fraction of intermetallides in each of the three alloys was about 1%. Figures 3, table 1; references 8 (Russian).

## Structural Distinctions of Ingots of the Alloy EP741NP Produced by the Method of Two-Electrode Vacuum Remelting

*927D0072A Kiev METALLOVEDENIYE I TERMICHESKAYA OBRABOTKA METALLOV in Russian No 12, Dec 91 pp 5-7*

[Article by O.Kh. Fatkullin, G.M. Rakovshchik, O.N. Vlasova, V.I. Yeremenko, G.V. Makhanek, and A.V. Filimonov]

UDC 669.245-154.9

[Abstract] The authors of the study examined the structural distinctions of ingots of the refractory nickel alloy EP741NP produced by the method of two-electrode vacuum remelting on a pilot remelting unit, the VDEP-400, which was developed at the All-Union Light Alloys Institute. The VDEP-400 makes it possible to remelt consumable electrodes up to 250 mm in diameter and 600 mm long into ingots with diameters of 200 to 400 mm. The new remelting unit is equipped with a drive to rotate chill molds at speeds up to 200 rpm and drives to move and turn the consumable electrodes. The new unit was used to remelt consumable electrodes with the aforesaid dimensions that were produced by using one of two techniques: vacuum induction melting + vacuum arm remelting or vacuum induction melting + electroslag remelting. The melting was conducted in built-up chill molds 200 and 300 mm in diameter with automatic maintenance of the length of the arc between the consumable electrode and a liquid-metal bath within specified limits. The electrodes were turned toward one another. The resultant ingots were subjected to homogenizing isostatic pressure treatment and studied both in their poured stage and after homogenization. The following are the main structural flaws discovered in the ingots produced by vacuum induction melting + vacuum arm remelting: significant structural and chemical nonuniformity, presence of large columnar grains and numerous coarse globules of γ-γ' eutectic, and microporosity. These flaws in turn result in the formation of different shapes and sizes of γ'-phase separations within the bounds of a dendrite cell, and this structural irregularity controls all of the processes occurring during subsequent deformation and heat treatment of the said alloys. Using two-electrode vacuum remelting, on the other hand, was found to result in a fine-grained structure. Furthermore, when the two-electrode vacuum remelting technique was used, the refining processes either did not take place at all or else were only slight. The two-electrode technique was also found to result in an isotropic polyhedral grain structure without columnar dendrites and with only small degrees of microchemical inhomogeneity and microporosity. In addition, the γ'-phase separations found were of identical shape and size throughout the cross section of a dendrite cell. The metal was, however, found to have a higher degree of contamination with slag and nonmetallic inclusions and with coarse aggregates of γ-γ' eutectic along the boundaries of the dendrite cells. When two-electrode vacuum remelting was combined with preliminary refining remelting, virtually the only problem remaining was that of microporosity. It too was largely eliminated by homogenizing pressure treatment. Triple remelting using two-electrode vacuum remelting was found to result in alloys with a higher degree of plasticity in their cast state and in better technological properties than are achieved by alternative manufacturing techniques. Figure 1, tables 2.

## Local Liquation in Ingots of the Alloy 1420 and the Structural Inhomogeneity of Intermediate Products

*927D0072A Kiev METALLOVEDENIYE I TERMICHESKAYA OBRABOTKA METALLOV in Russian No 12, Dec 91 pp 3-5*

[Article by A.G. Bratukhin, Yu.M. Vaynblat, and V.G. Davydov]

UDC 669.71'721'884:620.186

[Abstract] In the past few years the weldable alloy 1420 of the system Al-Li-Mg has come to enjoy increasingly wider-scale use in the aviation industry. Because 1420 contains chemically active lithium, the process conventionally used to manufacture aluminum intermediate products must be revised when used with 1420. Difficulties in producing intermediate products from 1420 also stem from the fact that ingots of the said alloy are plagued with the following forms of structural irregularities and defects: macroscopic bands that are more susceptible to etching, snakes, light and dark spots, flux inclusions, and inclusions consisting of the reaction products of the flux and melt. These types of local liquation characteristics of the alloy 1420 are geometrically transformed during the plastic metal working process and are preserved virtually unchanged in intermediate products made from the alloy, thus giving the said intermediate products the same structural irregularities inherent to the starting alloy. All of these particular types of local liquation are discussed herein and attributed primarily to the practice of the use of a protective flux during the process of casting ingots of the alloy 1420. The authors go on to discuss recent research directed toward eliminating the said types of liquation by modifying the technique used to produce type 1420 ingots. Included among the possible modifications mentioned are modification of the flux's composition, changing the way it is added to the crystallizer, developing precision flux-metering techniques, protecting the melt from contact with the argon atmosphere throughout the entire manufacturing process, and reducing the amounts of hydrogen and sodium used in the manufacturing process. Figures 4; references 7 (Russian).

## A Quantitative Analysis of the Intermetallides in the Structure of a Hard Disk's Base

*927D0072F Kiev METALLOVEDENIYE I TERMICHESKAYA OBRABOTKA METALLOV in Russian No 12, Dec 91 pp 14-16*

[Article by V.G. Davydov, B.N. Stepanov, A.A. Koltsova, and Yu.P. Pimenov]

UDC 669.71'721:620.186.12

[Abstract] Both in the USSR and abroad, the bases of the hard disks used to store information in computers are generally made of alloys of the system Al-4% Mg. Up until the mid-eighties, the surfaces of sheets of Al-4% Mg alloys, such as the alloy 1541, were required to have a roughness ($R_a$) of less than 0.02 μm. The grain size established for the said sheets was set at $<30$ μm. The size and quantity of intermetallide particles in the sheets were not controlled. Then, as disk storages designed to hold informat on written with a much greater density (300-600 or more magnetic flux reversals per millimeter of track) began to be produced, stricter requirements began to be established for the process used to manufacture the alloys and disks. Alloys began to appear for which the amount of intermetallides per unit surface in the lengthwise direction of a given specimen is an important quality indicator. In view of this fact, the authors of the study examined the relationship existing between alloy structure and disk coating quality on the one hand and selection of permissible amount of intermetallides by size group on the other. A Kvantimet-720 automatic image analyzer was used for the measurements. During the study, a polished specimen surface was placed in the plane of the sheet or base of the disc at a distance of 0.1 to 0.15 mm from the starting surface. Each specimen was subjected to 10 measurements, and the results were averaged. Several techniques of preparing alloy specimens for testing were compared, including the conventional method of preparing polished microsections for metallographic analysis, diamond turning, preliminary etching in Keller's reagent, and using unetched specimens. On the basis of this comparison the authors concluded that the most stable quantitative estimates of the intermetallides in sheets of type 1541 alloy for use in manufacturing hard disks are obtained by using either unetched specimens or else after subjecting etched specimens to electric polishing in weak electrolytes. Diamond turning was also found to be preferable over other polishing. Further investigation revealed that the structure of sheets obtained from an ingot 165 mm thick was virtually the same as that of sheets obtained from ingots of commercial size (265 to 300 mm), i.e., the maximum size of the intermetallides is between 9 and 11 μm. When ingots 70 mm thick were used, the maximum dimensions of the intermetallides were somewhat less, but most often by no more than 7 to 9 μm. In sheets obtained from a band 17 mm thick cast in an electromagnetic crystallizer and bands 6 to 8 mm thick, the maximum size of the intermetallides was between 5 and 7 μm, and virtually no crushing of the intermetallides during the rolling process occurred. The studies performed led the authors to conclude that quantitative estimation of the intermetallides in the structure of sheets of type 1541 alloy with a stability adequate for practical application is indeed possible. Figure 1, tables 6; references 3 (Russian).

## The Effect of Heat Treatment on the Segregation of Impurities in Pore-Containing Molybdenum

*927D0071C Kiev METALLOFIZIKA in Russian Vol 13 No 9, Sep 91 (manuscript received 10 Jan 91) pp 86-92*

[Article by Yu.V. Milman, Yu.N. Ivashchenko, I.V. Gridneva, I.V. Goncharova, and N.P. Korzhova, Material Science Problems Institute, Ukraine Academy of Sciences, Kiev]

UDC 620.192:621.762.669.28:621.78

[Abstract] The authors of the study studied the segregation of potassium and sulfur impurities in the pores of an alloy consisting of molybdenum and 0.03% carbon. They also studied the effect of heat treatment on segregation of impurity elements. Pores were created in pore-free molybdenum rolled stock produced by the powder metallurgy technique. Specifically, pieces of the rolled stock were welded, and round pores formed in the welds. The small round pores formed contained 0.03% carbon and 0.015% oxygen. Sintered blanks were subjected to forging and rolled into sheets 1 mm thick. The sheets were fused with a nonconsumable tungsten electrode in a helium atmosphere, thus simulating the welding process. The study specimens were subjected to 4 hours of annealing at temperatures ranging from 800 to 2,200°C. At 1,000, 1,500, and 2,200°C the annealing time was varied from 15 minutes to 4 hours. The annealing was implemented in a vacuum of no worse than $10^{-3}$ Pa. The segregation phenomena occurring on the surface of the pores and break were studied by Auger electron spectroscopy. The distribution of impurity elements by depth was studied by recording their Auger electron spectra during the process of argon-beam etching with an energy of 1 keV at an etching rate of 0.015 nm/s. The studies performed demonstrated that the segregation of impurity elements on the pore surface in molybdenum is significantly and nonmonotonically dependent on the temperature of the prior annealing. Specifically, the segregation phenomena are due to the structural and (possibly) phase changes occurring during annealing, and those annealing temperatures that resulted in the maximum segregation of impurities in the pores were approximately coincident with the temperatures of maximal segregation on the grain boundaries. The segregation of carbon and oxygen in the pore surfaces was found to be slightly greater than its segregation on the grain boundaries. The segregation of potassium and sulfur in the pores was much greater than that on the intercrystallite surfaces. Potassium tended to segregate on pore surfaces much more than on other crystal-structure defects. This finding made it possible to refine the effect

mechanism of potassium additives on the properties of wire made of refractory metals (molybdenum and tungsten). Halos around pores representing a layer of of potassium of close-to-monatomic thickness and 10 to 30 μm in diameter were discovered on the surface of the breaks passing through pores with a high potassium segregation. The formation of these halos was deemed a consequence of the flowing of potassium form the pores by means of surface diffusion at an anomalously high speed. Figures 5; references 10: 8 Russian, 2 Western.

### The Effect of a Copper Additive on the Properties of the Alloy 01970

*927D0072E Kiev METALLOVEDENIYE I TERMICHESKAYA OBRABOTKA METALLOV in Russian No 12, Dec 91 pp 12-13*

[Article by V.V. Zakharov, T.D. Rostova, I.A. Fisenko, V.E. Silio, V.S. Yevstifeyev, and N.S. Serova]

UDC 669.715'5'721'3

[Abstract] The authors of the study examined the effect that a copper additive in amounts exceeding 0.2% has on the properties of the Al-Zn-Mg weldable alloy 01970. Such amounts of copper have previously been demonstrated to increase the incidence of crack formation in Al-Zn-Mg alloys. In the study reported here, the authors tested the previously published suggestion that this effect of copper additives be compensated for by also adding a complex modifier consisting of scandium, zirconium, and titanium. Another problem associated with copper additives addressed in the study was that of the formation of a W-phase containing copper, scandium, and aluminum when the ingots are poured. After a phase diagram analysis, the authors concluded that up to about 1.5% Cu could be added to the Al-Zn-Mg alloy 01970 without any danger of formation of a W-phase regardless of how much scandium was added. The experiments performed established that up to 0.5% Cu may be added to the alloy 01970 without impairing its good combination of strength and plasticity properties provided that a strong scandium-containing modifier is also added. Comparisons of 01970 plates to which 0.24 and 0.34% copper was added revealed that the plates with 0.34% copper were more resistant to corrosion under stress than were the plates containing only 0.24%. Both sets of plates had a good mix of strength and plasticity properties and high fracture toughness and low-cycle fatigue resistance parameters, however. Figures 3, table 1; references 5 (Russian).

### The Electric Conduction and Thermoelectromotive Force of FeZr and NiZr Amorphous Alloys

*927D0071B Kiev METALLOFIZIKA in Russian Vol 13 No 9, Sep 91 (manuscript received 21 Feb 91; after revision 1 Jul 91) pp 18-27, 78*

[Article by I.Kh. Khalilov, S.A. Ninalalov, and M.M. Gekhtman (Jr.), Dagestan Polytechnic Institute, Makhachkala, Dagestan affiliate, Energoinformatika SNPP (not further identified), Makhachkala, and Geothermy Problems Institute, Dagestan affiliate, USSR Academy of Sciences, Makhachkala]

UDC 539.2

[Abstract] The authors of the study worked to calculate and construct a theory of the electric conduction and thermoelectromotive force of $Fe_xZr_{1-x}$ and $Ni_xZr_{1-x}$ amorphous alloys. They did so by using the results of a calculation of the electron structure of amorphous alloys of transition metals in an approximation of a coherent locator with consideration of nondiagonal disorder. Electric conduction was calculated on the basis of several models. The results obtained based on the model using integration throughout the Brillouin zone turned out to conform best to data obtained by experimentation. In the case of the alloy NiZr, the discrepancy between the calculated and experimental results did not exceed the error of the experimental determination of electric conduction. The calculation results obtained by using an isotropic model were not as good as those obtained from calculating velocity based on interaction throughout the Brillouin zone. This fact was compensated for by the comparative simplicity of the isotropic model-based method, however. The authors also calculated thermoelectromotive force based on the Faber-Ziman model and in an approximation of a coherent locator. The sign of the thermoelectromotive force for the alloy FeZr was found to be positive throughout the entire range of component concentration variations examined, whereas in the case of NiZr the sign changes when $x > 84\%$ (atomic). Curves of the concentration dependences of the resistance anisotropy and relationship of the different spin directions of the study ferromagnetic alloys were also plotted. In the case of $Ni_xZr_{1-x}$, the ratio of downward to upward spin was found to be weakly dependent on the direction of spin and to approximate 1 in the concentration range of $x = 50$ to 90% (atomic). In the case of the alloy FeZr, the said relationship was found to change slowly in the concentration range from 50 to 75% (atomic) and to increase when $x > 75\%$ (atomic) Fe. The authors thus managed to demonstrate that the approach of approximation of a coherent locator with consideration for nondiagonal disorder is a reliable basis for investigating the kinetic properties of amorphous alloys. Figures 5, references 31: 9 Russian, 22 Western.

### The Effect of Low-Temperature Heating-Cooling on Heat Expansion of Commerical-Grade Beryllium

*927D0071E Kiev METALLOFIZIKA in Russian Vol 13 No 9, Sep 91 (manuscript received 16 Jun 91) pp 119-124*

[Article by F.F. Lavrentyev, V.P. Popov, I.V. Gektina, O.V. Matsiyevskiy, and Yu.P. Khimich, Physics Technology Institute of Low-Temperatures, Ukraine Academy of Sciences, Kharkov]

UDC 539.2

[Abstract] The authors of the study examined the temperature dependence of the coefficient of thermal expansion of commercial-grade beryllium on cycles of low-temperature heating and cooling. Commercial-grade polycrystalline beryllium with an impurity content of about 1.2% was produced by the method of hot uniaxial pressing of powder with grain sizes ranging from 40 to 50 μm. The test specimens of commercial-grade beryllium used were in the form of cylinders 3 mm in diameter and 140 mm long. The axis of the specimens was oriented perpendicular to the pressing axis. A precision dilatometer and method described elsewhere were used for precise determination of the coefficient of thermal expansion. The determination error did not exceed +/-2 x $10^{-7}$/K at temperatures below 60 K and +/-5 x $10^{-7}$/K at temperatures between 60 and 300 K. A differential method relative to pure aluminum was used to measure the changes in the length of the study specimens. The studies performed revealed that the reduction in a test specimen's temperature during cooling occurs unevenly. The kinetic curve plotted for the temperature change occurring when a specimen is cooled during the first measurement cycle contained a number of sharp bends. The first appeared at about 100 K. Between 100 and 300 K the curve was smooth. A nonmonotonic change in specimen length as the temperature decreased was also discovered. Throughout the entire interval of temperatures below 100 K, the segments of the dilatogram where the slope of d/dT(ΔL/L) was either a negative or zero slope corresponded to those segments of the kinetic curve that had a small slope. Both these facts were explained within the framework of the hypothesis that the main reason for the structural and size stability of commercial-grade powder beryllium is the occurrence and development of twins in favorably oriented grains under the effect of internal streses occurring as the specimens' temperature changed. Two competing mechanisms were found to contribute to the change in specimen length that occurred as the temperature decreased: 1) a lattice mechanism that results in a regular decrease in specimen length and 2) a deformation mechanism that involves a "restoration" of the specimen's length due to twinning. The average magnitude of the deformation characterizing the separate act of "restoration" of a specimen's length as the temperature decreases was found to gradually decrease from about 10 x $10^{-6}$ in the range from 80 to 100 K to about 5 x $10^{-6}$ at 10 K. The three cycles of measurements taken indicated that the structure of commercial-grade beryllium stabilizes primarily during the first thermal cycles. Figures 3; references 10: 8 Russian, 2 Western.

## A 190,000 rpm Low-Power Magnetic Rotor

*927D0071A Kiev METALLOFIZIKA in Russian Vol 13 No 9, Sep 91 (manuscript received 23 Sep 91) pp 11-17*

[Article by V.V. Nemoshkalenko, A.A. Kordyuk, V.F. Los, A.D. Morozovskiy, B.G. Nikitin, and V.A. Rafalovskiy, Metal Physics Institute, Ukraine Academy of Sciences, Kiev]

UDC 537.312.62

[Abstract] A new self-stabilizing magnetic rotor has been developed. The new rotor, which is mounted on superconducting bearings made of $YBa_2Cu_3O_{7-\delta}$, rotates at a rate of about 79,000 rpm in air and about 190,000 rpm in a vacuum of about 1 Pa. It has a power requirement of about 3.1 mW. The new rotor has a number of advantages over conventional rotors, including its capability of self-stabilization while rotating, its quick damping of nutation vibrations while turning, and the low energy capacity of its suspension system. The authors of the study examined the energy losses occurring when the magnetic rotor interacts with air at various pressures, with a superconductor, and with a ferromagnetic magnetically soft amorphous powder material. They also determined selected physical parameters determining the interaction between the magnetic rotor and the medium in which it is located for the rotation frequency range from 0 to 2000 Hz. The Q-factor of the new rotor was estimated at $2\pi W_0/W = 4\pi^2 I\omega^2$ ($\omega$ being the rotor's rotation frequency and $W_0$ being the rotor's energy margin at a rotation frequency of 2000 Hz). The hysteresis energy loses of the new rotor were estimated at 1.76 x $10^{-5}$ J, which conforms to the previously published figure of Q = 4.5 x $10^4$. Figures 3; references 14: 10 Russian, 4 Western.

## The Temperature Dependence of the Young Modulus of Titanium Carbide and Eutectic Alloys of Chromium With Titanium Carbide

*927D0071D Kiev METALLOFIZIKA in Russian Vol 13 No 9, Sep 91 (manuscript received 24 Jan 91) pp 114-118*

[Article by T.V. Golub, V.G. Ivanchenko, and O.N. Kashevskaya, Metal Physics Institute, Ukraine Academy of Sciences, Kiev]

UDC 669.26'295'784.539.2

[Abstract] Published reports have shown that a eutectic-type quasi-double break exists between the chromium and titanium carbide in alloys of the system Cr-Ti-C and that its position does not coincide with the Cr-TiC connecting line. Rather, this break is shifted to the region of high titanium concentrations and is located on the ray $Cr_{0.969}Ti_{0.031}$-$TiC_{0.82}$. The alloys located on this ray possess rather high strength properties all the way to temperatures of 1,000°C. The authors of the study conducted a series of experiments to determine the temperature dependences of the normal elasticity moduli of the said alloys and to determine whether the concentration dependence of the modulus is subordinate to the rule of additivity within the bounds of the two-phase region examined. The alloys used in the studies weighed 70 g and were produced by melting in a copper-cooled crucible in an atmosphere of purified argon in a laboratory electric arc furnace with a nonconsumable tungsten electrode and molding in a copper chill mold. ItM-1 yttrium in the amount of 0.35% (mass) was used as a

deoxidizing agent. The temperature dependences of the Young moduli of the test specimens were determined by the acoustic method, which is based on the interconnection between the modulus of normal elasticity, the specimen's natural vibration frequency, and its geometric dimensions and mass. Calculations for measurements taken in the temperature range from 20 to 750°C indicated that at temperatures between 20 and 130°C, the Young modulus of the the study alloys decreases. This decrease in the said temperature range was found to be slower than that occurring at higher temperatures. The experiments also indicated that doping chromium with titanium causes the Neel temperature to decrease and, consequently, causes the maximum on the curve plotted for the temperature dependence of the elasticity modulus to shift to the range of lower temperatures. The slow change in the study specimens' Young modulus observed at 20 to 130°C was deemed the result of a magnetic transformation occurring in the chromium matrix of the study alloys. The dissolution of titanium and carbon in chromium was also found to result in a decrease in the Young modulus of the solid solution relative to pure chromium owing to the different atomic dimensions of these elements. The change in the Young modulus observed for eutectic alloys was confirmed to be additive. The Young modulus of titanium carbide at 20°C was found to be 417.4 GPa. Figures 3; references 17: 10 Russian, 7 Western.

## Using Rapid Heating During the Deformation and Heat Treatment of Titanium Alloys

*927D0072K Kiev METALLOVEDENIYE I TERMICHESKAYA OBRABOTKA METALLOV in Russian No 12, Dec 91 pp 33-37*

[Article by M.Ya. Brun, A.I. Gordiyenko, L.A. Yelagina, and V.V. Ivashko]

UDC 669.295:621.78.014.5

[Abstract] The All-Union Institute of Light Alloys and the Physics Technology Institute of the Belarus Academy of Sciences conducted a set of studies examining the feasibility of using rapid heating during the deformation and heat treatment of titanium alloys. The studies were conducted on specimens and blanks made of the refractory and high-strength titanium alloys VT3-1, VT6, VT8, VT9, VT16, VT18, VT22, and VT23. For the rapid heating, the researchers used salts ($BaCl_2$) and metal (Al) melts along with electric discharge and induction units. Heating speeds ranging from 5 to 300°C/s (versus the conventional speeds of 0.5 to 2.5°C/s) were acheived. The following were identified as the most promising areas for application of the new rapid heating technique: 1) "structural" heat treatment of intermediate products with a globular structure to obtain a fine-grained plate structure; 2) bulk hardening heat treatment; 3) surface heat treatment to produce composites with a gradient structure (i.e., with a structure that changes along the component's cross section); 4) recrystallization heat treatment to break up a coarse-grained structure; and 5) quick heating before deformation. The advantages and disadvantages of using rapid heat treatment in each of these areas are discussed. Overall, the research conducted demonstrated that rapid heating during the production and final heat treatment of intermediate products made of titanium alloys can result in a plastic structure with a controlled β-grain size, can break up an initially coarsely grained structure, and can create composites with different structural gradations so as to improve the quality and serviceability of the components ultimately produced from the intermediate products. Rapid heating proved to be suitable for use with melts of salts, slags, and molten metals, as well as with electric discharge and induction units. The main drawbacks of rapid heating are related with the dimensions and shapes of the blanks and intermediate products, which often necessitate the creation and use of specialized equipment. The benefits of the rapid heating technique outweigh these problems, however, and more extensive use of the technique in the areas discussed herein as well as elsewhere is warranted. Figures 12.

## The Dependence of the Intragrain Structure of (α + β)-Titanium Alloys on Chemical Composition and Rate of Cooling During Phase Recrystallization

*927D0072C Kiev METALLOVEDENIYE I TERMICHESKAYA OBRABOTKA METALLOV in Russian No 12, Dec 91 pp 7-8*

[Article by G.A. Bochvar]

UDC 669.295.5:620.18

[Abstract] The intragrain structure of (α + β)-titanium alloys has been demonstrated to form during the process of their cooling from the temperatures of their single-phase β-state. Different types of intragrain structures may form depending on the rate at which the material is cooled in the phase recrystallization temperature range and depending on their chemical composition. In lightly and moderately doped alloys such as VT3-1 and VT6 cooled at fairly low rates, generation of the α-phase occurs along the boundaries of the β-grains, after which it grows inside the grain until the wafers of the α-phase growing from the other grain boundaries are encountered. The result of this process is the formation of colonies of α-wafers oriented in virtually a single direction. The angle of the disorientation of the wafers in the adjacent colonies ranged from 23 to 50°. More heavily doped alloys are characterized by a finer intragrain structure. This fact is explained by the higher concentration inhomogeneity of the starting β-phase and decrease in the diffusion coefficient as the degree of doping is increased. The thickness of the α-wafers decreases as the cooling rate in the range of recrystallization temperatures increases. Increases in cooling rate also result in the interweaving of colonies of individual α-wafers and, in a

number of cases, in the formation of a martensite structure. In the case of (α + β)-titanium-type alloys, cooling rates (v) equal to or faster than $v_1$ result in a martensite-type structure. When $v < v_3$, only diffusion β → α transformation with the generation and growth of α-wafers from the grain boundaries occurs. In the interval $v_3 \leq v < v_2$, phase recrystallization begins from the grain boundaries. When the temperature M is reached, phase recrystallization centers appear in the bulk of the crystal. The author notes that although his observations are a simplification of the actual process occurring in (α + β)-titanium alloys, they provide a good explanation of the distinctive features of the structural transformations that occur in various (α + β)-titanium alloys. Figures 4.

## The Structure, Mechanical Properties, and Heat Stability of the Refractory Nickel Granulated Alloy EP741NP

*927D0072H Kiev METALLOVEDENIYE I TERMICHESKAYA OBRABOTKA METALLOV in Russian No 12, Dec 91 pp 21-23*

[Article by N.M. Grits, V.I. Yeremenko, and Ye.A. Fedorenko]

UDC 669.245:621.762:620.17:620.18

[Abstract] The highly heat-resistant granulated alloy EP741NP was developed for use in manufacturing the heavily loaded components of gas turbine engines that are used in the aerospace and power industries and that are expected to operate at temperatures up to 750°C. EP741NP has high service properties, including a high long-range strength and high resistance to low-cycle fatigue. By combining an optimal doping regimen with an optimal hot isostatic pressing process, the developers of EP741NP have been able to achieve an even distribution of carbides and γ'-phase hardening particles. Because EP741NP has been designated for use at temperatures between 650 and 750°C, the authors of the study examined its structure, phase composition, and mechanical properties in its initial state and after having been held at 650°C for 1,000 and 5,000 hours. The said studies were conducted on series-produced disks intended for operation at 650°C. The specimens were found to undergo additional hardening during protracted holding at 650°C, with the most significant changes in properties occurring during the first 1,000 hours of holding. In the first 1,000 hours, for example, $\sigma_{0.2}$ increases by 12%, whereas in the next 4,000 hours it only increases by an additional 2%. Tests for low-cycle fatigue resistance were found to produce results agreeing with the results of short-term strength tests. After 5,000 hours of holding, the number of cycles until smooth specimens fractured increased significantly. In notched specimens, on the other hand, the number of cycles until fracture remained virtually unchanged. Long-range strength tests at 650°C showed that the minimum time to fracture of smooth specimens increases by 50% in the first 1,000 hours but does not increase further after 5,000 hours. These changes are explained on the basis of a phase analysis of EP741NP. During protracted holding, the amount of hardening γ'-phase separation increases, and the parameter of the γ-phase lattice decreases accordingly. Most of this change occurs in the first 1,000 hours of holding. After 5,000 hours of holding, the EP741NP specimens studied experienced a slight (only 0.15%) increase in their carbide phase. A slight amount of boride phase also appeared. No densely packed embrittling phases were detected even after 5,000 hours of holding. The studies performed thus confirmed that EP741NP is indeed suitable for long-term use at an operating temperature of 650°C. Figures 2, tables 3.

## The Rolling of Titanium Alloy Sheets and Foils

*927D0057A Moscow TSVETNYYE METALLY in Russian No 12, Dec 91 pp 30-34*

[Article by V.K. Aleksandrov and Yu.M. Sigalov]

UDC 621.771.6:669.295

[Abstract] The contemporary process used to produce thin sheets and foils from titanium alloys consists of three basic operations (production of hot-rolled blanks, warm and cold rolling of the roll-shaped blanks into sheet-shaped blanks, and further rolling to form thin strips and foils on multiple-roller mills) and four auxiliary operations (etching, degreasing, heat treatment, and cutting). Cold- or warm-rolled stock 1.2 to 1.5 mm thick is the main starting material for rolling thin titanium alloy strips and foils. After etching and annealing, this rolled stock is cold-rolled in several passes to achieve a total relative reduction of 20 to 40%. It is then subjected to the intermediate operations of degreasing and vacuum annealing until a specified thickness (generally 0.5 to 0.02 mm) is reached. When necessary, the edges of the rolled stock are trimmed on circular shears. Titanium strips and foils are generally produced on 20-roller mills. P28 mineral oil is generally used as the process cutting fluid. Annealing of the sheets and foils is generally performed in vacuum shaft furnaces at a temperature of 600 to 750°C in a vacuum of 0.01 Pa. Continuous strand-type vacuum furnaces or special units combining the process of annealing in a vacuum or inert gas atmosphere with the operations of cutting, welding, degreasing, and straightening are also used. The roll technique of producing sheet intermediate products from titanium alloys provides a number of benefits. Specifically, it increases labor productivity by making it possible to perform all of the basic and auxiliary operations involved in high-capacity continuous or semicontinuous units; it expands the range of products produced by permitting the production of thinner and larger-sized sheets than was previously possible; it improves the percentage of acceptable product by reducing the amount of metal because of geometric shape requirements; and it increases the mechanical properties and overall quality of the sheets and foils produced. Figures 4; references 6 (Russian).

## Selecting a Rational Method of Hot Plastic Metal Working in the Manufacture of Shaped Sections and Pipes Made of Light Alloys

*927D0057B Moscow TSVETNYYE METALLY in Russian No 12, Dec 91 pp 36-37*

[Article by M.Z. Yermanok]

UDC 621.7.016.2-97:669.7.018

[Abstract] A number of factors must be considered when selecting a rational method of hot plastic metal working for use in manufacturing shaped sections and pipes from light alloys. The following factors are especially important: 1) the configuration of the cross section of the product and its change throughout the length of the product, 2) the process plasticity of the metal to be deformed, 3) the processing and deformation speeds, 4) the size of the series in which the product is to be manufactured, 5) the amount of metal waste generated during the manufacturing process, 6) the durability of the tool required, 7) ecologic and labor hygiene considerations, 8) the precision of the geometry of the product being manufactured, and 9) the structure and properties of the product. Pressing is the preferred technique for producing light-alloy shaped sections and pipes when the following are true: 1) the sections and/or pipes have a complex shape, 2) the alloys being used have a low degree of plasticity, 3) the product is to be produced in a small series, 4) tool and accessory costs constitute a large percentage of the total cost of producing the product, 5) the process must be kept leaktight, and 6) the strength properties and performance characteristics of the product being produced must be improved. Rolling is the preferred process when the following are true: 1) the sections and/or pipes are being produced in relatively large quantities, 2) they have a comparatively simple cross section, 3) they are to be made of plastic metals and alloys, 4) it is important that the intermediate products required (whether produced in medium or small series) have a highly uniform structure, cross section, and length, and 5) the cost of reprocessing the wastes generated during pressing processes exceeds the cost differential between the manufacture and alignment of pressing and rolling equipment. References 6 (Russian).

## New Types of Shaped Sections Made of Aluminum Alloys

*927D0057C Moscow TSVETNYYE METALLY in Russian No 12, Dec 91 pp 38-40*

[Article by M.V. Kharitonovich]

UDC 621.771.26:669.715

[Abstract] Analysis of the new types of shaped sections made from aluminum alloys reveals three main trends in their manufacture. The first trend is the creation of a technology to manufacture large shaped sections and panels from high-alloy aluminum alloys. The second trend is the manufacture of a wide range of shaped sections and panels from aluminum-lithium alloys. The third main trend is that of the manufacture of a new construction material with variable properties throughout its cross section and length. One such group of shaped sections are those made of aluminum alloys reinforced with high-modulus materials. The creation of large-fuselage aircraft has necessitated the development of a process to produce unique pressed intermediate products with cross-sectional areas up to 1,500 $cm^2$, widths up to 960 mm, and lengths up to 30,000 mm. Work to develop such processes for use with the aluminum alloys V95och, V95pch, D16ch, 1161, 1973, and AK-4 has been conducted at the VSMPO [not further identified] and BKMZ [not further identified] under the scientific-technical supervision of the All-Union Light Alloys Institute and All-Union Scientific Research Institute of Aviation Materials. Research on the development of new materials with variable properties throughout their cross section and length is currently proceeding in three main directions. The first is that of combining conventional aluminum alloys (type D16 or V95) with alloys having special properties (such as Al-Be, Al-SiC, and Al-C) by producing combined blanks and optimizing their deformation parameters. The second direction is that of granule metallurgy. In granule metallurgy high crystallization rates are used not only to create unique alloys that could not be produced by other methods but also to design materials for specific product components. The third direction is based on the combined plastic deformation of materials with very different strengths (for example, combining aluminum with various alloys, aluminum and boron, aluminum and steel, or aluminum and AlC). Experimental batches of shaped-section products manufactured by using these three experimental technologies have been produced and are now being used in products in the aviation and aerospace industries as well as to create new transport systems.

## The Deformed State When Aluminum Alloy-Based Layered Sheets Are Rolled

*927D0057D Moscow TSVETNYYE METALLY in Russian No 12, Dec 91 pp 40-43*

[Article by V.I. Korol]

UDC 621.771.01

[Abstract] A study examined the role of the following factors of the deformed state resulting when aluminum alloy-based layered sheets are rolled: geometric parameters of the focus of the deformation ($l/h_{av}$, H/D, $\varepsilon$), friction conditions, design of the blank, and thickness of the cladding and intermediate soft layers. The studies were performed on blanks made of D16, V95, AMg6, and other aluminum alloys assembled in accordance with one of three schemes (soft-hard-soft, hard-soft-hard, and soft-hard-soft-hard-soft) with hard and soft layers arranged in such a way that the variation in the relative thickness of the soft and hard layers was between 0.3 and

4.0. The studies performed revealed that during rolling with a high focus of deformation, it is the shear component of deformation that is most sensitive to a change in contact friction, thickness, and location of the layers. Furthermore, it was shear deformation that was found to dictate the conditions of the connection of the layers and to exert a significant effect on unevenness of deformation. The studies also revealed that the shear deformation component close to the boundary between layers during rolling with a high focus of deformation under conditions of equal reductions of a layered blank arranged in a hard-soft-hard scheme is much larger than the shear deformation component that occurs in the case of layers arranged in a soft-hard-soft scheme. This difference was seen as an explanation for the reduction in the strength of the connection of the layers of the sheets of the hard-soft-hard type. The studies also demonstrated that when $l/h_{av} < 1$ and $H/D > 0.1$, only bundles assembled in a soft-hard-soft scheme may be rolled in the range of light amounts of reduction. In all other cases, bundles assembled in either soft-hard-soft or hard-soft-hard schemes may be rolled in light-reduction regimens. When sheets arranged in a soft-hard-soft-hard-soft scheme are rolled with a high focus of deformation, the component of shear deformation on the interlayer surfaces increases closer to the blank's surface and decrease as the inner and outer soft layers are increased. Finally, the studies confirmed that in the case of rolling with a low focus of deformation ($l/h_{av} > 2.0$ and $H/D < 0.01$), the effect of shear deformation is lost, and the effects of linear deformations and external and interlayer friction forces increase. For this reason, geometric factors such as the ratio of the soft and hard layers and the arrangement of the intermediate layers by height become secondary. Figures 3, table 1; references 6 (Russian).

## Assimilation of a Technology To Manufacture Light Alloy-Based Bimetallic Pressed Products

*927D0057E Moscow TSVETNYYE METALLY in Russian No 12, Dec 91 pp 43-45*

[Article by M.S. Gildengorn]

UDC 621.762.4:669.7.018

[Abstract] Work to develop and assimilate the commercial production of bimetallic pressed products based on light alloys began at the All-Union Light Alloys Institute in 1962-1963. A pilot technology was developed to manufacture the first thin-walled pipes (200 x 2.5 mm) made of AMg6 with an inner cladding of pure aluminum constituting about 10% of the pipe's wall thickness. Further research resulted in the development of a technology to press hollow bimetallic blanks measuring 93 x 30 x 150 mm through tapered dies with lubrication of the container. The technology was further refined, and processes were developed for pouring hollow ingots with no discontinuities or separation. According to the new process, depending on the ratio of the strength properties of the bimetal's components, either combined pressing or pressing with plastic deformation of just one material of the outer layer may be used to produce layered products. The combined pressing technique has been used to produce complexly shaped products and bimetallic ribbed panels of V95 high-strength aluminum alloy combined with AMg4 aluminum alloy. The technique has also been used to produce large AMg6 + AD1 + AMg6 trimetallic pipes. The technique of pressing coupled with plastic deformation of just one of the two materials constituting the bimetal has been used to produce steel-aluminum and steel-magnesium bars. The new light alloy-based bimetals have proved to be more durable and have better performance characteristics than their conventional counterparts. They have the additional advantages of weighing less and requiring less scarce materials to manufacture. Figures 4, references 5 (Russian).

## Improving the Manufacture of Bars and Wires Made of Titanium Alloys

*927D0057F Moscow TSVETNYYE METALLY in Russian No 12, Dec 91 pp 47-49*

[Article by V.V. Selivanov]

UDC 621.771.25-621.778.1:669.295

[Abstract] The increasing demand for bar and wire intermediate products made of titanium alloys over the past 20 years has resulted in a sizable increase in production volumes and spawned a number of improvements in the process used to make these products. The acquisition of domestic and imported contact and induction heating equipment to heat blanks before rolling as well as centerless lathes and centerless grinders made it possible to develop a commercial process to manufacture bars with diameters of 4.0 mm or more for use in producing such products as fasteners, engine blades, and springs. Titanium alloy bars are now being produced at the rate of hundreds of tons per year for use in such diverse sectors as aerospace, shipbuilding, and medicine. A lack of mills to produce hot-rolled blanks remains a serious problem in the production of titanium alloy bars and wires. The model 250 mills used at the Light Alloys Plant have been in operation for over 35 years. Modifications in its type of heating and sizing units have improved its technical and economic indicators but have not solved the problems associated with obsolete and worn equipment. One new process that appears promising from an economic standpoint is to use fluoride-phosphate coatings when manufacturing titanium alloy wires. Such coatings, which make it possible to obtain surfaces with class 6 or 7 roughness, have proved to be particularly effective on very thin wires less than 1.0 mm in diameter. The All-Union Light Alloys Institute and Magnitogorsk Mining and Metallurgy Institute imeni G.I. Nosov worked jointly to produce a process for producing aluminum-titanium alloy wires by rolling in multiroll passes instead of by intermediate drawing. The new process offers several important advantages. It requires 7 to 10% less metal and requires less (by a factor

of 2.5 to 3) electric power, and it results in higher-quality wire with fewer surface defects. The Beloretsk Metallurgy Combine has used the new technique to produce 100 tons of wire blanks 3.2 to 5.3 mm in diameter from the alloys VT1-00 and PT7M. The blanks were later sized at the Light Alloys Plant and delivered to customers. This year the Magnitogorsk Mining and Metallurgy Institute imeni G.I. Nosov will create a six-cage mill with three-roll passes and will deliver it to the Kirsinskiy Cable Plant to make welding wire from aluminum alloys. References 10 (Russian).

## Titanium Nickelide-Based Alloys With Shape Memory

*927D0057 Moscow TSVETNYYE METALLY in Russian No 12, Dec 91 pp 70-72*

[Article by L.P. Fatkullina]

UDC 669.018.6:669.295

[Abstract] Titanium nitride-based alloys with shape memory became the object of worldwide attention in July 1991 when Soviet cosmonauts successfully constructed a 14-m-long truss connected by sleeves of a titanium nitride-based alloy with shape memory. The main task in the field of titanium nitride-based alloys with shape memory at the present time is to set up the commercial manufacture of intermediate products and components made of them. The All-Union Light Alloys Institute Scientific Production Association has developed a process for smelting ingots weighing more than 500 kg by the technique of double remelting. The first remelting is performed in the cooled crucible of a vacuum skull furnace. The resultant ingots (electrodes) are remelted in a vacuum arc furnace with a consumable electrode. The production association has also developed pilot processes to manufacture the following intermediate products from Ti-Ni, Ti-Ni-Fe, and Ti-Ni-Cu alloys with shape memory: pressed bars 20 to 230 mm in diameter, rolled bars 8 to 20 mm in diameter, wires 2 to 7 mm in diameter, pressed pipes 24 to 60 and 14 to 26 mm in diameter, sheets 0.5 to 10.0 mm in diameter. Studies conducted for the purpose of improving the new processes revealed that increasing cooling speed results in a finer-grained internal structure and that the properties of the metal produced improve as the dispersivity of the grains is increased. Figures 4, table 1; references 4 (Russian).

## Structure Formation Characteristics of Fe-29%Mn-Al-C System Alloys During Sputtering and Hot Extrusion

*927D0110J Yekaterinburg FIZIKA METALLOV I METALLOVEDENIYE in Russian No 12, Dec 91 pp 130-138*

[Article by T.F. Volynova, I.Z. Yemelyanova, V.M. Mnasin, A.N. Svobodov, I.B. Sidorova, Central Scientific Research Institute of Ferrous Metallurgy imeni I.P. Bardin, Moscow]

UDC 669.15'71'74'784:620.186.1

[Abstract] Additional alloy doping opportunities being opened up by solidification during rapid quenching (at rates exceeding $10^6$ deg/s), especially for high-specific-strength Fe-Mn-Al-C alloys is discussed and the structure and properties of Fe-29 Mn-Al-C system alloys are examined as a function of the aluminum (from 4 to 16%) and carbon (from 0.8 to 1.5%) concentration and heat treatment conditions in order to maximize the specific strength. The chemical and phase composition of the Fe-29 Mn-Al-C alloys are summarized. The powders for compaction are produced by accelerated sputtering in a helium medium and represent a mixture of fractions within a 200-800 μm range. The samples are examined using a JSM-T300 scanning electron microscope and a Volumeter instrument and Neofot-3 microscope and Jamp-10 spectrometer made by the Jeol company as well as a BS-540 microscope made by the Tesla company. The powders are heated in evacuated glass vials for 1 h at temperatures of 900, 1,000, and 1,000°C. The impurity distribution in the granule is plotted and the heat treatment-induced mixture redistribution coefficient is determined. The study revealed and confirmed the high impurity and alloying element segregation effect which makes it possible to produce powder alloys with up to 15% Al and outlined a realistic possibility of increasing the specific strength of Fe-Mn-Al-C alloys by increasing the aluminum concentration and using powder metallurgy methods. Figures 8, tables 3, references 2.

## Phase Transitions in Pd-Cu-Pt Alloy System

*927D0110K Yekaterinburg FIZIKA METALLOV I METALLOVEDENIYE in Russian No 12, Dec 91 pp 139-143*

[Article by N.N. Golikova, A.S. Laptevskiy, G.M. Gushchin, V.I. Syutkina, Institute of Physics of Metals at the Urals Department of the USSR Academy of Sciences]

UDC 669.231'234'3:539.42

[Abstract] The low values of resistivity in ordered alloys combined with the need to ensure their high corrosion resistance in instrument applications prompted an investigation of the phase constitution diagram of the Pd-Cu-Pt system in the PdCu-PtCu cross sections which correspond to binary alloys with the maximum critical ordering temperature. An X-ray structural analysis is performed in a DRON-2 unit and an electron diffraction pattern and the temperature behavior of electric resistivity are plotted. The results show that an addition of platinum to the PdCu binary alloy with a B2 superstructure gradually decreases the critical ordering temperature while an increase in the platinum concentration to above 9% at. is accompanied by a total long-range order breakdown. As for the PtCu alloy with an $L1_0$ superstructure, its critical ordering temperature decreases continuously with an addition of palladium. The long-range atomic order breaks down completely at a palladium

concentration above 17% at. Palladium-copper-platinum system alloys in which the platinum or palladium alloying element concentration exceeds said values do not develop a superstructure and remain continuous solid solutions with an FCC lattice. Figures 4, tables 1, references 11: 4 Russian, 7 Western

## Effect of Partial Rh Substitution on FeRh Alloy's Magnetic and Electric Properties

*927D0099B Yekaterinburg FIZIKA METALLOV I METALLOVEDENIYE in Russian No 11, Nov 91 pp 72-78*

[Article by N.V. Baranov, Ye.A. Barabanova, A.I. Kozlov, Scientific Research Institute of Physics and Applied Mathematics at the Urals State University]

UDC 669.15'232'234'235:537.311.3:537.662

[Abstract] The characteristic features of first-kind antiferromagnetic (AF) and ferromagnetic (F) transitions in *d*-metals and their alloys are discussed and a study of the electric and magnetic properties of FeRh alloys in which rhodium is partially substituted with palladium and iridium is reported. $Fe_{50}(Rh_{1-x}T_x)_{51}$, where T is Ir or Pd or their combinations, are produced by the component fusion in an arc furnace in a helium atmosphere, then subjected to diffusion annealing at 1,000°C for 50-70 h and cooling together with the furnace. A radiographic analysis reveals that after the annealing, all alloys have a CsSl crystal structure. An investigation of the alloy resistivity, magnetization, and thermal expansion in a 4.2-700K temperature range in up to 7 T magnetic fields reveals that partial Rh substitution with Pd leads to a substantial nonmonotonic change in the antiferromagnetic state range and resistivity during the antiferromagnetic ordering, partial Rh substitution with Ir pushes up the critical antiferromagnetic-ferromagnetic transition temperature by almost 200K but has little effect on resistivity during the antiferromagnetic ordering at $T = 0$. The resistivity of substituted FeRh alloys during the antiferromagnetic-ferromagnetic transition may change by as much as 110 μΩ x cm. The results are attributed to the characteristics of the FeRh alloys' energy band structure. The authors are grateful to A.V. Andreyev for helping with the experiment. Figures 6, references 17: 11 Russian, 6 Western.

## $M_3B_3$ Borides in High-Temperature Nickel Alloys With 5 and 15-20% Cr by Mass

*927D0099C Yekaterinburg FIZIKA METALLOV I METALLOVEDENIYE in Russian No 11, Nov 91 pp 85-89*

[Article by Yu.R. Nemirovskiy, M.S. Khadyyev, V.V. Poleva, V.P. Lesnikov, Urals Polytechnic Institute imeni S.M. Kirov]

UDC 665.245:620.186.1

[Abstract] The probability of the $M_3B_3$ boride development and its structural properties in high-temperature alloys (ZhS) for various purposes are considered from the viewpoint of the alloy corrosion and/or strength properties and borated N65Kh5V11K9Yu6T1M1B2 (alloy 1) with 5% Cr and 10-12% W and N60Kh15-20V4K5-10Yu3T4M3B1 (alloy 2) with 15-20% Cr and 3-5% W are examined by the method of transmission electron microscopy; to this end, the morphology and crystallography of $M_3B_3$ borides are analyzed in high-temperature nickel alloys. The morphological modifications of borides and their orientational bond to the γ+γ' base as well as the effect of the segregation, phase, and structural inhomogeneities on the boride distribution in the alloy volume are described. The findings confirm that the $M_3B_3$ boride formation is one of the principal and widespread phase transition processes in boron-doped nickel superalloys for various purposes. It is speculated that this process has a significant effect on the performance of these high-temperature alloys. These findings are important for assessing the performance of existing alloys, for predicting the effect of boron and the expediency of its use in order to develop new alloys, and for optimizing heat treatment conditions. Figures 3; references 5: 4 Russian, 1 Western.

## Texture and Mechanical Properties of VT32 Titanium Alloy

*927D0099I Yekaterinburg FIZIKA METALLOV I METALLOVEDENIYE in Russian No 11, Nov 91 pp 188-191*

[Article by R.A. Adamescu, A.I. Gordiyenko, R.S. Novik, M.V. Frolova, Urals Polytechnic Institute imeni S.M. Kirov]

UDC 669.295:669-176:539.4.015

[Abstract] The scarcity of data on the recrystallization structure of Ti β-alloys prompted an investigation of the texture formation characteristics and mechanical properties of cold-rolled 3.5 mm sheets of the VT32 titanium alloy after furnace heating and high-speed heating. The alloy is rolled in a DUO-200 laboratory mill with a 50% reduction. The texture is examined by X-ray methods of direct and inverse pole figures using a microcomputer-aided DRON-3M X-ray machine in molybdenum radiation. The effect of the heating temperature on the pole density of VT32 samples and the behavior of mechanical properties of cold rolled sheets of VT32 alloys in the temperature domain are plotted. In the hardened state, the sheet ductility peaks at 18% when it is hardened at an 800°C temperature; the tensile strength in this state drops to 940 N/mm$^2$ and the alloy has a partially recrystallized structure with a 40-42 μm grain. A comparison of optimum mechanical properties of cold rolled VT32 alloy with a 50% reduction in the hardened state after both types of heating shows that continuous fast heating expands the treatment range which ensures

stable properties while isothermal heating in a furnace does not lead to such stability. Figures 5; references 2.

**Mechanical Properties and Hydrogen Permeability of Pd-Pt Systems Alloyed by Nb and Ta**

*927D0099H Yekaterinburg FIZIKA METALLOV I METALLOVEDENIYE in Russian No 11, Nov 91 pp 150-154*

[Article by F.N. Berseneva, G.P. Zhmurko, S.V. Neuymina, N.I. Timofeyev, Mechanical Engineering Institute at the Urals Branch of the USSR Academy of Sciences]

UDC 669.231'234:539.4.015

[Abstract] The search for optimum palladium alloying in order to produce new membrane materials for diffusive purification of hydrogen prompted a study of the effect of hydrogen on the mechanical properties of Pd-Pt systems doped with Nb and Ta and an investigation of their hydrogen permeability. To this end, four binary alloys, two with a $Pd_{90}Pt_{10}$ content with 5% at. Nb and Ta additions at the expense of palladium and two with a $Pd_{95}Pt_5$ content and the same admixtures are prepared and hydrogenated electrochemically. The dependence of the amount of absorbed hydrogen on the hydrogenation duration, the crystal lattice parameter behavior as a function of the dissolved hydrogen amount, and the dependence of the mechanical properties of alloys with 5 and 10% Pt on the amount of dissolved hydrogen is investigated and plotted and the parameters of the above alloys' interaction with hydrogen are summarized. An analysis demonstrates that joint alloying of palladium with platinum and group VB metals considerably improves the strength properties while helping to maintain good ductility. It is noted that a decrease in the platinum concentration in the alloys does not worsen their mechanical characteristics during hydrogenation: they have good strength properties and are more ductile than alloys containing 10% Pt. Pd-Pt alloys with Nb and Ta are characterized by high hydrogen permeability, making it possible to recommend them as heat-resistant membrane materials for diffusive purification. Figures 4; tables 1; references 6: 2 Russian, 4 Western.

## Refractory Products for Filtration Refining of Molten Metals

*927D0065A Moscow OGNEUPORY in Russian No 12, Dec 91 pp 5-6*

[Article by S.A. Suvorov, N.B. Tebuyev, V.N. Fishchev, Leningrad Technological Institute]

UDC 666.76:669.18.046.518.054.2

[Abstract] Filtration refining of molten metals which makes it possible to attain a high melt purity degree relative to nonmetallic inclusions (NV) and eliminate rejects caused by blow-holes in the casting is considered and the premises of the filtration refining theory are outlined. The results of an investigation of the dependence of filtering capacity of "foamy" cellular filters on their properties are presented; the effect of the specific surface of the disperse phase in the initial suspension on the specific surface of the filter, the porosity of its links, the pore size distribution in the links, and the molten metal filtering ratio as well as the porosity and pore size variation during the filter operation are examined. The analytical procedure is described. The results show that cellular porous filters on the basis of a composite material containing aluminum oxide, zirconium dioxide, and yttrium oxide in a 34:63:3 ratio has the maximum absorption of nonmetallic inclusions; it is also shown that pores with a 30-60 μm diameter have the highest sorption ability. To attain an optimum pore structure of sintered filters, it is necessary to ensure that the specific surface of the disperse phase does not exceed a certain specified value for each material. Figures 1; tables 1; references 6: 2 Russian; 4 Western.

## Rheological Properties of Plastic Bodies From Aluminum Nitride With Anhydrous Temporary Bonds

*927D0065D Moscow OGNEUPORY in Russian No 12, Dec 91 pp 17-19*

[Article by Yu.M. Mosin, V.G. Leonov, Moscow Chemical Engineering Institute]

UDC 666.762.93.3.022:532.135

[Abstract] Ceramic and refractory body molding methods are discussed and an attempt is made to assess the effect of the origin and type of anhydrous temporary process binders on the properties of plastic molding bodies on the basis of aluminum nitride containing 93.3% of the main substance with a specific surface of 3.5 $m^2/g$; to this end, compressor oil, rubber solutions in gasoline, and polyvinylbutyral were used as highly viscous binders in order to obtain a plastic refractory body. The range of plastic state of the aluminum nitride and corundum-based body is summarized and the dependence of the solid phase packing coefficient on the disperse medium concentration, the dependence of the body's relaxation time, plasticity, and elasticity on the disperse medium concentration, the relationship between various types of deformation with an increase in the disperse medium and polymer concentration, and the dependence of the relaxation time, plasticity, and elasticity on the polymer concentration are investigated and plotted. In addition, the effect of the binder type on the density of bodies, semifinished products, and roasted ceramics is established. A similar character of the behavior of deformation properties of bodies with aqueous and anhydrous temporary process binders is established and it is shown that an expansion in the plastic range of the bodies is accompanied by a decrease in the solid phase concentration in the system. The bodies under study are suitable for making elongated products, e.g., tubes and rods, with a close-to-design density whereby the billet density must be at least 2.05 $g/cm^3$. Figures 4; tables 2; references 19: 14 Russian; 5 Western.

## Investigation of Possibility to Produce $CeO_2$-SrO-Based Solid Electrolytes

*927D0065C Moscow OGNEUPORY in Russian No 12, Dec 91 pp 9-12*

[Article by N.A. Likhomanova, Yu.S. Toropov, M.G. Tretnikova, VostIO]

UDC 541.138:661.865

[Abstract] Limited substitution solid solutions with vacancies in the anion sublattice forming in the $CeO_2$-SrO system and their properties within a broad temperature range prompted an investigation of the conditions for synthesizing $CeO_2$-SrO solid solutions from mechanical component mixtures as well as chemically—from mixtures of salt solutions—and for manufacturing and sintering samples on the basis of these solutions. To this end, TseO-Zh cerium dioxide with a 99.99% mass fraction of cerium (OST 48-195—81), pure strontium carbonate (TY 6-09-4165—84) with a 99.0% mass fraction of strontium, and analytically pure (ch.d.a) cerium nitrate hexahydrate (TU 6-09-4081—84) were used. An analysis of materials synthesized from a salt solution mixture and from a mechanical mixture reveals the presence of several exothermal effects in their behavior. The linear shrinkage, open porosity, and apparent density of $CeO_2$-SrO-based samples and samples with various additions as a function of composition and roasting temperature are summarized and the volume resistivity of samples is analyzed as a function of open porosity and composition. A general trend toward a decrease in the sample resistivity with an addition of Pr or Dy is observed. The study makes it possible to draw the conclusion that materials on the basis of $CeO_2$-SrO solid solutions with an 8, 9, and 15% molar fraction of SrO are suitable for producing solid electrolytes; it is recommended that in order to increase their density and reduce resistivity, 0.5% $Dy_2O_3$ or 2% $Pr_6O_{11}$ be added to the composition. Figures 2; tables 3; references 3.

### Refractory Oxide Fiber-Based Heat Insulating Materials

*927D0065B Moscow OGNEUPORY in Russian No 12, Dec 91 pp 7-9*

[Article by N.M. Kovalchuk, S.P. Listovnichaya, Yu.L. Pilipovskiy (Mechanics Problems Institute at the Ukrainian Academy of Sciences)]

UDC 666.76-486

[Abstract] Progress in the area of fibrous insulating materials prompted by the development of aerospace technology, metallurgy, and power engineering is described and the types of materials suitable for use as fibers are considered. Special attention is focused on fibrous heat insulating materials made on the basis of refractory oxides which can be used at high temperatures as well as in corrosive media. In general, the type of fiber used is dictated mostly by the anticipated operating temperature. The composition, fiber diameter, fiber density, operating temperature, modulus of elasticity, and tensile strength of various oxide high-temperature fibers manufactured by the 3M Company, Quartz Slice, Du Pont, and Shinagawa Refr. Company are summarized and the apparent density, composition, maximum operating temperature, and thermal conductivity of several fibrous heat insulating materials, both foreign and domestic, are cited. The fiber type, binder, density, and maximum operating temperature of several heat insulating materials with an inorganic binder are examined. It is speculated that functionally gradient materials being developed in Japan and bilayer materials bound by a 0.03 cm-thick glass layer being developed in the United States represent the trend of the future since they are capable of more fully realizing the potential of materials with diverse properties. Tables 3; references 14: 6 Russian; 8 Western.

### Protective Atmosphere Composition and Water Resistance of Soda Lime Glass Surface

*927D0075A Moscow STEKLO I KERAMIKA in Russian No 12, Dec 91 pp 2-3*

[Article by V.F. Solinov, T.V. Kaplina, A.V. Gorokhovskiy, NITS, Tekhstroysteklo Scientific Production Association, and Saratov Polytechnic Institute]

UDC 666.11.01:620.193.23

[Abstract] The effect of the molecular hydrogen concentration in the protective atmosphere of the molten pool on the water resistance of the lower and upper surfaces of thermally polished glass is investigated. The studies were carried out at the Avtosteklo plant and the following process parameters were manipulated: the hydrogen content (within 2.7-6%) by volume and the glass body temperature (within 1,114-1,120°C). The dependence of the water resistance on the leaching duration of glass samples produced by various methods is examined and plotted. The conclusion is drawn that increasing the water resistance of the surface of thermally polished glass by changing the process parameters represents an optimization problem in which the hydrogen content in the protective atmosphere of the molten pool and the glass body temperature are the objective variables; the need to take into account the different water resistance characteristics of surfaces formed under various conditions as well as the time factor is identified. It is shown that as hydrogen concentration in the protective atmosphere increases, the spread of water resistance values of the upper surface decreases while the spread of water resistance values of the lower surface increases; in addition, the lower the hydrogen concentration, the smaller the water resistance spread between the upper and lower surfaces. Figures 2; references 5: 4 Russian, 1 Western.

### Identification of Tinting Agents in Glass by X-Ray Fluorescence Analysis

*927D0075I Moscow STEKLO I KERAMIKA in Russian No 12, Dec 91 pp 25-26*

[Article by V.Ye. Sankov, V.B. Bragin, L.A. Samsonova, S.Ya. Shulov, Tekhstroysteklo Scientific Production Association]

UDC 666.11.01:666.124.2:543.422.8

[Abstract] The work on developing two techniques for X-ray fluorescence analysis of bulk-tinted glass being carried out at the Tekhstroysteklo Scientific Production Association is described. The first technique makes it possible to determine the concentration of both principal elements in the glass and dyes (Fe, Ti, Ni, Co, Cr, and Cu) while the second is capable of quantitatively measuring the concentration of Cu, Cd, Mn, Se, Cr, and Sb in zinc, lead, and barium-containing glass. Both methods require 5-7 min for analyzing a sample. A VRA-30 X-ray fluorescence analyzer (German-made) was used in the analysis. Analytical data on the concentration ranges of individual tinting agents in glass are summarized. The technique is recommended for research work as well as routine process monitoring. Tables 2; references 2: 1 Russian; 1 Western.

### Method of Ceramic Part Molding for Integrated Circuit Packages

*927D0075H Moscow STEKLO I KERAMIKA in Russian No 12, Dec 91 pp 20-21*

[Article by M.I. Timokhova, L.I. Medvedeva, Elektrofarfor Scientific Production Association]

UDC 666.65.032.6

[Abstract] The need to design a high-output method of molding ceramic packages for integrated circuits to replace existing hot die casting methods is identified and the development of an efficient technique for molding IC packages from the VK94-1 aluminum oxide material and

VK100-2 high-alumina material is reported. Hydraulic and mechanical presses with metal molds are used for this purpose. The results of an examination of 15 types of ceramic integrated circuit packages of various shapes and dimensions are presented. The parts were molded at a unit pressure of 120-200 MPa, depending on the geometrical configuration, and sent directly to roasting without drying. Molding of ceramic integrated circuit packages by this method makes it possible to ensure a high dimensional accuracy without additional machining, reduce the size spread to 0.01-0.04 mm, and attain a sag of less than 0.05 mm. Figures 2.

### New Electromagnetic Separators

*927D0075G Moscow STEKLO I KERAMIKA in Russian No 12, Dec 91 pp 17-19*

[Article by B.I. Gaydash, V.A. Aleko, B.I. Nevolnichenko, M.B. Lebedev, K.N. Logvinov, Slavyansk Branch of the All-Union Scientific Research Institute of Electric Grade Ceramics and Elektrofarfor Scientific Production Association]

UDC 666.3:621.928.8

[Abstract] The importance of magnetic separation for removing iron and iron oxide particles from the liquid suspensions of porcelain and faience mixtures in order to improve their mechanical and electric properties is discussed and the results of an investigation of four different type of magnetic separators (Author's Certificate Nos. 998492, 1029990, 1142140, 1178469) for this purpose are presented. The separators' design diagrams are presented and their operating principle is described in detail. The results of commercial tests of the separator operation with glaze slip, fine ceramic slip, and electric-grade porcelain slip are summarized; when separating slip with a moisture content of 62%, the separator output is 1-8 $m^3/h$ while in separating a slip and electrolyte mixture and glaze slip, its output reaches 4-5 $m^3/h$; the separating screens must be removed and washed every 60-80 min. A microscopic analysis shows that the processed slip contains magnetic iron particles with a size of less than 50 μm. A study of a pilot batch of products sintered from the slip treated by the separator shows that the number of iron-related defects decreased by 53%. Figures 1; references 1.

### Increasing Heat Resistance of Silicon Nitride-Based Ceramic Materials

*927D0075F Moscow STEKLO I KERAMIKA in Russian No 12, Dec 91 pp 15-17*

[Article by N.M. Bobkova, A.A. Stepanchuk, A.V. Deshkovets, Belarus Technological Institute]

UDC 666.762.93:539.434

[Abstract] The need for structural materials with high strength and good heat and temperature resistance as well as improved heat insulating properties is identified and it is shown that silicon nitride-based ceramics have some of these qualities. As a result, attempts to obtain high-strength heat resistant ceramics with a low heat conduction by adding aluminum titanate to the matrix phase are described and the properties and synthesis technology of the new material are investigated. The effect of various substitutions in the ceramic composition on its properties is examined. As a result, a system consisting of $Si_3N_4$, $SiO_2$, $TiO_2$, $Eu_2O_3$, $Al_2O_3$, and MgO is synthesized and its properties are analyzed. The new ceramics' increased heat resistance is due to the formation of $Al_2TiO_5$ and solid solutions on the basis of $\beta$-$Si_3N_4$ in the end product. The dependence of the material's properties on the sintering temperature and the dependence of strength losses on the number of thermal loading cycles are plotted. The results make it possible to recommend the new ceramics for use as structural material for making engines and machines. Figures 2; references 3: 1 Russian; 2 Western.

### Effect of Process Parameters on Reflection by Thin Films

*927D0075E Moscow STEKLO I KERAMIKA in Russian No 12, Dec 91 p 11*

[Article by A.B. Atkarskaya, V.I. Borulko, V.Yu. Goykhman, T.A. Dudnik, L.I. Maricheva, S.A. Popovich, L.V. Yakubets, Scientific Research Institute of Automotive Glass]

UDC 666.657

[Abstract] The use of thin films applied to glass in order to change its properties is discussed and the effect of the solution concentration and treatment temperature and duration on the surface quality and reflectance of coats is investigated. It is shown that the coat's refractive index and reflectance are proportionate to each other. The thin film coat composition, application method, and heat treatment conditions are described. An analysis demonstrates that an increase in the films' exposure to a high temperature increases their reflectance by a factor of 1.1-1.3; this is attributed to an improvement in the coat homogeneity because the film-forming reaction occurs more fully. On the other hand, the film-forming solution concentration and treatment temperature within a 350-550°C range do not affect the surface reflectance. Tables 2.

### Process Chart of Making Bent Hardened Products

*927D0075D Moscow STEKLO I KERAMIKA in Russian No 12, Dec 91 pp 9-10*

[Article by A.G. Shabanov, A.I. Shutov, V.P. Markov, A.A. Chistyakov, Tekhstroysteklo Scientific Production Association and BTISM]

UDC 666.153.1:666.155

[Abstract] Two methods of making bent tempered glass items—horizontal sagging and vertical compaction—and their shortcomings are considered and a method of making such products by horizontal compaction which has a higher efficiency and makes it possible fully to mechanize and automate the process is examined in detail. The glass temperature in any layer and the quenching stress are used as the controlled variables. A process chart is presented and the temperature field parameters at the end of heating and intermediate cooling processes are summarized. The heat transfer coefficient and stress distribution in bent tempered glass products are cited. An algorithm and computer program for designing the complete cycle of this process have been developed; they are suitable for calculations with any initial parameters. Figures 1; tables 3; references 3.

## Low-Melting Glass for Sealing Thick-Film Integrated Circuits

*927D0075B Moscow STEKLO I KERAMIKA in Russian No 12, Dec 91 pp 4-5*

[Article by I.K. Nemkovich, O.V. Nevar, I.A. Formago, I.Ye. Maksimova, Belarus Polytechnic Institute]

UDC 666.11.01

[Abstract] The use of (soft) low-melting lead-containing borate glass for sealing thick-film integrated circuits is discussed and a $SiO_2$-$B_2O_3$-$Al_2O_3$-PbO system is investigated; in so doing, the effect of the composition on the glass formation, crystallization, physical and chemical properties, and compatibility of glass and substrates from ST-50-1 glass ceramic and steatite and high-alumina ceramic substrates is examined. The softening temperature, temperature coefficient of thermal expansion (TKLR), water resistance, and density of three brands of glass are summarized. An analysis of experimental data shows that various types of glass may be synthesized from the above borate system for use as protective coats for resistors and capacitors on thick-film integrated circuits, making it possible to create glass-encased hermetic capacitors and resistors with improved electric characteristics. Figures 2; tables 1.

## Analytical-Experimental Method of Estimating Limiting Stressed State of Cast-Melted Refractory Ingots During Crystallization and Annealing

*927D0075C Moscow STEKLO I KERAMIKA in Russian No 12, Dec 91 pp 6-8*

[Article by V.V. Kolomeytsev, Ye.F. Kolomeytseva, Bakor Scientific-Engineering Center and State Glass Institute]

UDC 666.76:666.19:539.3

[Abstract] An analytical-experimental method based on comparing the design critical casting surface cooling rate to the measured rate at fixed crystallization and annealing values is used to assess the limiting state of stress of cast-melted refractory materials; in so doing, the casting failure criterion is defined as the moment when the real cooling rate of its surface exceeds the calculated critical rate. Typical cooling curves of the center and bottom surface of cast-melted refractory ingots in sand and graphite molds heat-insulated with diatomite are plotted and the following characteristics of castings are summarized: thermal conductivity, heat capacity, apparent density and thermal diffusivity. The method's efficiency has been corroborated in practice; compared to known techniques, the method takes into account the nonuniformity of the properties and structure of cast-melted refractory materials and their deviation from linear fracture mechanics within a broad temperature range. The analytical-experimental method is therefore recommended for predicting the optimum crystallization and annealing conditions of new types of cast-melted refractory materials as well as for improving the production procedures of known refractory materials. Figures 5; tables 1; references 9: 8 Russian; 1 Western.

## Mechanical Properties of Zirconia Single Crystals for Structural Applications

*927D0025C Moscow OGNEUPORY in Russian No 8, Aug 91 pp 14-17*

[Article by G.A. Gogotsi, Institute of Bearings Industry at UkSSR Academy of Sciences, Ye.Ye. Lomonova and V.V. Osiko, Institute of General Physics at USSR Academy of Sciences]

UDC 666.762.52.001.4

[Abstract] An experimental study of $ZrO_2$:($Y_2O_3$ single crystals and their mechanical properties was made concerning their suitability for various structural applications, partly stabilized zirconia compacted into a single crystal known to be the strongest material at 1400°C and higher temperatures with adequate strength and cracking resistance at room temperature. Test specimens were cut with a diamond tool from single crystals which had been grown from melts of 97 % $ZrO_2$ + 3 % $Y_2O_3$ in a cold container, the melts having been produced by direct high-frequency induction heating. Directional crystal growth without limitation on the number of possible crystallization centers, without seeding or constriction, was facilitated by containers with flat walls and slag-lined bottoms. Single crystals up to 40 mm wide and up to 120 mm long were grown at a rate of 10 mm/h lengthwise, whereupon they were cooled at a rate of 10°C/min. Specimens were cut from randomly selected single crystals, a 45 mm long rectangular 3.5 mm thick and 5 mm wide with rounded edges serving as master. These specimens were tested for density (g/cm), speed of ultrasound (m/s), both dynamic and static moduli of

elasticity ($kN/mm^2$), strength in 3-point and 4-point flexure ($N/mm^2$ at 140-1400°C temperatures. The results of ultrasonic measurements indicated that specimens had been cut from two different batches of single crystals with approximately (111) and (001) orientation respectively, their other mechanical properties except density also being correspondingly different. Specimens of both batches were tested for cracking resistance, in terms of the critical stress intensity index ($N/mm^{3/2}$) and its relation to the length of a sharp crack. A statistical analysis of the data on the basis of 20-54 specimens indicates that this new partly stabilized zirconia ceramic is quite suitable, and competitively so, for industrial cutting tools and for tape transports as well as for orthopedic and stomatological prostheses. The authors thank V.I. Aleksandrov, M.A. Vishnyakov, Yu.K. Voronko, and V.F. Kalabukhov for participation in the research needed for producing the single crystals, V.I. Galenko, A.V. Drozdov, A.V. Cheboryukov, and A.I. Fesenko for participation in the mechanical testing. Figures 4; tables 3; references 11.

## High-Temperature Strain-Strength Characteristics of Refractory Magnesium Spinellides

*927D0025D Moscow OGNEUPORY in Russian No 8, Aug 91 pp 17-18*

[Article by R.A. Panfilov, V.M. Ustyantsev, T.I. Remezova, and S.P. Postinkova, Eastern Institute of Refractory Materials, M.Ya. Landa and V.V. Nikolayev, Ufa Institute of Aviation]

UDC 620.174.25.017:666.762.3

[Abstract] An experimental study of four refractory magnesium spinellides was made, for a determination of their high-temperature wear characteristics on the basis of flexural strength and strain-before-fracture measurements. These refractories were produced at the "Magnezit" Combine from heat-resistant chromite-periclase and from three varieties of periclase-chromite with different dispersions of the granular chromium ore, the latter coming from Kempirsay deposits and periclase coming from Satka deposit. The charges were finely comminuted so that grain size fraction below 0.06 mm constituted 95 % of the total volume. Technical-grade lignosulfonates having a density of 1.20-1.22 $g/cm^3$ were used as temporary binder. Compacts of these refractory materials were formed in a hydraulic press under 130 $kN/mm^2$ pressure and then fired in a tunnel furnace at 1700°C, at which they were held for 4 h. From the bricks were cut, with a saw, 70 mm long bars 15 mm thick and 20 mm wide. Strain and strength tests were performed at 20°C and then successively at 800-1000-1200-1350-1500°C. The data have been analyzed and evaluated in accordance with standard Resistance of Materials formulas. The results indicate that the strain-strength characteristics of these materials are determined by their heterogeneous phase composition. While sintered periclase spinellide being most compact and rigid so that it is more prone than the other three materials to chipping under heat loads, those three materials containing granular chromium ore have a structure with a network of microcracks making them more deformable and heat resistant. Figures 1; tables 4; references 10.

## Erosion Resistance of Zirconia Concrete Blocks in Hot Gas Stream

*927D0025A Moscow OGNEUPORY in Russian No 8, Aug 91 pp 8-11*

[Article by A.G. Karaulov, Ukrainian Scientific Research Institute of Refractory Materials, R.Y. Abraytis and V.Yu. Romashev, Institute of Problems in Engineering Physics of Energetics at LiSSR Academy of Sciences]

UDC 666.762.5.017:620.178.16

[Abstract] New formulations of highly refractory concrete have been developed with 90.3-91.6 wt.% ($ZrO_2$+ $HfO_2$) and 4.2-4.7 wt.% CaO in the filler and with a $SrZrO_3$-$SrAl_2O_4$ cement or with $MgAl_2O_4$ cement and $CaZrO_3$ as binder. The filler also contains metallic iron in amounts equivalent to 0.01-0.014 wt.% $Fe_2O_3$. The size distribution of filler grains is: 25.5-28.0 % 5-2 mm fraction, 13.2-24.2- 2-0.5 mm fraction, 9.0-11.8 % 0.5-0.09 mm fraction, 38.5-47.2 % smaller than 0.09 mm fraction. Cements of the Al-Mg class are produced by firing a mixture of $CaMg(CO_3)_2$ (dolomite) and $Al_2O_3$ (alumina) without or with addition of MgO so as to form a $CaO.2Al_2O_3$-$MgO.Al_2O_3$ mixture with or without $CaO.Al_2O_3$ and with or without MgO. Increasing the dolomite fraction and thus the CaO content is not advisable, inasmuch as curing of the cement would then begin and end sooner. Cement produced from mixture of 35 % $CaO.2Al_2O_3$ + 65 % $MgO.Al_2O_3$ was found to have the highest compressive strength after 7 days of curing. Tests performed on the $CaZrO_3$ binder have revealed that its activity decreases and the amount of water necessary for producing a cement of normal consistency becomes correspondingly smaller as the firing temperature is raised. Raising it from 1580° to 1650°C and then to 1750°C was found to increase the compressive strength of this cement from lower to successively higher than that of $MgAl_2O_4$ cement after 1-3-7 days of curing, a higher firing temperature evidently being more favorable for formation of crystalline hydrates. Differential thermal analysis has revealed exothermic decomposition of the hydrates with attendant removal of moisture at temperatures characteristic of each cement, addition of $CaZrO_3$ to $MgAl_2O_4$ reducing the loss of moisture. In cements of the Sr aluminate-zirconate class it is the $SrAl_2O_4$ compound which hydrates most actively and yields the strongest cement after 1-3-7-28 days of curing. Curing of the other compound, $Sr_2Al_{12}ZrO_{22}$, begins and ends much too soon so that this binder is not suitable for concrete. Cements produced from mixtures of 30 % $SrAl_2O_4$ + 70 % $SrZrO_3$ and of 40 % $SrAl_2O_4$ + 60 % $SrZrO_3$ have a lower compressive strength after 1-3-7-28

days of curing. Concrete blocks with $CaZrO_3$ and either $MgO.Al_2O_3$ or $SrO.Al_2O_3$ in the binder were tested for erosion in a high-speed (2200 m/s) stream of gaseous propane and butane combustion products, both hydrocarbons burning at 1800-1900°C in an oxygen stream flowing at a velocity of 250 m/s. This test was performed on cylindrical specimens, 28 mm high with a 28 outside diameter and an 8 mm inside diameter, which had been formed from concrete blocks under a 100 $N/mm^2$ pressure. Their erosive wear was found to be very small, and even smaller with silicone included as additional binder. This indicates that these binders do not vaporize at such high temperatures. Differential thermal analysis was performed by G.G. Yeliseyeva. Figures 5; tables 5; references 12.

## Improved X-Ray Method of Monitoring Refractory Materials Production

*927D0025E Moscow OGNEUPORY in Russian No 8, Aug 91 p 19*

[Article by V.S. Rybakov, F.F. Ocheretr yuk, N.K. Stelivanova, V.A. Yesipova, and A.A. Masentsov, Magnitogorsk Metallurgical Combine]

UDC 666.762.11:546.723-31:537.531

[Abstract] The x-ray diffraction method of inspection has been improved at the Magnitogorsk Metallurgical Combine for monitoring the oxides of light elements (Al,Si,Mg,Ca) in refractory materials, the earlier BARS-3L modified version of the automatic x-ray spectrometer for this purpose having been further modified as follows: 1) a small electric motor installed for rotating specimens at 1 rps and thus minimizing the influence of their nonhomogeneity on the results of measurements; 2) a small gang of flow counters installed so as to facilitate quantitative chemical analysis of a specimen for all oxides in the same instrument with the counters optimally positioned relative to the specimen; 3) two separate channels with differential discriminators built into the electric circuit; 4) results of analysis displayed as the ratio of pulse counts in the two channels, with either 10 or 2x10 pulses in one of the channels so as to retain the high accuracy over wide ranges of oxide concentrations in specimens; 5) timer circuit revised to allow changing the exposure time from 10 s for setup of the apparatus to 100 s for monitoring the chemical composition of a specimen. The key performance indicators of the new BARS-3LM version (based on control analyses of Berlin and Arkalyk clays for $Al_2O_3$ and $SiO_2$ contents) are: r.m.s. deviation 0.13 %, maximum difference between readings taken in parallel measurements 0.3 %, sensitivity 3000-5000 pulses per 1 % of monitored oxide, duration of one analysis 5 min. This version is in each respect better than the earlier BARS-3L version. Tables 1; references 2.

## Dependence of Ceramic Microstructure and Properties on Crystal Size

*927D0025B Moscow OGNEUPORY in Russian No 8, Aug 91 pp 11-14*

[Article by V.P. Tarasovskiy, Scientific Research Institute of Automobile Transportation Materials, Ye.S. Lukin and A.V. Belyakov, Moscow Institute of Chemical Technology]

UDC 666.3/7.017:620.186.6

[Abstract] An important problem in ceramics technology is considered, namely the dependence of their microstructure along with their mechanical and thermophysical properties on the characteristics of crystals a ceramic is made of. These characteristics include the degree of dimensional anisotropy and of attendant thermal expansion anisotropy as well as crystal size fraction. With regard to dimensional anisotropy, crystals of most common ceramic materials are classifiable into isotropic ones (cubic) with axes a = b = c, intermediately anisotropic ones (trigonal, tetragonal, hexagonal) with axes a = b > or < c, and fully anisotropic ones (rhombic, triclinic, monoclinic) with axes a > or < b > or >h c. The mechanical strength of a ceramic material will depend on the size to which its crystals have grown, and that size will in turn depend on the degree of crystal anisotropy. These relations are quantitatively analyzed for single-phase crystalline ceramic materials. The maximum tensile stress in such a material along the a-axis (longest) has been calculated according to the Bush-Hymmel formula $\sigma_a = E\Delta T(\alpha_a - \alpha_c\nu)(\alpha_a - \alpha_b)/(1 + \nu)(1 - 2\nu)$ (E—modulus of elasticity, $\Delta T$—temperature drop, $\alpha_{a,b,c}$—coefficients of linear thermal expansion along respective axes, $\nu$—Poisson's ratio). The width of a microcrack developing in a ceramic material when that maximum stress exceeds the tensile strength of that material in a given direction has been calculated according to the Bush-Hymmel formula $W = L(T_{rel} - T)\alpha_{max}\text{-}\alpha)$] (L—mean length of crystal in the direction of the maximum coefficient of linear thermal expansion $\alpha_{max}$, T—temperature of material, $T_{rel}$—stress relaxation temperature, $\alpha$—average coefficient of linear thermal expansion). The results of these calculations are compared with and found to agree closely with experimental data on crystals of $Al_2TiO_5$ (rhombic), $\alpha\text{-}Al_2O_3$ (trigonal), and BeO (hexagonal) ceramics as well as on MgO and $Y_2O_3$ (both cubic) ceramics. That the temperature dependence of mechanical and thermophysical properties of a ceramic material are determined by its microstructure, which in turn depends on the crystal size, is demonstrated on two such properties: 1) flexural strength of $Al_2TiO_5$ ceramic after firing at 1500°C and after firing at 1700°C, 2) thermal conductivity of $Fe_2TiO_5$ after hot-pressing and after firing at 1100°C. Tests have shown that addition of $Me_2O_3$ metal oxides to $Al_2TiO_5$ which form solid solutions with it will not only weaken the crystal anisotropy and thus increase the strength of the ceramic but also alter the crystal habit. Figures 6; tables 1; references 16.

## Properties of $ZrO_2$ Ceramic Partly Stabilized by $Y_2O_3$ Concentrate

*927D0023B Moscow OGNEUPORY in Russian No 6, Jun 91 pp 5-7*

[Article by T.V. Chusovitina, Experimental Materials Scientific- Industrial Association "Keramika", Yu.S. Toropov and M.G. Tretnikova, Eastern Institute of Refractory Materials]

UDC 666.762.52.001.4

[Abstract] An experimental study of $ZrO_2$ ceramic partly stabilized by either 4.0 mol.% or 2.5 mol.% $Y_2O_3$ in an 84 wt.% concentrate was made, for an evaluation of its suitability as solid electrolyte in preference to fully stabilized ceramic. Powders of both oxides were prepared by chemical precipitation of their chlorides from an ammonia solution, firing the precipitate at 1000°C temperature, and its subsequent comminution in copper ball mills to the 4 μm basic dimension of powder lumps. A technology of producing partly stabilized $ZrO_2$ powder with excellent thermomechanical properties, better than those of fully stabilized ceramic, has been developed which ensures retention of the tetragonal high-temperature phase at room temperature by slip casting ultrafine powder (U.S. Patent No 463,935; French patent application No 2,578,241) and subsequent sintering at temperatures within the 1300-1500°C range. The volume fractions of the three tetragonal, cubic, and monoclinic phases are then calculated in accordance with a system of three equations relating their volume fractions to the intensities of respective diffraction lines after reflection by a (111) plane (all three phases) and by a (111[bar over 1]) plane (monoclinic phase only). The results of physical and chemical tests indicate that $ZrO_2$ + 4.0 mol.% $Y_2O_3$ ceramic can be produced by sintering at 1350°C or at 1300°C, for a longer period of 10 h at the lower temperature, while $ZrO_2$ + 2.5 mol.% $Y_2O_3$ ceramic can be produced by sintering at 1300°C for only 3 h. The results of x-ray phase analysis indicate that as the sintering temperature is raised, the volume fraction of tetragonal phase decreases while the volume fractions of the other two phase increase. This is attributed to more intense diffusion of ions in the crystal lattice at higher temperatures with attendant transformation of more tetragonal crystals into more stable cubic ones and to recrystallization at higher temperatures resulting in transformation of more tetragonal crystals into monoclinic ones during subsequent cooling. Both ceramics were tested for apparent and true density, flexural strength, and dynamic modulus of elasticity under cyclic heat loads. This modulus was found not to be the same for $ZrO_2$ + 2.5 mol.% $Y_2O_3$ ceramic and almost the same for $ZrO_2$ + 4.0 mol.% $Y_2O_3$ ceramic after repeated heating to 200°C and cooling to 20°C in water, but much lower already after the first cycle of heating to a temperature higher than 200°C and cooling to 20°C. The electrical resistivity of $ZrO_2$ + 4.0 mol.% $Y_2O_3$ ceramic sintered at various temperatures from 1350°C up to 1500°C was measured at temperatures covering the 500-1000°C range. It was to remain almost the same after the sintering temperature had been raised from 1350°C to 1450°, but to be lower and especially so over the 500-800°C temperature range after the sintering temperature had been raised to 1500°C. This ceramic is a suitable material for a solid electrolyte operating under both mechanical and heat loads at temperatures above 800°C, an auxiliary heating arrangement being advisable for its operation at temperatures below 700°C, while the $ZrO_2$ + 2.5 mol.% $Y_2O_3$ ceramic is a suitable material for mechanically noncritical structural elements. Figures 1; tables 1; references 11.

## Tribochemical Activation of Polycrystalline Aluminum and Zirconium Oxides in Liquid Suspension

*927D0023C Moscow OGNEUPORY in Russian No 6, Jun 91 pp 7-11*

[Article by I.I. Nemets, N.S. Belmaz, and L.N. Semykina, Belgorod Institute of Structural Materials Technology]

UDC [666.762.11+666.762.52]:621.926.086

[Abstract] A method of increasing the initial mechanical strength and thus also the subsequent volumetric stability of structural $Al_2O_3$ and $ZrO_2$ structural ceramics is considered, namely by implantation of ions which readily form polymerizable compounds. Inasmuch as the chemical inertia of these oxides inhibits ion implantation, an amorphous layer of inorganic compounds into which ions can be readily implanted needs to be deposited on the surface of those oxides. In order to facilitate ion implantation in this layer, it is necessary to activate it mechanically as well as chemically. The product of such a tribochemical activation must, moreover, have the characteristics of a highly concentrated suspension of ceramic particles in a liquid such as water so as to ensure not only high strength and high density but also volumetric stability of the cast ceramic. The method was experimentally applied to corundum and to zirconia, the latter stabilized with 12 wt.% $Y_2O_3$. Aqueous solution of orthophosphoric acid was used as source of ions, its concentration being varied over the 4-30 wt.% range. The oxide charge was tribochemically activated in 2-4 $dm^3$ large porcelain containers serving as ball mills, with uralite balls (density 3.2 $g/cm^3$) pulverizing the charge and with $H_3PO_3$ solution implanting P ions in it. The weight ratio of components in this system was oxide:balls:implantor = 5:2:10. The slurry was slip cast into thermoplastic molds and held in them till it had completely hardened into solid bars. Upon removal from the molds, these bars were dried at 150°C and then heat treated at 300°C to a final 70 mm length and 10 mm square cross-section. The rheological behavior of the oxide suspensions throughout the process was monitored in a Reotest-2 rotary viscometer with coaxial cylinders, the speed of the rotating one being varied from 437 rps to 1

rps. The amount of free orthophosphoric acid was monitored by acid-base titration. Structural examination of ceramic powders produced by heat treatment of their suspensions at 150°C and at 1000°C was performed by the method of infrared spectroscopy covering the 200-4000 $cm^{-1}$ frequency range in a Specord M-80 instrument. New formations were identified on the basis of both petrographic analysis and x-ray phase analysis, the latter being performed in a DRON-3 x-ray diffractometer (tube voltage 30 kV, current 25 mA) with a $CuK_{\alpha}$-radiation source and a Ni filter. The optimum $H_3PO_3$ concentration in the solution was determined according to the criterion of imparting adequate fluidity to the ceramic powder suspension with the minimum possible water content so as to ensure high strength and low porosity in addition to volumetric stability of ceramic castings. Two suspensions satisfied these requirements: 1) pH 1.63, density 2.37 $g/cm^3$; 2) pH 1.42, density 3.04 $g/cm^3$. Both completely hardened in the molds within 60 h. A highly disperse solid phase of colloidal dimensions was found to form within the first 240 h molding period, one which spontaneously binded more of the still kinetically free water and thus contributed to compaction by pressure due to intermolecular attraction. As a result, the strength of corundum and zirconia ceramics had increased by a factor of 1.16 and 2.6 respectively. Within the next 240 h aging period, however, the viscosity of the broken down thixotropic structure in corundum and in zirconia increased by factors of 2.1 and 3-5 respectively. Petrographic analysis revealed a thin crystalline coating on the grains of the solid phase in both corundum and zirconia ceramics. The refractive index of the Al-P cryptophase in corundum ceramic could not be determined after drying at 150°, only after heat treatment at 1000°C. The refractive index of the Zr-P cryptophase in zirconia ceramic could not be determined at all. The results indicate three distinct successive stages of tribochemical activation: 1) intense interaction in the first stage lasting 5 h for corundum and 3 h for zirconia, 2) steady chemical reaction with constant supply of comminution energy in the ball mill, 3) interaction after comminution. The authors thank B.G. Alapin for performing the x-ray phase analysis, V.Yu. Prokudin for performing the petrographic analysis, and L.B. Degtyareva for performing the infrared spectroscopy. Figures 4; references 7.

## Phase Transformations in Al-Si-Mg Gels. Effect of Ti,Ce,Zr Additives

*927D0023D Moscow OGNEUPORY in Russian No 6, Jun 91 pp 11-13*

[Article by A.V. Galakhov, V.Ya. Shevchenko, and A.A. Stebunov, Interdepartmental Scientific Research Center for Industrial Ceramic, USSR Academy of Sciences]

UDC 666.762.14:62-404.8

[Abstract] An experimental study of phase transformations in cordierite powder produced by the sol-gel technology was made concerning the effect of $TiO_2$, $ZrO_2$, and $CeO_2$ additives on these transformations, these oxides being known to lower the crystallization temperature of Al-Si-Mg glasses. Gels for this study were produced with extra-pure tetraethoxysilane, chemically pure $Al(NO_3)_3 .9H_2O$, analytically pure $Mg(NO_3)_2 2O$, pure $TiCl_3$ in 20 % ethanol solution, analytically pure $ZrOCl_2.8H_2O$, and analytically pure $CeO_2$. The crystalline Al nitrate and Mg nitrate hydrates were dissolved in anhydrous ethanol in an $Al^{3+}:Mg^{2+}$ = 2:1 ratio, whereupon tetraethoxysilane was added to this solution of sols in an amount ensuring formation of the $2Al_2.2MgO.5SiO_2$ complex. Crystalline hydrates of alcoholic $TiCl_3C$ solution, $ZrOCl_2$, or $Ce(NO)_3$ were added, in amounts not exceeding respective oxide-equivalent 5 wt.%, while both Al and Mg nitrates were being dissolved in ethanol. The solutions were stirred and placed in a thermostat set at 60°C. All components gelled within about the same time, about of 4 h, forming translucent glassy structures. Specimens of each gel were dried at a temperature of 100°C and then heat treated at various temperatures from 700°C to 1300°C for 3 h at each temperature. The variously heat treated specimens of Al-Mg-Si:$Ti_2$, Al-Mg-Si:$ZrO_2$, Al-Mg-Si:$CeO_2$ gels and of pure Al-Mg-Si gel were examined analytically. Differential thermal analysis in a Paulik-Paulik Q-1500 apparatus with the temperature rising at a rate of 7.5°C/min revealed exothermic effects during heat treatment of all gels, but at different temperatures in each. Phase analysis in a DRON-3M x-ray diffractometer with a $CuK_{\alpha}$-radiation source revealed a completely amorphous structure of all gels except the partly crystalline Al-Mg-Si:$CeO_2$ gel at 700°C and subsequent usual phase transformations at higher temperatures, with a petalitic phase $Al_2 O_3.MgO.3SiO_2$ appearing above 1000°C. The results indicate that μ-cordierite and β-cordiertite can form gradually by the diffusion mechanism during heat treatment at temperatures lower than required for polymorphic transformations during fast heating. Figures 2; tables 1; references 7.

## Dependence of Mullite Synthesis Characteristics on Size of Alumina and Silica Grains

*927D0023E Moscow OGNEUPORY in Russian No 6, Jun 91 pp 13-14*

[Article by I.D. Kashchev, Ural Polytechnic Institute, and T.I. Nazarova, Eastern Institute of Refractory Materials]

UDC 666.762.14

[Abstract] The mullite production process, which involves the $3Al_2 + 2SiO_2$ synthesis and subsequent sintering of the aluminosilicate powder, is analyzed for dependence of the yield of this reaction on the $Al_2O_3$ and $SiO_2$ grain sizes during this reaction. Considering that diffusion is the governing factor in the mullite formation process, both Si in $SiO_2$ and Al in $Al_2$ self-diffusion coefficients $D^*$ at temperatures from 1300°C to 1600°C are evaluated, both being proportional to $e^{-/T}$. The

mullite yield is then calculated for a 75:25 ground alumina (99.5 % $\alpha$-$Al_2O_3$ and quartzite (98.5 % $SiO_2$) mixture. The results indicate that the mullite yield increases as diffusion becomes more intense, the diffusion factor $F = D^*S/r$ being inversely proportional to the grain size (S—specific surface of reacting grains, r—grain radius) in accordance with Fick's first law and being 2-3 orders of magnitude larger for Al — $Al_2O_3$ diffusion than for Si — $SiO_2$ diffusion. This is confirmed by a series of three experiments: 1) with 0.05 cm alumina grains and 0.001 cm quartzite grains, 2) with 0.001 cm alumina grains and 0.1 cm quartzite grains, 3) with 0.001 alumina grains and 0.001 cm quartzite grains. The mullite yield increases as the diffusion factor increases with rising temperature and is determined essentially by the alumina grain size distribution. Figures 1; tables 1; references 8.

## Dependence of Structure and Properties of $Al_2O_3$-$ZrO_2$-$Y_2O_3$ Ceramic on Method of Charge Processing

*927J0023A Moscow OGNEUPORY in Russian No 6, Jun 91 pp 2-5*

[Article by Yu.G. Gogotsi, O.N. Grigoryev, N.A. Orlovskaya, O.A. Babiy, G.Ye. Khomenko, and G.S. Krivoshey, Institute of Problems in Materials Science, UkSSR Academy of Sciences]

UDC 666.762.11.017:620.174:621.763

[Abstract] An experimental study of $Al_2$ + $ZrO_2$ ceramic with $Y_2O_3$ stabilizer produced from three different 70 wt.% $Al_2O_3$ + 30 wt.% $ZrO_2$ + 3 mol.% $Y_2O_3$ powder mixtures was made for a comparative evaluation of structural characteristics and mechanical properties, the powder mixtures having been prepared by: 1) plasmochemical synthesis of Al, Zr, and Y with oxygen; 2) chemical precipitation from solutions of Al, Zr, and Y salts; 3) mechanical mixing of industrial-grade $\alpha$-$Al_2O_3$, m-$ZrO_2$, and $Y_2O_3$ powders. Ceramic was produced by isothermal hot-pressing of the powder mixtures in graphite molds under a pressure of 25 N/mm$^2$ at 1500°C for 1 h. The fine structure of powders and the microstructure of ceramic were examined under a scanning transmission electron microscope. Their phase compositions were determined in a DRON-3M x-ray diffractometer with a $CuK_\alpha$-radiation source. The weight fractions of the crystalline (m,t,c)-$ZrO_2$ phases were measured by the Miller-Smialer-Garlick method (ADVANCES IN CERAMICS Vol 3, 1981). Dispersion and apparent specific surface were determined on the basis of laser beam scattering in a Laser Micron Sizer and on the basis of porosity readings in a Pore Sizer 9300. Density of powders was measured by the displacement-of-liquid method with a Seishin pycnometer. Impurity content ($SiO_2$, MgO, $TiO_2$, $Fe_2O_3$) in powders was determined on the basis of x-ray fluorescence analysis in a VRA-30 apparatus. The results indicate that during hot-pressing both $\gamma$-$Al_2O_3$ and $\delta$-$Al_2O_3$ phases transform into the $\alpha$-$Al_{O_3}$ phase, evidently with an appreciable attendant increase of porosity not reducible by application of high pressure on account of the low strength of ceramic agglomerates. Fracture of ceramic produced from powder obtained by chemical precipitation of salts and from powder obtained plasmochemical synthesis was found to be essentially intergranular, most of $ZrO_2$ inclusions in $Al_2O_3$ grains therefore not being involved in the transformation. Both powders yielded high-porosity and therefore low-strength ceramic. Ceramic produced from mechanically mixed powders had the highest strength, even though it did not have the highest t-$ZrO_2$ content and its $Al_2$ and $ZrO_2$ were not the smallest. The distribution of $Zr_2$ inclusions in the $Al_2O_3$ matrix was nevertheless as uniform as in the ceramic produced from the other two powders. Figures 5; tables 3; references 9

## Cold Extrusion in Floating Mandrels

*927D0111A Moscow*
*KUZNECHNO-SHTAMPOVOCHNOYE PROIZVODSTVO in Russian No 8, Aug 91 pp 7-8*

[Article by Ye.S. Serov, A.G. Mazurin]

UDC 621.777.4.001

[Abstract] The process of cold extrusion in free (floating) mandrels developed for producing long tubular forgings is discussed and the possibility of reducing the wall thickness variation of the initial blank for direct cold extrusion with inverse ejection during the making of cylindrical forgings with a flange is investigated. A formula is derived for describing the variation in the forging thickness and the effect of the initial forging wall thickness variation, its diameter, the clearance between the mandrel and the blank's inside surface, the die cone angle, and the relative deformation on the wall thickness variation of the forging is examined. A fractional factorial experiment (DFE) is conducted in order to assess all significant factors and interactions and assign their weight. The experiment design matrix, mean response values, and their standard deviations are determined. A regression analysis of the experimental data is performed and a model of the process is produced. The results indicate that the initial wall thickness variation decreases due to the use of the free mandrel process and that the mathematical model makes it possible to optimize the selection of process parameters. The wall thickness variation may be reduced by as much as 40%. Figures 3; tables 1; references 3.

## High-Output Automatic Cold Stamping Machines

*927D0111E Moscow*
*KUZNECHNO-SHTAMPOVOCHNOYE PROIZVODSTVO in Russian No 8, Aug 91 p 31*

[Article by V.A. Guskov]

UDC 621.979-52:621.7.016.3.004

[Abstract] More than three decades of design, fabrication, and operation experience accumulated at the Azov Forging Press Automatic Machine Plant culminated in large-scale production of five-position automatic cold stamping machines. The machines are intended for stamping normal, high-strength, and specialty M5-M16 nuts of strength classes 6 and 8 from coiled phosphatized gauged steel. The automatic machines are characterized by high output and reliability and improved working conditions as well as a modern design and various auxiliary devices. The five-position automatic machines have one cutting position and four stamping positions. The automatic machine's design and operating principle are described and its specifications are cited. It develops a force of up to 3,200 kN and has an up to 26.5 kW drive. The plant is offering machines built to customer specifications. The machines make nuts according to GOST 5927—70 and are equipped with noise protection devices stipulated by GOST 12.1.003—83. Figures 1; tables 1.

## Gaseous Detonation Spraying of Wear Resistant Coating on Mandrels for Hot Radial Forging of Hunting Gun Blanks

*927D0111D Moscow*
*KUZNECHNO-SHTAMPOVOCHNOYE PROIZVODSTVO in Russian No 8, Aug 91 p 30*

[Article by A.P. Stafeyev, Ye.P. Saputkin, G.T. Aleksandrova, A.P. Lapin]

UDC 621.793.7:621.735.34.074:639.1.081.2.002

[Abstract] The shortcomings of chrome-plated mandrels for hot radial forging of hunting guns—primarily their poor wear resistance and negative environmental impact—are discussed and a study carried out by the Perm Scientific Research Technological Institute, the Progress Scientific Research Technological Institute in Izhevsk, and the Izhevsk Mechanical Plant aimed at overcoming these shortcomings is reported. The gaseous detonation spraying process for making wear-resistant coats on RKM mandrels is developed as a result of the study. The resulting coats have a porosity of no more than 1.5% and an adhesion bond strength of up to 240 MPa, which is higher than that of plasma jet sprayed coats by almost twofold. The new VK-9s coats' hardness exceeds 1,100 kg/mm$^2$. The Dnepr-2 unit is used for spraying, the KIG-250 machine (Hungary) is used for polishing, and the SVD-412 (Austria) radial forging machine is used for full-scale tests which confirm the adequacy of the coat. The optimum coat thickness is 0.03-0.05 mm. Figures 2.

## Device for Making Large Shells and Rings by Burnishing Under Press

*927D0111C Moscow*
*KUZNECHNO-SHTAMPOVOCHNOYE PROIZVODSTVO in Russian No 8, Aug 91 pp 27-28*

[Article by A.N. Lemkin, L.S. Gusev, L.Ya. Kadigrobov]

UDC 621.735.002.51

[Abstract] The shortcomings of traditional methods of making shells by burnishing under forging presses, i.e., straining the annular billet walls between the flat die and a round mandrel, particularly the size limitations, are considered and a device for forge burnishing of shells and rings, whose diameter exceeds the range of press capabilities, outside the press's working zone is proposed. A photograph and schematic diagram of the prototype of the device on a scale of M1:10 assembled on a 1,000 kN hydraulic press are presented and its specifications are cited. The new prototype device develops a design pressure 300 kN while a full-scale burnisher is

expected to develop a 100,000 kN pressure. The prototype is tested by burnishing ring blanks from steel 20 heated to a forging temperature of approximately 1,100°C. In addition to its intended purpose, the burnishing device may also be used for straightening the curvature of large shells and for bending with the help of additional flat dies. The device requires low outlays and makes it possible to burnish shells which cannot be forged by conventional presses. Figures 3; tables 1.

## Experience of Polyurethane Stamping of Steel Parts With Complex Shape

*927D0111B Moscow*
*KUZNECHNO-SHTAMPOVOCHNOYE PROIZVODSTVO in Russian No 8, Aug 91 pp 17-18*

[Article by V.K. Moiseyev, A.D. Komarov, A.N. Dunayev, V.I. Usatov, Yu.D. Derksen, A.A. Sharov]

UDC 621.983.1.002

[Abstract] The need to forge 18 different small parts for Japanese designed truck crane cabs quickly and cheaply from steel 08kp at the Samara Mechanical Plant No. 1 prompted the use of polyurethane stamping. The parts are stamped in a universal container with polyurethane with the help of cut-out templates or using simple machine-tool attachments. The configuration of the parts produced by this method, their dimensions, blank dimensions, and the stamping arrangement are summarized and a formula is derived for computing the necessary straining pressure. The results show that a 40 MPa polyurethane pressure is sufficient for stamping all complex bent parts. An analysis shows that the polyurethane stamping method may be recommended for making small batches of complex-shaped steel parts in a short time. Yu.I. Beloglazov, A.V. Surgutanov, and N.A. Yefimov participated in the study. Figures 1; tables 1; references 4.

### Endurance Strength of Welded Tubular Structure Assemblies Under Composite Loading

*927D0095A Kiev AVTOMATICHESKAYA SVARKA in Russian No 9(462), Sep 91 pp 1-6*

[Article by E.F. Garf, Ye.P. Lisichenko, Electric Welding Institute imeni Ye.O. Paton at the Ukrainian Academy of Sciences]

UDC [621.791.052:621.774.21]:620.178.3

[Abstract] Fatigue resistance evaluation of welded tubular structure joints on the basis of full-scale or large-scale tests is discussed and the endurance strength of various types of welded tubular structure connections loaded simultaneously by two periodic forces is investigated; in addition, an attempt is made to develop recommendations for assessing the normal life of welded joints at the structural design stage. K-joints are simultaneously loaded by force and moment in a test bench. Test results reveal that under composite cyclical loading of welded tubular assemblies by longitudinal force and a bending moment directed in the assembly's plane, the fatigue resistance should be estimated by the total stress allowing for the damage inflicted. In welded K-joints, endurance strength should be estimated from the viewpoint of effective stresses; in this case greater stresses developing at the strut joint with the truss chord or another strut are responsible for failure. A correlation analysis of the test results from the effective and local stress viewpoints demonstrates that the methods are roughly equivalent in accuracy while with respect to versatility, the evaluation from the effective stress viewpoint has certain advantages. Figures 5; tables 5; references 5: 2 Russian; 3 Western.

### Fracture Propagation Mechanism Under Cyclical Loading of Shaft-Cladding System

*927D0095M Kiev AVTOMATICHESKAYA SVARKA in Russian No 9(462), Sep 91 pp 69-70*

[Article by L.N. Kopetman, St. Petersburg Water Transport Institute]

UDC [621.793.7.052:62-233.12]:620.178.4.001.4

[Abstract] Fracture propagation mechanism in the shaft-cladding system under cyclical loading is investigated and an attempt is made to check the validity of an assertion that thin cladding is more pliable than the base metal due to its noncompact nature and the presence of discontinuities, so the fracture process is initiated in it. An UMM-01 test bench developed at the Mechanics Institute at the Ukrainian Academy of Sciences is used in the study. To this end, fatigue cracks are made in two shafts before surfacing while the third shaft is surfaced intact. The shaft-cladding system behavior is then examined under cyclical loading. A study of longitudinal cross sections of the three samples reveals that the cladding peeling is observed only near the mouth of the crack due to the presence of the stress concentrator. It is speculated that peeling may develop in the absence of a cladding crack and the conclusion is drawn that under alternating-sign loading of clad shafts, e.g., steel with bronze, endurance failure starts in the base rather than the coat. It is thus recommended that the shaft surface be hardened prior to surfacing. Figures 2; references 1.

### Helium Arc Welding of VKA-2 Composite Material

*927D0095L Kiev AVTOMATICHESKAYA SVARKA in Russian No 9(462), Sep 91 pp 62-65*

[Article by V.R. Ryabov, I.S. Dykhno, V.P. Budnik, I.V. Zvolinskiy, M.G. Butsko, A.N. Linnik, Electric Welding Institute imeni Ye.O. Paton at the Ukrainian Academy of Sciences]

UDC 621.791.754'291:[669.715+669.781]:621-419

[Abstract] The VKA-2 metallic composite material consisting of the AD-33 aluminum alloy matrix with 0.14 mm dia. boron fibers and its advantages over polymer composite materials are discussed and the possibility of using helium arc welding with a filler material for joining sheets from the VKA-2 composite material in the fiber orientation direction is examined. The fusible filler material is made as a T-shaped insert designed to form a sheet-T-sheet joint configuration. Microsections of the welded joints produced under various conditions are examined and the weld strength is tested. An analysis shows that helium arc welding along the fiber direction ensures a welded joint strength at an 80-95% level of the base metal strength. It is demonstrated that helium arc welding of the VKA-2 alloy helps to localize the energy influx within a small weldpool volume and ensures complete insert fusion penetration, i.e., a high joint quality. The effect of the post-welding treatment on the welded joint strength is examined. Figures 6; tables 2; references 5.

### Use of Glow Discharge for Resistor Leads Brazing

*927D0095N Kiev AVTOMATICHESKAYA SVARKA in Russian No 9(462), Sep 91 pp 72-73*

[Article by G.P. Bolotov, Chernigov Technological Institute]

UDC [621.791.3:621.3.015.532]:621.316.8

[Abstract] Attempts to use the glow discharge as a heating source for brazing are reviewed and the possibility of using low-pressure glow discharge for brazing the leads to the bodies of resistors (MLT, MON, etc.) instead of resistance welding is investigated. POS-61 brazing solder rings are placed on the leads with rosin and brazing is then performed in a horizontal position. The glow discharge is ignited between the leads and the body. The contact pads are nickel-plated and a neutral helium shielding atmosphere is created in the chamber.

The brazing quality is estimated by tear tests using an RT-250 tensile testing machine within a 0-500 N range tunable in 2 N steps. A total of 50 samples are tested. In most experiments, the contact pad is torn off at a 40-70 N force. Figures 3; references 4: 3 Russian, 1 Western.

### Composition Optimization of Flux-Cored Wire for High-Temperature Aluminum Alloy Surfacing

*927D0095K Kiev AVTOMATICHESKAYA SVARKA in Russian No 9(462), Sep 91 pp 53-54*

[Article by L.S. Tonkikh, A.F. Kabanets, O.B. Nosovskaya, Mariupol Metallurgical Institute]

UDC [621.791.927.5.042:669.715.018.44]:519.2

[Abstract] The use of surfacing for rebuilding the worn-out surfaces of high-temperature aluminum alloy parts using pulsed-arc consumable-electrode welding in an inert gas shielding atmosphere is discussed and a multivariate mathematical model is derived for solving the problem of finding the optimum chemical composition of flux-cored wire electrodes which ensure the requisite surfaced metal properties, i.e., hardness, wear resistance, etc. The model is developed in two stages: deriving a multivariate linear regression equation and a nonlinear regression equation. The mathematical expectations, standard deviations, and correlations are statistically estimated, partial elasticity coefficients are derived, and the adequacy of the regression equation is tested. In addition, the multiple correlation is calculated and tested. As a result, the hypothesis that there is no correlation between the HB hardness and chromium, titanium, manganese, iron, and silicon factors is rejected and multiple correlation is recognized as being significant. The linear effect of the chemical elements in the flux-cored wire on the surfaced metal hardness is corroborated, thus confirming the adequacy of the model. Tables 1; references 2.

### Electrode Metal Transfer During Aluminum Cladding by PP-MA Flux-Cored Wire

*927D0095J Kiev AVTOMATICHESKAYA SVARKA in Russian No 9(462), Sep 91 pp 36-38*

[Article by V.Ya. Zusin, L.A. Glozman, V.A. Serenko, Mariupol Metallurgical Institute]

UDC 621.791.927.5.042:669.715

[Abstract] The difficulty of welding or surfacing aluminum or its alloys due to the presence of a refractory $Al_2O_3$ film on its surface and methods of breaking it down and stabilizing the welding process are discussed; it is shown that controlled-transfer consumable-electrode surfacing by the PP-MA-5 flux-cored wire electrode is the most advanced and efficient process. The flattened flux-cored electrode wire metal transfer mechanism is investigated using a unit which makes it possible to shoot a high-speed film of the surfacing process and examine it frame by frame. A cylindrical billet with a U-shaped beveled groove is surfaced in the study using direct current and 50 and 100 Hz alternating current. A block diagram of the rapid-filming unit and frames shot at a 50 and 100 Hz frequency are cited and the properties of the base and surfaced metal are compared. An analysis shows that when reversed polarity direct current with 50 Hz pulses is used, the charge spills out in the arc burning zone, so the alloying elements are depleted in the weld-pool. When the pulse frequency is increased to 100 Hz, the molten metal drop size decreases, the charge spilling ceases almost completely, and the chemical composition of the surfaced metal ensures its good operating properties. The optimum welding parameters are identified: a 750-800 A welding current, a 100 Hz pulse frequency, a 22-24 V voltage, a 1.6-22 μs duration, a 16-20 m/h welding rate, a 110-140 m/h wire feed rate, and an argon rate of 0.6-0.9 $m^3/h$. Figures 3; references 3.

### Electrostatic-Field Diffusion-Welding of Aluminum to Glass

*927D0095I Kiev AVTOMATICHESKAYA SVARKA in Russian No 9(462), Sep 91 pp 51-53*

[Article by S.E. Shlifer, V.M. Kosogorov, Moscow Aviation Engineering Institute imeni K.E. Tsiolkovskiy]

UDC [621.791.4:539.378.3]:621.319.7:621.315.612.6

[Abstract] The method of electrostatic-field diffusion-welding (DS in ESP)—one of the most efficient ways of producing vacuum-tight joints of semiconductor device units without straining at low temperatures, i.e., below the Al-Si eutectic melting point—is discussed and the use of the method for welding aluminum to S35-1, Pyrex, LK-105, and other types of glass is analyzed. A schematic diagram of the method is cited and optimum welding parameter ranges for glass with various chemical compositions are determined: a 673-753K temperature, a 600-800 V voltage, a 15-30 min isothermal exposure, and a 0-6 MPa compression force. Various welding methods—use of aluminum foils with 0.5% Cu additions, application of a $SiO_2$ layer, and preliminary treatment in an electrostatic force—are examined and welding machines, including multiposition ones, are tested. Methods of preventing NaOH precipitation on the interface in the electric field during welding are considered. The method is suitable for low-temperature nonstraining welding of aluminum-plated (both through sprayed aluminum layers and foils) Kovar, silicon, and GaAs to borosilicate glass containing alkali metal oxides and for producing multilayer welded Al-glass-Al structures in a single cycle. Figures 2; references 3.

### Effect of Sc-Doping on Weldability of Al+6% Mg Alloy

*927D0095H Kiev AVTOMATICHESKAYA SVARKA in Russian No 9(462), Sep 91 pp 34-38*

[Article by N.A. Makhmudova, A.G. Makarov, O.N. Yeryshev, Prometey Central Scientific Research Institute of Structural Materials]

UDC 621.791.011:[669.715+669.793]

[Abstract] The efficiency of doping the Al+6% Mg alloy with scandium in order to harden it is demonstrated and an attempt is made to investigate the effect of scandium doping on this alloy's weldability and the weld structure. To this end, the effect of scandium doping on the metal's tendency toward hot cracking is examined in cold rolled 4 mm-thick slabs containing 0.25% Sc as a dopant. For comparison, commercial alloy AMg61 as well as an Al-Mg-Zn system alloy with 6%Mg was also studied. The tests are carried out using a method developed at the Bauman Engineering University in Moscow whereby the critical tensile straining rate in the sample is measured while making the weld without filler wire. An analysis shows that scandium doping in an amount of 0.25% increases the alloy's hot cracking resistance during welding by a factor of 1.5 while scandium-doped alloy is not sensitive to brief overheating simulation welding in a 250-550°C temperature range. The loss of strength during brief welding simulation overheating usually starts at temperatures of above 550°C. The Sc-doped Al+6% Mg alloy can be recommended for use as a structural material for crucial welded joints since its strength is virtually identical to that of the thermally hardened Al-Mg-Zn system alloy. Figures 3.

## Spot Arc Welding of Aluminum Alloys With Metal Shielding by Elevated-Pressure Argon Jet

*927D0095G Kiev AVTOMATICHESKAYA SVARKA in Russian No 9(462), Sep 91 pp 49-50*

[Article by D.M. Pakhanyan, D.G. Glyanko, Agricultural Machinery Industry Institute, Rostov-na-Donu]

UDC 621.791.754'293.053.3:669.715'721

[Abstract] Extensive uses of aluminum and magnesium alloys due to their good mechanical and operating properties and the experience of welding these alloys under an elevated shielding gas pressure are discussed; in particular, the effect of elevated argon pressure on the geometric characteristics of spot welds made by arc welding is investigated. In so doing, a specially designed welding torch capable of creating an elevated shielding gas pressure directly in the arc burning zone is used, making it possible to use this method for welding large-scale structures. The SvAMg6 electrode wire is used for welding 2 and 4 mm-thick slabs from alloys AMg5. The fusion penetration depth and cast core diameters of the welded spots are examined and regression equations are derived for determining them as a function of the welding condition. The process is recommended for welding stacks of sheets with a total thickness of 8-10 mm and 1 5 mm thickness of the upper sheet. Figures 1; references 3: 2 Russian, 1 Western.

## Nonferrous Metal and Alloy Welding and Surfacing at Mariupol Regional Enterprises

*927D0095F Kiev AVTOMATICHESKAYA SVARKA in Russian No 9(462), Sep 91 pp 45-47*

[Article by V.Ya. Zusin, A.V. Tsyplyukhin, Mariupol Metallurgical Institute and Azovmash Production Association]

UDC [621.791.75+621.791.92]:669.2/.8

[Abstract] The studies of the metallurgical, technological, and energy characteristics of welding of aluminum, copper, and their alloy in shielding gases with flux as well as electron beam welding which have been carried out in the Mariupol region for many years, primarily at the Mariupol Metallurgical Institute, the "Azovmash" Production Association, the metalwork plant, and the shipyard, are summarized and the methods of mechanized consumable-electrode helium-argon welding of railroad tank cars from technical aluminum AD40 with a thickness of 16-28 mm developed at the "Azovmash" Production Association in close cooperation with the Electric Welding Institute imeni Ye.O. Paton at the Ukrainian Academy of Sciences in order to replace automatic submerged arc welding and manual covered-electrode arc welding are described. Other methods of ferrous metal and alloy welding and surfacing developed at enterprises in the Mariupol region, including hidden arc welding, flux-cored wire welding, circumferential welding, etc., are considered. Rebuilding of worn-out parts by surfacing is examined.

## Problems of Welded Structure Fabrication From Titanium and Aluminum Alloys

*927D0095E Kiev AVTOMATICHESKAYA SVARKA in Russian No 9(462), Sep 91 pp 43-45*

[Article by V.V. Redchits, Moscow Aviation Engineering Institute imeni K.E. Tsiolkovskiy]

UDC 621.791.052:[669.715+669.295]

[Abstract] An urgent need to decrease the specific quantity of metal per structure necessitated a transition from various types of machining, casting, and fastening methods to welding; as a result, an attempt is made to summarize available experience in this field and outline a range of problems related to the design, development, and fabrication of crucial welded structures from titanium and aluminum alloys for the new generation of products. To this end, three principles of industrial engineer's work—creating a certain scientific and technical lead, creatively participating in the design of the product at all stages, and using a comprehensive approach to the development of the item and its production and fabrication—are formulated and ways of implementing them are suggested. For this purpose, all welded structures are divided into two categories: load-bearing structures from semifinished components of the beam,

truss, girder, chassis, etc., type and welded structures fabricated mostly from sheet metal. Optimum technologies, materials, and equipment for each category of aluminum and titanium alloys are outlined, reliability and mechanical property stability requirements are considered, and quality control measures are proposed.

### Principal Weldability Characteristics of Alloys 1151 and 1201

*927D0095D Kiev AVTOMATICHESKAYA SVARKA in Russian No 9(462), Sep 91 pp 31-33*

[Article by N.G. Tretyak, R.V. Ilyushenko, M.R. Yavorskaya, V.I. Zaytsev, Electric Welding Institute imeni Ye.O. Paton at the Ukrainian Academy of Sciences and Mashinostroyeniye Scientific Production Association, Reutovo, Moscow oblast]

UDC 621.791.754'293.011:669.715

[Abstract] The weldability of alloys 1151 and 1201 is investigated using the weld metal resistance to hot cracking, mechanical properties of the joints at room temperature, and the metal's tendency toward stress corrosion cracking as the evaluation criteria. Two, 3, and 4 mm-thick sheets of alloys 1151 and 1201 with an ultimate strength of 400-439 and 393-420 MPa, respectively are argon arc welded in a "herringbone" and other patterns. The study reveals that the alloys have a roughly equal tendency to hot cracking while the hot shortness of alloy 1151 may be decreased by three- to fivefold by using the Sv1177 filler wire. This alloy is also distinguished by hot crack propagation during welding both through the middle of the weld and in the fusion zone with the base metal while the base metal and welded joint strength of alloy 1151 at elevated temperatures during slow heating is some 35-40 and 20-25 MPa higher than that of alloy 1201 or its welded joints, respectively. In addition, the resistance to stress corrosion cracking of alloy 1151 in a 3% NaCl solution is higher than that of alloy 1201 by fourfold. Joints of alloy 1151 fail both along the weld and heat affected zone (ZTV) but alloy 1201 fails mostly along the fusion zone and heat affected area. Figures 3; tables 4; references 6.

### Effect of Activated Wire Design and Diameter on Efficiency of Metal Shielding During Welding

*927D0095C Kiev AVTOMATICHESKAYA SVARKA in Russian No 9(462), Sep 91 pp 19-21, 25*

[Article by N.M. Voropay, V.I. Rogatyuk, A.A. Sanko-Novik, Electric Welding Institute imeni Ye.O. Paton at the Ukrainian Academy of Sciences]

UDC 621.791.753.042.3:669

[Abstract] The efficiency of metal shielding during welding by flux-cored electrode wires is discussed and the effect of the activated wire design and diameter on the efficiency of molten metal shielding during open arc welding of low-carbon and low-alloyed steels is investigated. The wire diameter ranges from 1.2 to 2.5 mm. Open self-shielding activated flux-cored $MgCO_3$-$CaF_2$-$TiO_2SiO_2R_2O$ carbonate-fluorite wires are used; to prevent the denitration of molten metal, active nitride-forming elements, such as aluminum, titanium, and rare earth metals are added at the pool stage. Two wire designs are used: one with one central channel and one with two parallel longitudinal channels located on the cross section periphery. Test data demonstrate that for wires with a 2 mm or larger diameter, the shielding efficiency can be increased by complicating the wire design, i.e., placing a part of the steel base in the inner cavity and removing the gas- and slag-forming components to the periphery; when using wire with a 1.2-1.6 mm diameter, its design has virtually no effect on the molten metal shielding. Moreover, when using activated wires with a 1.2-1.6 mm diameter, the flux core filler should ensure a low gas gas evolution and slag protection. Figures 4; references 8: 7 Russian, 1 Western.

### Stresses and Strain During Electron Beam Welding of Thin-Walled Tubes From Single Crystal Tungsten

*927D0095B Kiev AVTOMATICHESKAYA SVARKA in Russian No 9(462), Sep 91 pp 7-12*

[Article by V.I. Makhnenko, Ye.A. Velikoivanenko, B.A. Zaderiy, S.S. Kotenko, Electric Welding Institute imeni Ye.O. Paton at the Ukrainian Academy of Sciences]

UDC [621.791.72.053:669.27]:539.4.013

[Abstract] Problems raised by the increasing use of refractory metals and the issue of their weldability are addressed and the stresses and strain developing during the welding of circumferential seams on thin-walled tubes from single crystal tungsten by electron beam welding are considered. The study is performed numerically; in so doing, the problem of thermoplasticity related to the welding-induced heating of thin-walled tubes is considered and the boundary value problem determining the temperature pattern in the tubes is solved. An analysis shows that during the fusion welding of refractory metals, e.g., W, the material's heating largely depends on the radiant heat transfer between the welded element surface and the environment while the residual stress developing in the circumferential welds made by electron beam fusion welding on thin-walled single crystal tungsten pipes largely depends on their geometrical parameters. The plastic strain zone size also depends on the geometrical parameters and may increase by twofold while the residual radial displacements in the girth weld zone at equal geometrical parameters are proportionate to the shell radius. Figures 7; tables 1; references 7.

## On Two Gas Bubble Nucleation Mechanisms During Li-Doped Aluminum Alloy Welding

*927D0107E Moscow SVAROCHNOYE PROIZVODSTVO in Russian No 9(683), Sep 91 pp 40-43*

[Article by V.V. Ovchinnikov, V.V. Redchits, Moscow Aviation Production Association imeni P.V. Dementyev and Moscow Aviation Engineering Institute imeni K.E. Tsiolkovskiy]

UDC 621.791.01:548.5:669.71

[Abstract] The pore formation during the welding of high-strength lithium-doped aluminum alloys used in the aerospace industry and its negative impact on the weld strength and reliability prompted a study of the gas bubble nucleation stage during the welding of such alloys from the viewpoint of assessing the probability of endogenic and exogenic mechanisms. To this end, experiments are conducted on 3 mm thick slabs of the AMg6 and 1420 alloys which are welded by alternating current using an ISVU-315 source at a 12-15 m/h rate. Some samples are welded using the Sv-AMg63 filler wire with a 2 mm diameter. The dependence of the number of stratifications on the hydrogen concentration in the base metal in the case of incomplete penetration and the dependence of the pore volume in the weld metal on the alloy 1420 sample exposure in a thermostat and under shop room conditions are plotted and the weld and base metal microstructure are examined. The results indicate that exogenic gas bubble nucleation on the face surface of the welded edges is possible although the endogenic mechanism is dominant. Methods of preventing the gas bubble nucleation, e.g., edge scraping, removal of the surface layer from the base metal and filler wire, etc., are suggested. Figures 5; tables 1; references 10.

## Change in Carbon Concentration in Metal During Plasma-Jet Welding in $CO_2$

*927D0107D Moscow SVAROCHNOYE PROIZVODSTVO in Russian No 9(683), Sep 91 pp 25-27*

[Article by B.L. Bozhenko, [illegible]halimov, A.F. Shepelev, Volga-Don Department of the Novocherkassk Polytechnic Institute and Rostov Scientific Research Institute of Machine Building Technology]

UDC 621.791(754'264+755).01:669

[Abstract] The effect of the interaction conditions of $CO_2$ and molten metal on the carbon concentration in the weld made by plasma-arc welding and surfacing is investigated. To this end, the chemical reactions occurring in the gaseous phase and on the plasma arc-melted metal surface which determine the equilibrium carbon concentration in the weld are derived and the activity coefficient of carbon dissolved in steel is calculated. The equilibrium carbon concentration in steel during welding as a function of the correction factor is plotted and microsections of the weld with a filler wire are examined. The weld HV hardness of steels St3p, 15G2AFDps, 45, and 65G as a function of the welding method, i.e., in $CO_2$, air, and argon, as well as after oil and water quenching is summarized. The results show that in contrast to arc welding, the equilibrium carbon concentration in the weld metal increases to >0.1% during the plasma-jet welding in $CO_2$; this is attributed to an increase in the gas composition imbalance near the interface due to the lag of the gas molecule recombination process during the filler metal heating by the plasma jet. Figures 2; tables 4; references 11.

## PVR-UMZ-001 Plasma Generator for Metal Cutting

*927D0107C Moscow SVAROCHNOYE PROIZVODSTVO in Russian No 9(683), Sep 91 pp 20-21*

[Article by V.I. Kondratyev, V.V. Zakharov]

UDC 621.791.947.55.03

[Abstract] The PVR-UMZ-001 plasma generator developed and implemented at the Uzlovoye Machine-Building Plant imeni I.I. Fedunets of the Kran Production Association is described; the plasma generator developed by the authors employs vortical direct-action arc stabilization; the metal strip being cut serves as the anode. A schematic diagram of the plasma generator is presented and its operation is explained. The plasma generator is water-cooled and uses 400 A direct current with a 270 V rating. It operates with other plasma-air cutting units, APR-402UKhL4, APR-403UKhL4, and APR-404UKhL4, used for cutting low carbon and low alloyed steel with an up to 30-mm thickness. Manuals and specifications are available upon request. Figures 2; tables 1.

## Characteristics of Cr-Containing Vacuum Tube Material Brazing by PSr 72 Solder

*927D0107B Moscow SVAROCHNOYE PROIZVODSTVO in Russian No 9(683), Sep 91 pp 4-6*

[Article by V.V. Kraft, All-Union Electrical Engineering Institute]

UDC 621.791.3.016.61:621.06

[Abstract] The poor wettability of corrosion-resistant, and particularly Cr-containing, steels by the silver-based solders used in brazing of vacuum tube components are discussed and the spreading of the PSr 72 solder on steel 12Kh18N10T as well as the mechanical strength and microstructure of brazed joints of this steel with copper M0b are examined and the issue of brazing the KhD50V-MP powder contact material containing ≤50% Cr by the PSr 72 solder is addressed. All experiments are conducted in an SGV-2.3/15 vacuum electric furnace and

the solder spreading on steel is examined by the GOST 23904—79 method. The dependence of the ultimate rupture strength of joints from steel 12Kh18N10T and copper M0b on the brazing temperature is plotted. An analysis shows that wetting by the PSr 72 solder occurs at temperatures above 850°C and a residual gas pressure of $<1.33 \times 10^{-2}$ Pa and that spreading is generally completed at 900°C. The 1-2 μm steel surface layer is saturated with copper. As for butt-joints of copper with the KhD50V-MP composite materials or steel 12Kh18N10T, a much better wetting of the Cr-containing material is observed, making it possible to attain a good mechanical strength of >100 MPa at a 820-850°C soldering temperature; yet vacuum-tight contacts require an 850°C temperature. A microstructural analysis of copper-steel joints demonstrates that the solder is gradually "dispersed" and the zone of its diffusive penetration into copper increases. Figures 3; tables 1; references 5: 4 Russian, 1 Western.

### Welding of Beryllium-Doped Copper Alloy Strips

*927D0107A Moscow SVAROCHNOYE PROIZVODSTVO in Russian No 9(683), Sep 91 pp 2-4*

[Article by K.A. Yushchenko, A.A, Nakonechnyy, Yu.G. Vysotskiy, L.B. Kuznetsov, L.B. Alekseyev, Electric Welding Institute imeni Ye.O. Paton and Kolchugino Nonferrous Metal Works]

UDC 621.791.75.037:669.725

[Abstract] Attempts to develop a welding technology for joining strips of Cu-based alloys doped with beryllium made by rolling from small ingots (and thus requiring welding due to their short length) and to develop a unit which would make it possible to mechanize and automate the preparation, assembly, and welding processes are reported. Experiments are conducted using samples cut from commercial coils; lap, butt, seam resistance, and pulsed arc methods are tested and the welding process and weld parameters are summarized. An analysis demonstrates that nonconsumable electrode pulsed arc welding is the most efficient for welding strips from heavy nonferrous alloys doped with Be. A good joint quality is obtained in welding strips with a 0.3-0.9 mm thickness as well as strips with different thicknesses within a 0.3-2.5 mm range by using the lap welding methods while butt welding is more advantageous for joining strips of different thicknesses within a 0.9-2.5 mm range. The unit developed for the strip welding makes it possible to cut, center, and weld strips in an automatic mode and ensures satisfactory strength and ductility properties of the resulting continuous strip welds. Figures 3; tables 1.

### Erection Welding of One-Sided Joints of Stationary Deep-Water Marine Platform Structure

*927D0108A Moscow SVAROCHNOYE PROIZVODSTVO in Russian No 11(685), Nov 91 pp 2-5*

[Article by Ye.I. Okupnik, S.N. Zhiznyakov, L.L. Rubanovich, V.I. Novikov, V.N. Gorpenyuk, O.I. Steklov, E.A. Makhmudov, G.I. Khanguliyev, T.Sh. Shirinov, Promstalkonstruktsiya All-Union Scientific Research and Design Institute, Electric Welding Institute imeni Ye.O. Paton, MING imeni I.M. Gubkin, and Shelfproyektstroy PPSO]

UDC 621.791.75:629.12

[Abstract] The load-carrying supporting structures of the stationary sea platform intended for crude oil production in the deep-water sections of the Caspian Sea which is an all-welded lattice framework shaped as a truncated tetrahedral pyramid designed by the EPTM Company (France) is described; the principal structural member is a pipe with a 277-1,820 mm diameter and a 10-60 mm thickness. The structure is made from steel 09G2S-12 and is designed to U.S. specifications on the basis of one-sided butt and T-joints. The design features of the welded edges, welding features of the covered electrodes, parameters of the welding process, electrode and weld-pool control methods, and the welder skill requirements are summarized and schematic diagrams of the unsupported welding procedures and welded joints are cited. The operating experience gained by the Shelfproyektstroy PPSO indicates that this method of unsupported welding may also be used in other fields of mechanical engineering and construction for erecting load-bearing, process, and building structures from steel allowing for the characteristic features of their welding. The procedure requires a rather high welder skill level. Figures 2; tables 3; references 12: 9 Russian, 3 Western.

### Welded Joint Properties of Low Alloyed Steel X42 After Use in Hydrogen Sulfide

*927D0108D Moscow SVAROCHNOYE PROIZVODSTVO in Russian No 11(685), Nov 91 p 18*

[Article by S.M. Chashin, S.A. Yermolayev, I.Yu. Gavrilina, V.V. Antonova, G.N. Osipova, All-Union Scientific Research Institute of Natural Gas]

UDC 621.791.052:620.17:669.15-194.2

[Abstract] The properties of welded joints from low alloyed steel X42 are examined after being used in an $H_2S$ environment in order to determine their residual life under the operating conditions of the Astrakhan gas condensate deposit characterized by an elevated hydrogen concentration (25% above normal). Two tube-assembly welded joints and four stagger-wound Lorenz coils from steel MWX42NS (made by Mannesmann) are examined after one year and 2.5 years of operation; to this end, their mechanical properties—the KCV and KCU toughness—are measured and their corrosion resistance is tested. Metallographic studies and test data indicate that the joints and coils may indeed operate efficiently under the Astrakhan deposit conditions where the average monthly air temperature in January does not drop below -15°C (GOST 156350—80). Tables 2.

## Laser Unit Selection Optimization by Their Material Treatment Parameters

*927D0108E Moscow SVAROCHNOYE PROIZVODSTVO in Russian No 11(685), Nov 91 pp 19-21*

[Article by A.G. Grigoryants, A.V. Bogdanov, Yu.V. Ivanov, V.S. Gavrilyuk, Yu.V. Golubenko, B.I. Krivov, Moscow State Engineering University imeni N.E. Bauman]

UDC 621.791.947.72.03:621.375.826

[Abstract] The complex effect of the polarization, space-time, and energy characteristics of laser radiation on the hydro- and gas dynamics of the weldpool, the weld width and depth, the mechanical strength of the welded materials, and their corrosion resistance is discussed and an attempt is made to optimize the laser selection on the basis of the treatment parameters. A physico-mathematical model offered by Vvedenov and Gladush (*Fizicheskiye protsessy pri lazernoy obrabotke materialov*, Moscow: Energoatomizdat, 1985) is used as the basis for the study. The dependence of the mean output power, energy divergence, and bean diameter on the radiator's output window on the pump power is plotted experimentally and on the basis of regression models; topograms of the pump power function and the experimental dependence of the output power, penetration depth, and weld width on the mean pump power are plotted. An analysis demonstrates that the method is suitable for assessing the ambiguous effect of the laser radiation parameters on the process parameters and select the laser system operating condition which ensures the most efficient material processing. Figures 4; references 7.

## Characteristics of Power Valve Seal Metal Formation During Build-up in Vacuum Furnaces

*927D0108C Moscow SVAROCHNOYE PROIZVODSTVO in Russian No 11(685), Nov 91 pp 11-12*

[Article by A.S. Zubchenko, N.A. Chertkov, Scientific Production Association of the Central Scientific Research Institute of Machine-Building Technology and Chekhov Power Machine-Building Plant]

UDC 621.791.052:620.18

[Abstract] The characteristics of the metal build-up formation during the surfacing of power fitting seals in a vacuum furnace are investigated, the practical feasibility of using the standard PSGr2 powder is evaluated, and the serviceability of the resulting seals is determined. Prototypes and regular housings of valves from steel 25 and 12Kh1MF were surfaced with the PGSr2 powder in a vacuum furnace at 1,100°C at a 0.133 Pa pressure; the surfaced parts were then cooled in an argon atmosphere. The microstructure of the seal area is examined and the surfaced metal HRC hardness is measured as a function of the exposure duration and cooling duration. An analysis shows that the PGSr2 chromium-nickel powder lends itself to streamlined application and may produce a high-quality built-up surface with a 1-30 min exposure and a 1-5 h cooling. Hardness test data attest to the sufficient hardness of the built-up metal at working temperatures. The seal metal's corrosion resistance tests and service life tests of valves form steel 12Kh1MF surfaced in vacuum furnaces confirm the adequacy of the method. Figures 1; tables 3.

## Calculation of High-Frequency Current Field Heating Duration During Centrifugal Plain Bearing Build-up

*927D0108B Moscow SVAROCHNOYE PROIZVODSTVO in Russian No 11(685), Nov 91 pp 7-8*

[Article by Yu.I. Veslopolov, I.Yu. Veslopolov, Integral Scientific Industrial Complex]

UDC 621.791.77.011:331.01

[Abstract] Ways of extending the life of clad metal plain bearings by build-up with heating in a high-frequency current field are considered and an attempt is made to describe mathematically the laws governing the thermal and electromagnetic fields in a differential or integral form in order to find the optimum microwave field heating duration. To this end, the heat balance equation of the plain bearing build-up in a microwave current field is derived in a differential form allowing for the total heat losses and then solved, resulting in an integral equation; the integral equation, in turn, makes it possible to determine the heating duration. The dependence of the bearing heating duration on the induction heater current is plotted. The resulting formulas can be used for building up the surface of plain bearings for the NDV-24 diesel engine. Figures 1; references 2.

## Tribological Forms of Diamond Drill Bits and Their Classification

*927D0109A Moscow RAZVEDKA I OKHRANA NEDR in Russian No 10, Oct 91 pp 14-18*

[Article by Kh.M. Khristov, Bulgarian Geological Committee]

UDC 622.24.051.71.004.62/.63.001.33

[Abstract] The diversity of the physical and chemical origin, manifestations, and patterns of diamond drill bit (ABPI) wear prompted an effort to classify the tribological forms or drill bit wear and outline the principal classification criteria. The resulting classification of the principal tribological forms of diamond drill bits covers several objects of wear—the threaded housing, matrix, diamonds, and the tool as a whole—and addresses the tribological forms and symptoms, the nature of the processes, wear rate, and the end result of wear; in so doing, the physical, chemical, and economic features are considered. The occurrence of various types of diamond drill bit wear at various Bulgarian deposits are summarized and three main tribological diamond forms are identified: normal wear, polishing, and pitting. The classification's usefulness for practical applications is noted and the need for further research is emphasized. Figures 3; tables 3.

## Mobile Diesel Electric Power Plant With Sump

*927D0109B Moscow RAZVEDKA I OKHRANA NEDR in Russian No 10, Oct 91 pp 18-19*

[Article by R.G. Bondarev, S.V. Dmitriyev, S.K. Matveyev, Dalgeologiya Production Geology Association]

UDC 621.311.28:621.436

[Abstract] A mobile diesel-driven electric power plant with a sump (PEZS-60) designed by a pilot methodological party of the Dalgeologiya Production Geology Association allowing for the specific natural and climatic conditions is described; the PEZS-60 is intended for supplying drilling rigs with electric power as well as for household purposes. A schematic diagram of the power plant is cited and its specifications are listed. The plant employs DES-60 or ADS-100 diesel engines, can travel at 30 km/h, and can be mounted on wheels or skids. The sump design is described. Depending on the distance and road conditions, the PEZS-60 can be transported as a single unit by rail or by water as well as pulled or towed. Figures 1; tables 1.

## Using Biolocation for Solving Engineering Geophysics Problems

*927D0109C Moscow RAZVEDKA I OKHRANA NEDR in Russian No 10, Oct 91 pp 26-28*

[Article by G.G. Arkhangleskiy, A.S. Zaytsev, Tsentrgeologiya]

UDC 577.3:550.83

[Abstract] The shortcomings of traditional engineering geophysics methods for assessing the state of soil and buildings, locating underground cavities, and finding soil mass loosening areas in cities are summarized and the need for utilizing the natural abilities of the human organism capable of perceiving even the smallest changes in the physical and information-bearing characteristics of the environment for this purpose is recognized. It is stated that such abilities may be used to locate water, mineral deposits, items of worship, etc. In biolocation, man himself serves as the sensor, so other instruments are not needed. The authors' experience in investigating the biolocation phenomenon is summarized and examples of its successful use for assessing the state of the soil and building structures in Moscow are cited. The possibility of combining biolocation with other geophysical methods is investigated. Good correlation of the biolocation results with seismic data is emphasized. References 2.

## Factors Determining Diversity of Tungsten's Mineral Forms

*927D0109E Moscow RAZVEDKA I OKHRANA NEDR in Russian No 10, Oct 91 pp 32-34*

[Article by V.N. Voyevodin, S.A. Voyevodina, N.S. Prokopov, Far Eastern Institute of Mineral Raw Materials and Rostov State University]

UDC 553.46:550.4

[Abstract] The diversity of tungsten's mineral forms at various deposits prompted an attempt to ascertain how they depend on the physical, chemical, and geological conditions of their mineralization development. Consequently, the factors determining the development of various mineral forms of tungsten at certain deposits are examined. To this end, the redox environment of the geothermal solutions which determine the valent state of tungsten, the degree of the initial ancestral mineralization magmatism basicity, and the role of the enclosing rock are investigated. The redox environment is determined indirectly as a ratio of the sum of reduced gases to the sum of oxidized gases measured by gas chromatography. The principal conclusion of the study is that the basicity degree of the magmatic rock ancestral to mineralization and the magnitude of the redox value of the geothermal solutions which determines tungsten's valent state, as well as the possibility of the geothermal solutions' interaction with the enclosing rock with various chemical compositions along their path are the dominant factors affecting the occurrence of the scheelite, wolframite, and tungstenite mineralization form. References 2.

## Role of All-Union Scientific and Engineering Geology Society in Improving Work Condition and Protection

*927D0109D Moscow RAZVEDKA I OKHRANA NEDR in Russian No 10, Oct 91 p 31*

[Article by E.I. Romashevskiy, Kazakh Republican Directorate of the All-Union Scientific and Engineering Geology Society]

UDC 331.45:550.8

[Abstract] The role of the All-Union Scientific and Engineering Geology Society (VNTGeO) in improving the work conditions and work safety and the specific tasks facing Kazakhstan's geological service are outlined. Today, the Kazakh Republican Directorate of the All-Union Scientific and Engineering Geology Society has ten sections involved in various aspects of the geological activity, including a Work Safety and Industrial Engineering Section which was set up in 1973. The activities of the section in cooperation with the Kazakh Scientific Research Work Safety Institute (KNIGOT) and other organizations aimed at preventing accidents resulting in injuries, disseminating safe work procedures, and improving the efficiency of work protection measures as well as training staff in the areas of safety engineering and accident prevention are summarized. The need to set up work safety groups and organize relevant advice centers at all territorial departments of the All-Union Scientific and Engineering Geology Society is emphasized.

## Hygienic Efficiency of Welding Aerosol Removal by 'Kemper' Air Filtration and Ventilation Systems

*927D0108F Moscow SVAROCHNOYE PROIZVODSTVO in Russian No 11(685), Nov 91 pp 32-33*

[Article by L.N. Gorban, T.K. Kucheruk, P.P. Tikhonchuk, V.I. Bova, Kiev Scientific Research Institute of Work Hygiene and Occupational Diseases and Bolshevik Production Association]

UDC 621.791:658.34:613,647

[Abstract] The negative health impact of air contamination with welding aerosols and the human and economic cost of the resulting occupational illness are discussed and the sanitary and hygienic efficiency of the mobile "Kemper" (FRG) air filtration and ventilation system which captures welding aerosols by mechanical (FVU-1) and electrostatic (FVU-2) filtering systems is evaluated. The Kemper system is capable of delivering 2,000 $m^3$/h, has an exhaust capacity of 1,200 $m^3$/h, and has a power demand of 0.75 kW. Its noise level is 68 or 70 dB depending on the type of filter used. The FVU-1 and FVU-2 efficiency is assesed for various types of welding and the toxic substance concentration in the respiratory zone is measured. The studies reveal the high efficiency of the Kemper system in preventing the effect of welding aerosols on the welders. The concentration of gaseous and solid substances in the breathing zone meets the specifications of GOST 12.1.005—88. It is recommended that the welders learn how to operate the system correctly. Figures 1; tables 2; references 4.

# END OF FICHE DATE FILMED

5 May 1992